University of California
Los Angeles

Pattern Formation in Particle Interactions

A dissertation submitted in partial satisfaction
of the requirements for the degree
Doctor of Philosophy in Mathematics

by

James Holladay von Brecht

2012

Abstract of the Dissertation

Pattern Formation in Particle Interactions

by

James Holladay von Brecht

Doctor of Philosophy in Mathematics

University of California, Los Angeles, 2012

Professor Andrea L. Bertozzi, Chair

Large systems of particles interacting pairwise in d-dimensions give rise to extraordinarily rich patterns. These patterns generally occur in two types. On one hand, the particles may concentrate on a co-dimension one manifold such as a sphere in three dimensions or a ring in two dimensions. Localized, space-filling, co-dimension zero patterns can occur as well. This work develops an understanding of such patterns by exploring how the prediction and design of patterns relates to the stability and well-posedness properties of the underlying mathematical equations.

At the outset we use dynamical systems theory to predict the types behaviors a given system of particles will exhibit. Specifically, we develop a non-local linear stability analysis for particles that distribute uniformly on a $d-1$ sphere. Remarkably, this linear theory accurately characterizes the patterns in the ground states from the instabilities in the pairwise potential. We then leverage this aspect of the theory to address the issue of inverse statistical mechanics in self-assembly, i.e. the construction of a potential that will produce a desired pattern. As the linear theory indicates that potentials with a small number of spherical harmonic instabilities may produce very complex patterns, we naturally arrive at the linearized inverse statistical mechanics question: given a finite set of unstable modes, can we construct a potential that possesses precisely these linear instabilities? An affirmative answer would allow for the design of potentials with arbitrarily intricate spherical symmetries in the ground state. We solve the linearized inverse problem in full, and present a wide

variety of designed ground states.

To conclude we begin the task of transferring aspects of the linear theory apply to the fully nonlinear problem. In particular, we address the well-posedness of distribution solutions to the aggregation equation $\rho_t + \mathrm{div}(\rho \mathbf{u}) = 0,\ \mathbf{u} = -\nabla V * \rho$ in $\mathbb{R}^d$ where the density ρ concentrates on a co-dimension one manifold. When the equation for such a solution is linearly well-posed, we show that the fully non-linear evolution is also well-posed locally in time for the class of bi-Lipschitz surfaces. In this aspect at least, the linear and non-linear theories therefore coincide.

The dissertation of James Holladay von Brecht is approved.

Inwon C. Kim

James Ralston

P. Jeffrey Brantingham

Andrea L. Bertozzi, Committee Chair

University of California, Los Angeles

2012

Table of Contents

List of Figures

List of Tables

Acknowledgments

I have had a tremendous amount of good fortune throughout the course of my academic career and my life as a whole. I am forever indebted to all of my family, friends and mentors for the love, support and guidance they have provided me during my journey. This dissertation would not have happened without them.

Foremost I must thank my academic mentor and thesis advisor Andrea Bertozzi. Outside of my parents, she has played the largest role in guiding my adult life. She started me on the path toward a Ph. D. in mathematics as an undergraduate, and has continued to give me invaluable advice and encouragement at every step along it. Words cannot express my gratitue, and I will forever be grateful to her. I would also like to thank the rest of my thesis committee as a whole, Inwon Kim, Jeff Brantingham and Jim Ralston, for their assistance in reviewing my dissertation and their interest in my work, and Professor Ralston specifically for teaching me differential equations.

I must also express my gratitute to a number of other mathematicians for their roles in my career. Theodore Kolokolnikov first suggested the problem that formed the basis for my dissertation and current line of research. He has been a terrific collaborator and showed me tremendous hospitality in my visit to Halifax. I would also like to express my gratitude to my friend and collaborator David Uminsky. He has provided me with help and advice in more ways than I can hope to remember. I would also like to thank Professors Luminita Vese, Tony Chan and Stan Osher for their assistance in gaining entrance to graduate school.

The second chapter of this thesis is based on the article "Predicting Pattern Formation in Particle Interactions," Mathematical Models and Methods in Applied Sciences, Suppl. 4, 2012. It was done in collaboration with David Uminsky, Theodore Kolokolnikov and Andrea L. Bertozzi and was supported by NSF grants EFRI-1024765 and DMS-0907931, ONR grant N000141010641 and NSERC grant 47050. The third chapter is based on the article "On Soccer Balls and Linearized Inverse Statistical Mechanics," Journal of Nonlinear Science, 2012. It was done in collaboration with David Uminsky and was supported by NSF

grant DMS-0902792. The final chapter is based on the article "Well-Posedness Theory for Aggregation Sheets," submitted to Communications in Mathematical Physics, 2012. It was done in collaboration with Andrea L. Bertozzi and was supported by NSF grants DMS-0907931 and EFRI-1024765.

Without doubt, the greatest support has come from my friends and family. I hope the great frienships I have made in graduate school will last a lifetime. Erik Lewis went above and beyond in helping me throughout the job application process. Hem Wadhar also gave me great career advice, and somehow put up with me sleeping throughout our trip to Europe. I want to thank Michael Moeller for his hospitality in Germany and for just being a great friend. You're still late to lunch, though. Thanks to Rachel Hegemann for all the hugs and high-fives, to Laura Smith for putting up with my wit and to Hayden Schaeffer for his constant sarcasm this last year. My half-brother Carlos Guzman is the best friend I will ever have. I relied on him almost every day throughout the past four years and he somehow managed to keep me sane. More importantly, he got me obsessed with playing blues guitar. My apologies to his wonderful wife Erika Lara, who is kind enough to let me borrow him from time to time. Above all I want to thank my Mom and Dad for their eternal love and support. With every day that goes by I realize how lucky I am to have them as parents. I love you, and hope I made you proud.

Vita

2008	B.S. in Applied Mathematics, *Summa Cum Laude* University of California, Los Angeles
2008	Phi Beta Kappa, Departmental Highest Honors University of California, Los Angeles
2008	Sherwood Prize in Mathematics University of California, Los Angeles
2008	M.A. in Applied Mathematics, University of California, Los Angeles
2008-2011	NSF VIGRE Fellowship, Department of Mathematics University of California, Los Angeles
2012	Postdoctoral Scholar University of California, Los Angeles

CHAPTER 1

Introduction

The mathematics of interacting particles pervades many disciplines, from physics and biology to control theory and engineering. Classical examples from physics and chemistry range from the distribution of electrons in the Thomson problem, to VSEPR[1] theory, self-assembly processes and protein folding. In biology, similar mathematical models help explain the complex phenomena observed in viruses, locust swarms and bacterial colonies. In engineering, particle models have been successfully used in many areas of cooperative control, including applications to robotic swarming.

In each of these examples, the overall collective behavior of the particle group is a minimizer of the total energy of all interactions between two particles. Specifically, if N denotes the total number of individuals in the group and $\mathbf{x}_i$ the position of the i^{th} individual then the formula

$$E(\mathbf{x}_1, \ldots, \mathbf{x}_N) := \sum_{j,k \neq j} V\left(\frac{1}{2}|\mathbf{x}_j - \mathbf{x}_k|^2\right). \tag{1.1}$$

defines the interaction energy of the whole group. In this formulation, the distance between two individuals alone determines their pairwise interaction. The potential $V(s)$ encodes the precise dependence of the interaction on inter-particle distance, and therefore widely varies between applications and across disciplines. While (1.1) takes a simple form and presupposes isotropic interactions, energies of this type still prove useful for modeling a wide variety of complex, collective behaviors and natural phenomena.

Modeling collective behavior in this manner applies regardless of whether a given "particle" happens to represent, say, an electron, atomic colloid, biological organism or autonomous robot. The simplest example involves performing a gradient flow directly on the interaction

[1] VSEPR = Valence Shell Electron Pair Repulsion

energy (1.1), which yields the equation

$$\frac{\mathrm{d}\mathbf{x}_i}{\mathrm{d}t} = \sum_{\substack{j=1\ldots N \\ j\neq i}} g\left(\frac{1}{2}\left|\mathbf{x}_i - \mathbf{x}_j\right|^2\right)(\mathbf{x}_i - \mathbf{x}_j), \quad g(s) = -\frac{\mathrm{d}V}{\mathrm{d}s}(s), \tag{1.2}$$

for the motion of each individual. This coupled system of N ordinary differential equations also has a closely related continuum limit, i.e. the well-known aggregation equation

$$\frac{\partial \rho}{\partial t} + \operatorname{div}(\rho \mathbf{u}) = 0, \quad \mathbf{u} = \int_{\mathbb{R}^d} g\left(\frac{|\mathbf{x}-\mathbf{y}|^2}{2}\right)(\mathbf{x}-\mathbf{y})\rho(\mathbf{y},t)\,\mathrm{d}\mathbf{y} \tag{1.3}$$

for the density $\rho(\mathbf{x}, t)$ of particles. In models of biological aggregates, the non-locality provides a means to incorporate the endogenous forces that occur between individuals [38]. These social interactions manifest as a short-range repulsion, so that each individual maintains its identity, and a long-range attraction to preserve the cohesiveness of the swarm [45, 46, 64]. Purely attractive potentials can arise in biology as well, most notably in simplified versions of the famous Keller-Segel model for bacterial chemotaxis [33]. In this case the non-locality represents the response of a bacterium to the presence of chemo-attractant. An additional diffusive term in (1.3) then provides a repulsion-like effect. In models for granular media, (1.3) describes the temporal evolution of the velocities in a spatially homogenous distribution of particles, and the non-locality models velocity fluctuations due to the quasi-elastic collisions that occur between granules in the medium [67, 15, 4].

Dynamic versions of (1.2) also frequently arise in models for biological swarming. The system of N self-propelled particles

$$\frac{\mathrm{d}\mathbf{x}_i}{\mathrm{d}t} = \mathbf{v}_i, \quad \frac{\mathrm{d}\mathbf{v}_i}{\mathrm{d}t} = \left(\alpha - \beta|\mathbf{v}_i|^2\right)\mathbf{v}_i + \sum_{j\neq i} g\left(\frac{1}{2}\left|\mathbf{x}_i - \mathbf{x}_j\right|^2\right)(\mathbf{x}_i - \mathbf{x}_j) \tag{1.4}$$

and its variants often arise as a model for the self-organization of large, localized groups of animals such as flocks of birds or schools of fish [39, 17, 65]. These models also help to explain similar complex collective motions observed at smaller scales, such as the emergence vortex swarms in *Daphnia* [42]. When $\alpha = \beta = 0$, the dynamical system (1.4) arises in classical molecular dynamics. In this context, the dynamics describe the motion of gas or fluid particles, and in the appropriate limit yield the equations of fluid dynamics [30].

The presence of a non-zero the local velocity contribution $(\alpha - \beta|\mathbf{v}_i|^2)\,\mathbf{v}_i$ reflects the self-propulsion of an individual animal or particle: in the absence of the non-local interactions each individual will eventually travel at the preferred speed $\sqrt{\alpha/\beta}$ of the group. The non-locality once again reflects social forces between individuals. Due to the presence of these forces, many behaviors exhibited by the system (1.2) also occur in the dynamic variant (1.4). For instance, the flocking behaviors of the dynamic model precisely correspond to equilibrium states of (1.2) translating at the group velocity $\sqrt{\alpha/\beta}$. A proper understanding of (1.2) is therefore essential in order to fully characterize the range of possible swarming dynamics.

Regardless of the specific physical or biological interactions the non-locality models, the primary aim lies in understanding the emergent behavior and long-time properties of the solutions to both equations. For the first order system (1.4), this naturally leads to the study of local minimizers of the interaction energy

$$(\mathbf{x}_1, \ldots, \mathbf{x}_N) = \underset{\mathbf{y}_1,\ldots,\mathbf{y}_N}{\arg\min}\, E(\mathbf{y}_1, \ldots, \mathbf{y}_N) := \sum_{i,j\neq i} V\left(\frac{1}{2}|\mathbf{y}_i - \mathbf{y}_j|^2\right). \tag{1.5}$$

The interest in and study of such minimizers has at least a century-old history. In 1904, J. J. Thomson proposed minimizing (1.5) with an electrostatic potential $V(s) \propto s^{-1/2}$ as part of his model of the atom [63]. He constrained the particles to lie on the sphere due to the purely repulsive nature of the electrostatic potential. This constraint then gives rise to a variety of rich, non-trivial minimizing structures. Characterizing these structures remains an unresolved problem, and it continues to generate interest in modern times [37, 18] as one of Smale's problems for the 21$^{\text{st}}$ century [59]. Formulations related to Thomson's problem have also found a wide range of applications, from the algorithmic design of self-assembled nanostructures [19] to models for the structure of spherical shells of viral capsids [75]. When the potential $V(s)$ exhibits short-range repulsion and long-range attraction, the artifical restriction of particles to a sphere proves unnecessary. In this case, the minimizers of (1.5) may remain naturally localized in space independently of the size of the particle group. A variety of rich minimizing structures naturally arise as a result. Since localized, cohesive groups like as flocks and schools dominate swarming dynamics, this aspect of attractive-repulsive potentials in large part motivates their use in biological modeling [45, 28].

The Forward Problem

Analysis of local optima of (1.5) involves two conversely related aspects. The first aspect entails understanding the types of grounds states that a given interaction potential may produce, and we refer to this aspect as the forward problem. This task is highly non-trivial as even a simple two-parameter potential can yield a plethora of diverse minima. To illustrate this fact, we numerically integrate (1.2) to steady-state with the regularized step function from [35]

$$-\frac{\mathrm{d}V}{\mathrm{d}s} = g(s) = \frac{\tanh(a(1-\sqrt{2s}))+b}{\sqrt{2s}}, \quad 0<a, \quad -\tanh(a)<b<1, \tag{1.6}$$

as the interaction potential. Simply by controlling the amount of local repulsion at the origin (b) and the slope of the transition between repulsion and attraction (a), many types of patterns emerge. These range from a uniform distribution of particles on a sphere to ground states characterized by higher symmetry and full three dimensionality. We begin our study of the forward problem by attempting to explain these transitions, so our primary interest therefore lies in co-dimension one solutions.

Such patterns frequently arise in applications. For instance, in the discrete setting (1.2) they arise in both point vortex theory [48, 47, 31, 2] as well as the previously mentioned Thomson problem [50, 1, 72, 18, 19]. In the context of point vortex theory, vortices restricted to a sphere can organize into both platonic solid and ring configurations [48, 47, 31]. In the classical Thomson problem, the minimizers exhibit platonic solid configurations for small numbers of electrons. As the number of electrons increases, a wide variety of spherical lattices may form, including non-platonic solids as well as lattices with higher order defects. Complex patterns also arise in biology, and have inspired researchers to develop mathematical models that can help explain, both evolutionarily and biologically, why and how these self-assembled patterns form [13, 52, 49, 32, 46, 25, 20, 41, 3]. Such models have proven fruitful in modeling locust swarms [5, 38, 65], where the techniques capture the unique swarm shapes of locusts. These models also help explain rings, annuli, and other complex, spotted patterns in bacterial colonies that form under stress in the lab [68, 21, 34, 11]. Many of these same models have been exploited in the area of cooperative control [74] and boundary tracking

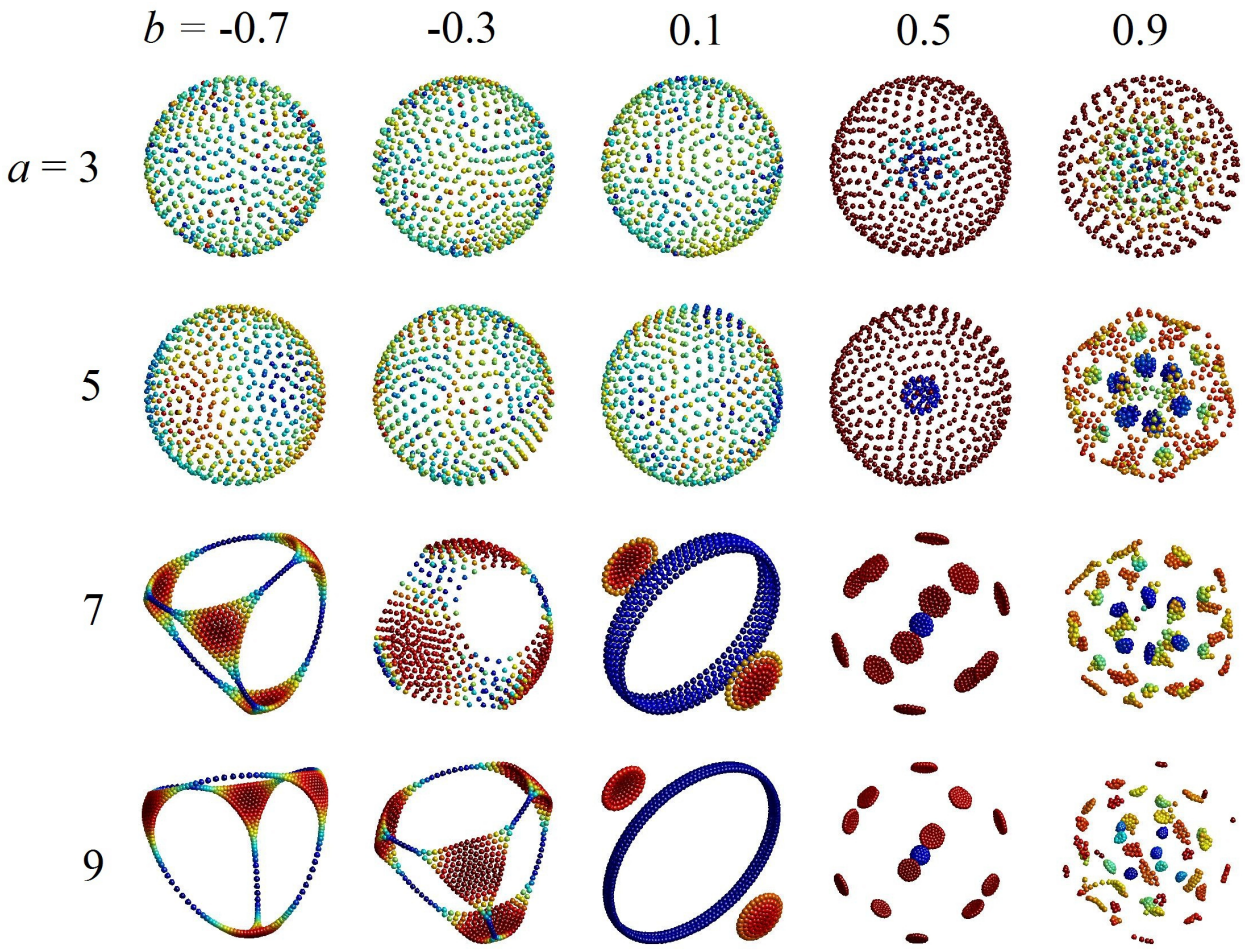

Figure 1.1: Minimizers of the energy (1.5) with force law (1.6).

algorithms for autonomous, flocking robots [17] as well.

The Inverse Problem

The converse aspect, known as inverse statistical mechanics or the inverse problem, requires constructing a pairwise interaction potential to yield a desired ground state with particular features. A successful resolution of the inverse problem would provide a means to control the collective behavior of an animal group, a robotic swarm of unmanned vehicles or to produce a self-assembled molecular strucutre that exhibits desired properties. Approaches to inverse statistical mechanics vary widely in terms of algorithmic simplicity and mathematical rigor. Algorithms that aim to self-assemble nanoparticles into square, diamond, and honeycomb

lattices add targeted potential wells to Lennard-Jones like potentials [54, 55, 56, 66]. The final potentials result from a computationally intensive optimization scheme coupled with a series of necessary conditions that suggest a working solution that produces the desired co-dimension zero lattice. For structures restricted to spherical geometries, the authors in [18, 19] developed a fully rigorous approach to construct potentials that provably yield their targeted configurations. The authors present a linear program to build potentials, but only apply their technique to produce a few, select configurations with a fixed number of particles, e.g. $N = 8$ or $N = 20$. As our approach to inverse statistical mechanics heavily leverages our work on the forward problem, we also concern ourselves with spherical, co-dimension one structures. However, we design attractive-repulsive potentials and therefore do not constrain the particles to a surface artificially. Instead, the particles assemble into a co-dimension one structure naturally. We focus our attention on proving that our closed form potentials possess prescribed instabilities. The resulting ground state then reflects these instabilities for any sufficiently large number of particles. In an approach similar to ours, the authors in [28] use a continuum formulation to rigorously construct potentials which yield a given radially symmetric particle density.

Derivation and Mathematical Analysis of the Aggregation Sheet Equation

We address both problems in the case where the patterns and collective behavior remain confined near the center of mass of the particles, and in the case where the number of particles is large. In this setting a continuum approach proves appropriate: in the limit of an infinite number of particles, the minimizers of (1.1) permit a consistent continuum description in terms of a density of particles ρ with support that lies in a bounded region of space. As the number of particles increases, the resulting ground state converges to this continuum description in the sense of probability measures. We will therefore use the continuum approximation (1.3) of (1.2) to study the minimizers of (1.5). However, to study surface-like structures we must derive an analogue of (1.3) that constrains the density of particles to a surface. We refer to the resulting equation (1.13) as the aggregation sheet equation and to its solutions as aggregation sheets.

To be precise, we consider solutions to (1.3) where the density $\rho(\mathbf{x}, t)$ has support homeomorphic to $\mathcal{S}^{d-1}$, i.e. the unit $(d-1)$ sphere. We therefore postulate that solutions will take the form

$$\rho(\mathbf{y}, t) := \int_{\mathcal{S}^{d-1}} \delta\left(\mathbf{y} - \Phi(\mathbf{x}, t)\right) f(\mathbf{x}, t) \, \mathrm{d}\mathcal{S}^{d-1}(\mathbf{x}). \tag{1.7}$$

The relation (1.7) simply denotes the fact that $\rho \in \mathcal{D}'(\mathbb{R}^d \times \mathbb{R})$ acts as a distribution on $\psi \in C_0^\infty(\mathbb{R}^d \times \mathbb{R})$ through the formula

$$\rho[\psi] = \int_{-\infty}^{\infty} \int_{\mathcal{S}^{d-1}} \psi(\Phi(\mathbf{x}, t), t) f(\mathbf{x}, t) \, \mathrm{d}\mathcal{S}^{d-1}(\mathbf{x}) \mathrm{d}t.$$

The image of the homeomorphism $\Phi(\mathbf{x}, t) : \mathcal{S}^{d-1} \to \mathbb{R}^d$ describes the dynamically evolving manifold itself, whereas the scalar function $f(\mathbf{x}, t) : \mathcal{S}^{d-1} \to \mathbb{R}$ relates to the density of particles along it. More specifically, let $\rho_\Phi(\mathbf{x}, t)$ denote the density of particles along the manifold and $\mathrm{d}\mathcal{H}_\Phi(\mathbf{x})$ denote the natural surface measure on the image of the homeomorphism. Then we define $f(\mathbf{y}, t)$ so that

$$f(\mathbf{x}, t) \mathrm{d}\mathcal{S}^{d-1}(\mathbf{x}) = \rho_\Phi(\mathbf{x}, t) \mathrm{d}\mathcal{H}_\Phi(\mathbf{x}). \tag{1.8}$$

From this relation, we can always recover the density of particles solely from the evolutions of the function $f(\mathbf{y}, t)$ and the homeomorphism $\Phi(\mathbf{x}, t)$ itself.

To derive the aggregation sheet equation, we simply impose that (1.7) defines a solution to (1.3) in the sense of distributions. By multiplying (1.3) by an arbitrary test function $\psi \in C_0^\infty(\mathbb{R}^d \times \mathbb{R})$ and integrating by parts, we find that the relation

$$\int_{-\infty}^{\infty} \int_{\mathcal{S}^{d-1}} \left(\psi_t + \langle \mathbf{u}, \nabla \psi \rangle\right) \left(\Phi(\mathbf{x}, t), t\right) f(\mathbf{x}, t) \, \mathrm{d}\mathcal{S}^{d-1}(\mathbf{x}) \mathrm{d}t \;=\; 0, \tag{1.9}$$

must hold for all such test functions. As in (1.3), we obtain the non-local velocity field $\mathbf{u}(\mathbf{y}, t)$ by convolving the interaction kernel $g(|\mathbf{y}|^2/2)\mathbf{y} = -\nabla_{\mathbf{y}} V(|\mathbf{y}|^2/2)$ with the density. After a formal application of (1.7), this yields a velocity field given by

$$\mathbf{u}(\mathbf{y}, t) \;=\; \int_{\mathcal{S}^{d-1}} g\left(\frac{1}{2}|\mathbf{y} - \Phi(\mathbf{w}, t)|^2\right) \left(\mathbf{y} - \Phi(\mathbf{w}, t)\right) f(\mathbf{w}, t) \, \mathrm{d}\mathcal{S}^{d-1}(\mathbf{w}). \tag{1.10}$$

Note that the homeomorphism $\Phi(\mathbf{x}, t)$ gives a Lagrangian parametrization of the manifold, so that each point on the manifold must move according to the velocity field at that point.

In other words,it follows that $\Phi(\mathbf{x},t)$ evolves in time according to

$$\frac{\partial \Phi}{\partial t}(\mathbf{x},t) = \mathbf{u}(\Phi(\mathbf{x},t),t) = \int_{\mathcal{S}^{d-1}} g\left(\frac{1}{2}|\Phi(\mathbf{x},t)-\Phi(\mathbf{w},t)|^2\right)(\Phi(\mathbf{x},t)-\Phi(\mathbf{w},t))\, f(\mathbf{w},t)\, \mathrm{d}\mathcal{S}^{d-1}(\mathbf{w}). \tag{1.11}$$

Substituting the relation

$$\frac{\partial}{\partial t}\{\psi(\Phi(\mathbf{x},t),t)\} = \left(\psi_t + \left\langle \frac{\partial \Phi}{\partial t}, \nabla \psi \right\rangle\right)(\Phi(\mathbf{x},t),t),$$

into (1.9) and using (1.11) then shows that $f(\mathbf{x},t)$ must satisfy

$$0 = \int_{-\infty}^{\infty}\int_{\mathcal{S}^{d-1}} \frac{\partial}{\partial t}\{\psi(\Phi(\mathbf{x},t),t)\}\, f(\mathbf{x},t)\, \mathrm{d}\mathcal{S}^{d-1}(\mathbf{x})\mathrm{d}t$$

for all test functions. An integration by parts in time then gives

$$\int_{-\infty}^{\infty}\int_{\mathcal{S}^{d-1}} \psi(\Phi(\mathbf{x},t),t)\frac{\partial f}{\partial t}(\mathbf{x},t)\, \mathrm{d}\mathcal{S}^{d-1}(\mathbf{x})\mathrm{d}t = 0.$$

As ψ is an arbitrary test function it follows that $f(\mathbf{x},t)$ must be constant in time:

$$f(\mathbf{x},t) \equiv f(\mathbf{x},0). \tag{1.12}$$

Therefore, starting with a given initial density

$$\rho(\mathbf{y},0) = \rho_0(\mathbf{y}) = \int_{\mathcal{S}^{d-1}} \delta\left(\mathbf{y}-\Phi_0(\mathbf{w})\right) f_0(\mathbf{w})\, \mathrm{d}\mathcal{S}^{d-1}(\mathbf{w}),$$

we formally obtain a distribution solution to (1.3) by evolving the homeomorphism $\Phi(\mathbf{x},t),\ \mathbf{x} \in \mathcal{S}^{d-1}$ according to the equation

$$\frac{\partial \Phi}{\partial t} = \int_{\mathcal{S}^{d-1}} g\left(\frac{1}{2}|\Phi(\mathbf{x},t)-\Phi(\mathbf{w},t)|^2\right)(\Phi(\mathbf{x},t)-\Phi(\mathbf{w},t))\, f_0(\mathbf{w})\, \mathrm{d}\mathcal{S}^{d-1}(\mathbf{w}), \tag{1.13}$$

starting from the initial condition $\Phi(\mathbf{x},0) = \Phi_0(\mathbf{x})$. We use this formulation in our analysis as opposed to (1.3) directly, since (1.13) ultimately proves more appropriate for studying particles that distribute along a manifold.

While the standard aggregation equation (4.1) has received significant attention in recent years, and a large theory has developed as a result, even the most basic well-posedness results do not yet exist for (1.13). We therefore begin the process of extending the theory for the

aggregation to cover the co-dimension one equation. The majority of the theory for the aggregation equation falls into two categories. Treatments from a classical perspective focus on densities that are absolutely continuous with respect to Lebesgue measure, usually those lying in $L^1(\mathbb{R}^d) \cap L^p(\mathbb{R}^d)$ for some $1 < p \leq \infty$. [10, 6, 7, 8, 23, 22, 28, 9]. These works have developed a rather complete local and global existence theory for such densities. For locally attractive potentials the well-known Osgood condition from ODE theory differentiates whether mass concentrates to a point in finite time or in infinite time [7, 8], and therefore provides a useful characterization of global (in L^p) existence. We extend their arguments to demonstrate the same condition differentiates local and global existence for aggregation sheets as well.

Treatments from a more modern perspective focus on more singular densities that merely define a Borel measure on $\mathbb{R}^d$, such as sums of Dirac masses [14, 51, 27, 26, 53]. In this case, ideas from optimal transport have proven fruitful for demonstrating the well-posedness of (1.3) for λ-convex interaction kernels, i.e. when $V(s) - \lambda s,\ s = |\mathbf{y}|^2/2$, is convex for some $\lambda \in \mathbb{R}$. For such potentials the aggregation equation defines a gradient flow with respect to the 2-Wasserstein metric on probability measures [14]. This observation provides a notion of solution for which global existence always holds in the class of Borel densities with finite second moment. This notion of solution provides no information regarding the temporal evolution of the support of the density, however. Moreover, λ-convexity fails for most of the potentials we consider. In this manner, the well-posedness theory we develop for aggregation sheets fills a gap in the overall theory of the aggregation equation.

The aggregation sheet equation (1.13) bears the most resemblance to similar equations that appear in the context of fluid dynamics. For instance, the classical Birkhoff-Rott equation in two dimensions formally results from taking $g(s) = -(\pi s)^{-1}$ and then rotating the resulting velocity field by $\pi/2$ to make it incompressible. In fact, the first derivation of the two-dimensional aggregation sheet equation arose from an attempt to generalize the Birkhoff-Rott equation itself [61]. This generalization includes velocity fields of mixed-type, i.e. a velocity field that contains both an incompressible component and a gradient component. This mixed-type of non-locality arises in vortex models for superfluids and superconductors

[16, 40]. The general aggregation sheet equation (1.13), then, simply extends their generalized equation to arbitrary dimensions. Although we do not consider the fully general, mixed-type case, local well-posedness for two dimensional mixed kernels does follow from our arguments as well.

In Chapter 2, we use our continuum formulation (1.13) to address the transition that motivates our study of the forward problem, i.e. the bifurcation that occurs between the uniformly distributed spherical solutions and the more complicated surfaces in figure 1.1. Specifically, we develop a non-local linear stability analysis of spherical solutions to (1.13). This analysis results in a decoupled, and therefore easy-to-analyze, sequence of symmetric eigenvalue problems. Each eigenvalue problem determines a solution to the linearized equations in terms of spherical harmonics. The eigenvalue problems allow us to detect the possible instabilities that may occur from knowledge of the potential $V(s)$ alone. These instabilities manifest in the minimizers. This chapter is based on collaborative work with David Uminsky, Theodore Kolokolnikov and Andrea Bertozzi that appears in [71]. The linear theory provides a powerful tool in addressing the forward problem, and also offers us a novel means to address the inverse problem. In Chapter 3 we provide an explicit construction that produces a potential with any finite, arbitrary set of spherical harmonic instabilities. Numerical simulations indicate that these instabilities properly manifest as the desired features in the minimizers, i.e. concentrations of particles along the unstable spherical harmonics. The material of chapter 3 follows from a collaboration with David Uminsky and appears in [70]. The final chapter develops the fully non-linear well-posedness theory for the aggregation sheet equation, and is based on joint work with Andrea Bertozzi that appears in [69].

CHAPTER 2

Stability Analysis of $\mathcal{S}^{d-1}$

This chapter studies the stability of a uniform sphere $\mathcal{S}^{d-1}$ using the continuum formulation (1.13) and a non-local linear stability analysis of the ODE system (1.2). For concreteness we first re-write the continuum formulation (1.13) using spherical coordinates on $\mathcal{S}^2$. This formulation simplifies the derivation of our main result in §2.1, i.e. that the eigenvalue problem associated to the 2-sphere of radius R reduces to a decoupled series of 2×2 scalar eigenvalue problems. Each eigenvalue problem determines a solution to the linearized equations in terms of spherical harmonics. We use this characterization to predict how instabilities perturb the density away from uniform in §§2.1.2. We complete the eigenvalue problem for arbitrary dimensions $d \geq 2$ in §2.2. Remarkably, the eigenvalue problem remains 2×2 and scalar independently of the dimension of space. Moreover, our analysis depends only on values of the potential and its derivatives on $[0, 2R^2]$. Thus, once we know the length scale of the radius our analysis applies regardless of the far-field behavior of the potential. In §2.3 we derive asymptotic expressions for the eigenvalues in theorem 2.3.1. As a first corollary we establish the linear well-posedness of uniformly distributed sphere solutions, which serves as the analogue in our context of the classic Kelvin-Helmholtz instability for vortex sheets [36, 44, 61]. In a second corollary, we consider potentials V with the form

$$-V_s(s) := g(s) = \sum_{i=1}^{\infty} c_i s^{p_i}, \tag{2.1}$$

where $p_i < p_{i+1}$ and $c_1 > 0$ to ensure an interaction kernel with repulsion in the short-range. We show that only finitely many unstable modes exist precisely when

$$\text{(i)} \quad \int_{-1}^{1} g\left(R^2(1-s)\right)(1-s^2)^{\frac{d-3}{2}}\mathrm{d}s + R^2 g_s\left(R^2(1-s)\right)(1-s^2)^{\frac{d-3}{2}} < 0 \tag{2.2}$$

$$\text{(ii)} \quad p_1 \in \left(-\frac{d-1}{2}, 0\right) \cup \bigcup_{n=0}^{\infty}(2n+1, 2n+2). \tag{2.3}$$

In this case, we can predict complex patterns in the resulting ground state from the unstable spherical harmonics. These conditions also allow us to predict the co-dimension of the ground state. We highlight these aspects of the theory in §2.4 with several examples.

To fix notation, let (ξ, η) denote coordinates on $\mathcal{S}^2$ with $-\pi \leq \xi \leq \pi$ and $0 \leq \eta \leq \pi$. If $\mathbf{X}(\xi, \eta, t)$ represents the position of the particle with label (ξ, η), the equation (1.13) dictates that the surface evolves according to

$$\mathbf{X}_t = \int_D g\left(\frac{1}{2}|\mathbf{X} - \mathbf{X}'|^2\right)(\mathbf{X} - \mathbf{X}')\, f_0(\xi', \eta')\, \mathrm{d}\xi'\mathrm{d}\eta'$$

$$\mathbf{X} = \mathbf{X}(\xi, \eta, t) \;\; \mathbf{X}' = \mathbf{X}(\xi', \eta', t) \;\; \mathbf{X}(\xi, \eta, 0) = \mathbf{X}_0(\xi, \eta). \tag{2.4}$$

This concrete formulation using coordinates proves vital in the section that follows. Moreover, although it is superfluous for determining the evolution of the surface, it will prove useful at times to re-write the distributional density in a more conventional form,

$$\rho(\mathbf{x}, t) := \int_D \delta(\mathbf{x} - \mathbf{X})\rho_S(\xi, \eta, t)|\mathbf{X}_\xi \times \mathbf{X}_\eta|(t)\, \mathrm{d}\xi\mathrm{d}\eta, \;\; \mathbf{x} \in \mathbb{R}^3.$$

The auxiliary quantity $\rho_S(\xi, \eta, t)$ then has the natural interpretation as the density of particles along the surface. Conservation of mass implies that the density evolves according to $\frac{\partial \rho_S}{\partial t} = -\rho_S \frac{|\mathbf{X}_\xi \times \mathbf{X}_\eta|_t}{|\mathbf{X}_\xi \times \mathbf{X}_\eta|}$, which when coupled to (2.4) becomes the extension to three dimensions of the corresponding equations from [61] for curves in two dimensions. In this manner, the evolution of the surface alone determines the density of particles along it; the surface $\mathbf{X}(\xi, \eta)$ is fundamental and the density is derived. For this reason, we focus our analysis on $\mathbf{X}$, and use this to determine properties of ρ_S.

2.1 Eigenvalue Problem in Three Dimensions

We now determine when a sphere of uniform density defines a linearly stable solution to (2.4). In §§2.1.1, we linearize (2.4) about a uniform sphere, and then reduce the problem to a decoupled series of scalar eigenvalue problems involving a single spherical harmonic. We proceed with the calculations in a manner that makes the appearance of spherical harmonics self-evident, as the ideas behind the calculation itself prove useful for other problems. The existence of uniform sphere solutions follows as an easy application, for instance, so we postpone it until after we derive the eigenvalue problem. In §§ 2.1.2, we use knowledge of the eigenvalue problem to linearize the density ρ_S about the uniform distribution on the sphere. This later proves useful for interpreting our stability conditions in § 2.3, and also in § 2.4 for comparing our analysis against numerics.

2.1.1 Linearization of the Surface

We begin by considering the evolution equations for a surface (2.4) for the particular instance of f_0 which yields a sphere of radius R and uniform density as steady-state,

$$\mathbf{X}_t = \int_{-\pi}^{\pi}\int_{0}^{\pi} g\left(\frac{1}{2}|\mathbf{X}-\mathbf{X}'|^2\right)(\mathbf{X}-\mathbf{X}')\sin\eta'\ \mathrm{d}\eta'\mathrm{d}\xi'. \tag{2.5}$$

Here, we parameterize a sphere of radius R as $\mathbf{X}(\xi,\eta) = \Theta_1(\xi)\Theta_2(\eta)R\mathbf{e}_1$ for $-\pi \le \xi \le \pi$ and $0 \le \eta \le \pi$. The 3×3 matrix Θ_1 represents rotation in the y-z plane, Θ_2 rotates in the x-y plane, and of course $\mathbf{e}_1 = (1,0,0)^t$.

Write a perturbation $\delta\mathbf{X}$ of the steady-state in the form

$$\delta\mathbf{X} = \Theta_1(\xi)\Theta_2(\eta)(R\mathbf{e}_1 + \epsilon(\xi,\eta)e^{\lambda t}), \tag{2.6}$$

with the goal of choosing the ansatz for $\epsilon \in \mathbb{R}^3$ in such a way that the linear equations for ϵ reduce to a scalar eigenvalue problem for λ and scalar coefficients that will determine ϵ. First, we substitute $\delta\mathbf{X}$ into (2.5) and obtain

$$\lambda\Theta_1(\xi)\Theta_2(\eta)\epsilon(\xi,\eta) = \int_{-\pi}^{\pi}\int_{0}^{\pi} g\left(\frac{1}{2}|\delta\mathbf{X}-\delta\mathbf{X}'|^2\right)(\delta\mathbf{X}-\delta\mathbf{X}')\sin\eta'\ \mathrm{d}\eta'\mathrm{d}\xi'. \tag{2.7}$$

Decomposing $\delta\mathbf{X} - \delta\mathbf{X}' := \mathbf{X}_1 + \mathbf{X}_2$, where $\mathbf{X}_1 = [\Theta_1(\xi)\Theta_2(\eta) - \Theta_1(\xi')\Theta_2(\eta')]\, R\mathbf{e}_1$ and $\mathbf{X}_2 = \Theta_1(\xi)\Theta_2(\eta)\epsilon(\xi,\eta) - \Theta_1(\xi')\Theta_2(\eta')\epsilon(\xi',\eta')$, we expand to first order in $\mathbf{X}_2$ and use the fact that the sphere is a steady-state to obtain

$$\lambda\Theta_1(\xi)\Theta_2(\eta)\epsilon(\xi,\eta) =$$
$$\int_{-\pi}^{\pi}\int_{0}^{\pi}\left\{g\left(\frac{1}{2}|\mathbf{X}_1|^2\right)\mathbf{X}_2 + g_s\left(\frac{1}{2}|\mathbf{X}_1|^2\right)(\mathbf{X}_1\cdot\mathbf{X}_2)\mathbf{X}_1\right\}\sin\eta'\,\mathrm{d}\eta'\mathrm{d}\xi'. \tag{2.8}$$

Denoting by M the matrix $M := \Theta_2^{-1}(\eta)\Theta_1(\xi'-\xi)\Theta_2(\eta')$ and by I the 3×3 identity matrix, simple calculations yield

$$\Theta_2^{-1}(\eta)\Theta_1^{-1}(\xi)\mathbf{X}_1 = (I-M)R\mathbf{e}_1,\;\; \Theta_2^{-1}(\eta)\Theta_1^{-1}(\xi)\mathbf{X}_2 = \epsilon(\xi,\eta) - M\epsilon(\xi',\eta')$$

$$\mathbf{X}_1\cdot\mathbf{X}_2 = (I-M)R\mathbf{e}_1\cdot\epsilon(\xi,\eta) + (I-M^t)R\mathbf{e}_1\cdot\epsilon(\xi',\eta'),\;\; |\mathbf{X}_1| = |(I-M)R\mathbf{e}_1|.$$

By premultiplying (2.8) with $\Theta_2^{-1}\Theta_1^{-1}$ and separating terms involving $\epsilon(\xi,\eta)$ from terms involving $\epsilon(\xi',\eta')$, we obtain the linearized problem

$$\lambda\epsilon(\xi,\eta) = \int_{-\pi}^{\pi}\int_{0}^{\pi}\left\{g\left(\frac{1}{2}|\mathbf{v}|^2\right)I + g_s\left(\frac{1}{2}|\mathbf{v}|^2\right)\mathbf{v}\otimes\mathbf{v}\right\}\epsilon(\xi,\eta)\sin\eta'\,\mathrm{d}\eta'\mathrm{d}\xi' +$$
$$\int_{-\pi}^{\pi}\int_{0}^{\pi}\left\{g_s\left(\frac{1}{2}|\mathbf{v}|^2\right)\mathbf{v}\otimes\underline{\mathbf{v}} - g\left(\frac{1}{2}|\mathbf{v}|^2\right)M\right\}\epsilon(\xi',\eta')\sin\eta'\,\mathrm{d}\eta'\mathrm{d}\xi', \tag{2.9}$$

where we define $\mathbf{v} := (I-M)R\mathbf{e}_1$ and $\underline{\mathbf{v}} := (I-M^t)R\mathbf{e}_1$.

The difficulty now lies in choosing $\epsilon(\xi,\eta)$ in such a way that the continuous eigenvalue problem (2.9) reduces to a simple scalar eigenvalue problem. To find the way forward, we recall the analogous situation in two dimensions, as detailed in [35]. In that setting, the continuous eigenvalue problem reads

$$\lambda\epsilon(s) = \int_{-\pi}^{\pi}\left\{g\left(\frac{1}{2}|\mathbf{v}|^2\right)I + g_s\left(\frac{1}{2}|\mathbf{v}|^2\right)\mathbf{v}\otimes\mathbf{v}\right\}\epsilon(s)\,\mathrm{d}s' +$$
$$\int_{-\pi}^{\pi}\left\{g_s\left(\frac{1}{2}|\mathbf{v}|^2\right)\mathbf{v}\otimes\underline{\mathbf{v}} - g\left(\frac{1}{2}|\mathbf{v}|^2\right)\Theta(s'-s)\right\}\epsilon(s')\,\mathrm{d}s'$$

where $\mathbf{v} = (I-\Theta(s'-s))R\mathbf{e}_1$, $\underline{\mathbf{v}} = (I-\Theta(s-s'))R\mathbf{e}_1$ and $\Theta(s)$ denotes a 2×2 rotation matrix. We can write this as

$$\lambda\epsilon(s) = \int_{-\pi}^{\pi}M_1(s-s')\epsilon(s)\,\mathrm{d}s' + \int_{-\pi}^{\pi}M_2(s-s')\epsilon(s')\,\mathrm{d}s', \tag{2.10}$$

for some 2×2 matrices M_i. Letting M_i^{jk} denote the (j,k) entry of the matrix M_i, we find that both matrices possess even, periodic entries in $s - s'$ whenever $j = k$, and odd, periodic entries whenever $j \neq k$. Changing variables (i.e. reparameterizing the circle) in the first integral, we have

$$\int_{-\pi}^{\pi} M_i^{jk}(s - s') \, \mathrm{d}s' = \int_{-\pi}^{\pi} M_i^{jk}(\theta) \, \mathrm{d}\theta \propto \delta_{jk}.$$

Thus, the first term on the RHS of (2.10) simplifies to a constant diagonal matrix times $\epsilon(s)$. We then substitute the known ansatz for ϵ from [35] into the second integral,

$$\epsilon(s') = (c_1 \cos(ms'), c_2 \sin(ms'))^t$$

for some constants c_1 and c_2, change variables and simplify. Along the first column of M_2, we find

$$\int_{-\pi}^{\pi} M_2^{11}(s - s') c_1 \cos(ms') \, \mathrm{d}s' = \int_{-\pi}^{\pi} M_2^{11}(\theta) c_1 \cos(m\theta + ms) \, \mathrm{d}\theta \propto \cos(ms) \tag{2.11}$$

$$\int_{-\pi}^{\pi} M_2^{21}(s - s') c_1 \cos(ms') \, \mathrm{d}s' = \int_{-\pi}^{\pi} M_2^{21}(\theta) c_2 \cos(m\theta + ms) \, \mathrm{d}\theta \propto \sin(ms) \tag{2.12}$$

due to the even-odd structure of M_2. Arguing similarly along the second column, the second term on the RHS of (2.10) simplifies as

$$\int_{-\pi}^{\pi} M_2(s - s') \epsilon(s') \, \mathrm{d}s' = D(c_1, c_2, m)(\cos(ms), \sin(ms))^t,$$

where D denotes a constant, diagonal matrix depending upon c_1, c_2 and the Fourier coefficients of the entries of M_2. Moreover, $D(c_1, c_2, m)$ is linear in the coefficients (c_1, c_2) that determine ϵ. As the first integral also results in something of this form, the continuous problem reduces to a scalar eigenvalue problem in (c_1, c_2). From (2.12), then, we deduce the essential property of the ansatz: $\int_{-\pi}^{\pi} M_2^{ij}(s - s') \epsilon_j(s') \, \mathrm{d}s' \propto \epsilon_i(s)$.

Returning now to the three-dimensional case, regardless of the choice of the ansatz $\epsilon(\xi, \eta)$, we first must show the first integral in (2.9) yields a constant, diagonal matrix. To do this, note the integrand depends only upon the vector $\mathbf{v}$. Looking at the definition of $\mathbf{v}$, for fixed (ξ, η) and for $-\pi \leq \xi' \leq \pi, 0 \leq \eta' \leq \pi$, we see that $\mathbf{v}$ simply represents a parameterization of $\partial B(R\mathbf{e}_1, R)$, i.e. the sphere of radius R centered at the point $(R, 0, 0)^t$. Moreover,

$|\mathbf{v}_{\xi'} \times \mathbf{v}_{\eta'}| = \sin\eta'$, so that by definition

$$\int_{-\pi}^{\pi}\int_{0}^{\pi} \left\{ g\left(\frac{1}{2}|\mathbf{v}|^2\right) I + g_s\left(\frac{1}{2}|\mathbf{v}|^2\right) \mathbf{v}\otimes\mathbf{v} \right\} \epsilon(\xi,\eta)\sin\eta' \, \mathrm{d}\eta'\mathrm{d}\xi' = \left(\int_{\partial B(R\mathbf{e}_1,R)} G(\mathbf{x})\mathrm{d}S(\mathbf{x}) \right) \epsilon(\xi,\eta),$$

where the 3×3 matrix valued function $G(\mathbf{x}) = g(\frac{1}{2}|\mathbf{x}|^2)I + g_s(\frac{1}{2}|\mathbf{x}|^2)\mathbf{x}\otimes\mathbf{x}$ for $\mathbf{x}\in\mathbb{R}^3$. As in the two-dimensional case, we re-parameterize $\partial B(R\mathbf{e}_1, R)$ and compute the first integral above to obtain a diagonal matrix times $\epsilon(\xi,\eta)$. Therefore, analagous to the two-dimensional case, we should choose the ansatz for $\epsilon(\xi,\eta)$ in such a way so that

$$\int_{-\pi}^{\pi}\int_{0}^{\pi} M_2^{ij}(\xi,\xi',\eta,\eta')\epsilon_j(\xi',\eta')\sin\eta' \, \mathrm{d}\eta'\mathrm{d}\xi' \propto \epsilon_i(\xi,\eta).$$

Let us now turn to this task. To simplify the notation, let $\mathbf{x} := \mathbf{X}(\xi,\eta)$ and $\mathbf{w} := \mathbf{X}(\xi',\eta')$ with $\mathbf{X}(\xi,\eta)$ denoting our parameterization of the sphere. Consider the quantity $\mathbf{x}\cdot\mathbf{w} := \mathbf{X}(\xi,\eta)\cdot\mathbf{X}(\xi',\eta')$. As $\mathbf{v} = (I-M)R\mathbf{e}_1$ and $\underline{\mathbf{v}} = (I-M^t)R\mathbf{e}_1$, straightforward calculations yield

$$\mathbf{v} = R\left(1-\mathbf{x}\cdot\mathbf{w}, -(\mathbf{x}\cdot\mathbf{w})_\eta, -\frac{(\mathbf{x}\cdot\mathbf{w})_\xi}{\sin(\eta)}\right)^t \quad |\mathbf{v}|^2 = 2R^2(1-\mathbf{x}\cdot\mathbf{w}) \tag{2.13}$$

$$\underline{\mathbf{v}} = R\left(1-\mathbf{x}\cdot\mathbf{w}, -(\mathbf{x}\cdot\mathbf{w})_{\eta'}, -\frac{(\mathbf{x}\cdot\mathbf{w})_{\xi'}}{\sin(\eta')}\right)^t. \tag{2.14}$$

We now make the key observation that M_2^{11} depends only upon the quantity $\mathbf{x}\cdot\mathbf{w}$, in that $M_2^{11}(\xi,\xi',\eta,\eta') = g_1(\mathbf{x}\cdot\mathbf{w})$ for $g_1(s) = R^2 g_s(R^2(1-s))(1-s)^2 - g(R^2(1-s))s$. For such functions, we shall make repeated use the following (c.f. [57]):

Theorem 2.1.1. *(Funk-Hecke Theorem in 3D) Let $f(s)\in L^1([-1,1])$. Then for any spherical harmonic $S^l(\mathbf{x})$ of degree l and $\mathbf{x}\in\mathcal{S}^2$,*

$$\lambda S^l(\mathbf{x}) = \int_{\mathcal{S}^2} f(\mathbf{x}\cdot\mathbf{w}) S^l(\mathbf{w}) \, \mathrm{d}\mathcal{S}_{\mathbf{w}}. \tag{2.15}$$

The eigenvalue λ depends only on the function f and the degree l of the harmonic, where we will now write $\lambda = \lambda_l(f)$ to make explicit the dependencies of the eigenvalues on the functions involved. More specifically,

$$\lambda_l(f) = 2\pi\int_{-1}^{1} f(s)P_l(s) \, \mathrm{d}s, \tag{2.16}$$

where $P_l(s)$ denotes the Legendre polynomial of degree l, normalized to $P_l(1) = 1$. In three dimensions, equation (2.15) plays the role that equation (2.12) serves in two dimensions.

Together with our observation regarding M_2^{11}, this theorem suggests we choose ansatz with $\epsilon_1(\xi, \eta) = c_1 S^l(\mathbf{x}(\xi, \eta))$ for some coefficient $c_1 \in \mathbb{R}$. Indeed, then

$$\int_{-\pi}^{\pi}\int_{0}^{\pi} M_2^{11}(\xi, \xi', \eta, \eta')\epsilon_1(\xi', \eta') \sin\eta' \, \mathrm{d}\eta' \mathrm{d}\xi' = c_1 \int_{\mathcal{S}^2} g_1(\mathbf{x}\cdot\mathbf{w}) S^l(\mathbf{w}) \, \mathrm{d}\mathcal{S}_{\mathbf{w}}$$

so that by a straightforward application of the Funk-Hecke (F-H) theorem,

$$\int_{-\pi}^{\pi}\int_{0}^{\pi} M_2^{11}(\xi, \xi', \eta, \eta')\epsilon_1(\xi', \eta') \sin\eta' \, \mathrm{d}\eta' \mathrm{d}\xi' = \lambda_l(g_1) c_1 S^l(\mathbf{x}) \propto \epsilon_1$$

as desired. With ϵ_1 now in hand, we can use the requirement that

$$\int_{-\pi}^{\pi}\int_{0}^{\pi} M_2^{i1}(\xi, \xi', \eta, \eta')\epsilon_1(\xi', \eta') \sin\eta' \, \mathrm{d}\eta' \mathrm{d}\xi' \propto \epsilon_i(\xi, \eta) \tag{2.17}$$

to determine the remainder of the ansatz. For this, we observe that the relations (2.13) and (2.14) imply

$$M_2^{21} = \left(g\left(\frac{1}{2}|\mathbf{v}|^2\right)(1 - \mathbf{x}\cdot\mathbf{w})\right)_\eta \quad M_2^{31} = \frac{1}{\sin(\eta)}\left(g\left(\frac{1}{2}|\mathbf{v}|^2\right)(1 - \mathbf{x}\cdot\mathbf{w})\right)_\xi .$$

Using this with the known choice of ϵ_1, we find the relation (2.17) for $i = 2$ becomes

$$\epsilon_2(\xi, \eta) \propto \int_{\mathcal{S}^2} \left(g\left(\frac{1}{2}|\mathbf{v}|^2\right)(1 - \mathbf{x}\cdot\mathbf{w})\right)_\eta c_1 S^l(\mathbf{w}) \, \mathrm{d}\mathcal{S}_{\mathbf{w}} = c_1 \left(\int_{\mathcal{S}^2} g_2(\mathbf{x}\cdot\mathbf{w}) S^l \, \mathrm{d}\mathcal{S}_{\mathbf{w}} \right)_\eta ,$$

where $g_2(s) = g(R^2(1 - s))(1 - s)$, by passing the derivative through the integral in the primed variables. Again using the F-H theorem, we recover $\epsilon_2(\xi, \eta) \propto c_1\lambda_l(g_2) S^l_\eta$. Arguing similarly from (2.17) with $i = 3$ yields $\epsilon_3(\xi, \eta) \propto \frac{c_1\lambda_l(g_2)}{\sin(\eta)} S^l_\xi$. All together, we recover

$$\epsilon(\xi, \eta) = \left(c_1 S^l(\mathbf{x}), c_2 (S^l(\mathbf{x}))_\eta, c_3 \frac{(S^l(\mathbf{x}))_\xi}{\sin(\eta)} \right)^t \tag{2.18}$$

for real coefficients c_i.

Proceeding as in the two-dimensional case, it remains to show that this choice of $\epsilon(\xi, \eta)$ yields

$$\int_{-\pi}^{\pi}\int_{0}^{\pi} M_2(\cdot)\epsilon(\xi', \eta') \sin\eta' \, \mathrm{d}\eta' \mathrm{d}\xi' = D(c_1, c_2, c_3, l) \left(S^l, S^l_\eta, \frac{S^l_\xi}{\sin(\eta)} \right)^t ,$$

where $D(c_1, c_2, c_3, l)$ is a constant, diagonal matrix that is linear in the coefficients. The derivation of the ansatz has demonstrated this claim for the first column of M_2. Continuing with the remainder first row of M_2, in light of (2.13) and (2.14) we see

$$M_2^{12} = \left(g\left(\frac{1}{2}|\mathbf{v}|^2\right)(1 - \mathbf{x}\cdot\mathbf{w})\right)_{\eta'} M_2^{13} = \frac{1}{\sin(\eta')}\left(g\left(\frac{1}{2}|\mathbf{v}|^2\right)(1 - \mathbf{x}\cdot\mathbf{w})\right)_{\xi'}.$$

In setting $c_2 = c_3$, we compute that

$$\int_{-\pi}^{\pi}\int_{0}^{\pi}(M_2^{12}\epsilon_2 + M_2^{13}\epsilon_3)\sin\eta'\ \mathrm{d}\eta'\mathrm{d}\xi' = \\ c_2\int_{-\pi}^{\pi}\int_{0}^{\pi}(g_2(\mathbf{x}\cdot\mathbf{w}))_{\eta'}S^l(\mathbf{w})_{\eta'}\sin\eta'\ \mathrm{d}\eta'\mathrm{d}\xi' + \\ c_2\int_{-\pi}^{\pi}\int_{0}^{\pi}\frac{(g_2(\mathbf{x}\cdot\mathbf{w}))_{\xi'}S^l_{\xi'}}{\sin(\eta')^2}\sin\eta'\ \mathrm{d}\eta'\mathrm{d}\xi'.$$

Integrating by parts in η' in the first term and in ξ' in the second term, we have

$$\int_{-\pi}^{\pi}\int_{0}^{\pi}(M_2^{12}\epsilon_2 + M_2^{13}\epsilon_3)\sin\eta'\ \mathrm{d}\eta'\mathrm{d}\xi' = -c_2\int_{-\pi}^{\pi}\int_{0}^{\pi}(\Delta_{\mathcal{S}^2}S^l)g_2(\mathbf{x}\cdot\mathbf{w})\sin\eta'\ \mathrm{d}\eta'\mathrm{d}\xi'.$$

Using that $\Delta_{\mathcal{S}^2}S^l = -l(l+1)S^l$ and the F-H theorem, we obtain

$$\int_{-\pi}^{\pi}\int_{0}^{\pi}(M_2^{12}\epsilon_2 + M_2^{13}\epsilon_3)\sin\eta'\ \mathrm{d}\eta'\mathrm{d}\xi' = c_2 l(l+1)\lambda_l(g_2)S^l(\mathbf{x}) \propto \epsilon_1$$

as desired. Proceeding similarly with the remainder of the second row of M_2, the facts

$$M_2^{22} = -(g(|\mathbf{v}|^2/2))_{\eta'}(\mathbf{x}\cdot\mathbf{w})_{\eta} - g(|\mathbf{v}|^2/2)(\mathbf{x}\cdot\mathbf{w})_{\eta\eta'}\ , \\ M_2^{23} = \frac{-(g(\frac{1}{2}|\mathbf{v}|^2))_{\xi'}(\mathbf{x}\cdot\mathbf{w})_{\eta} - g(\frac{1}{2}|\mathbf{v}|^2)(\mathbf{x}\cdot\mathbf{w})_{\eta\xi'}}{\sin(\eta')}$$

and a similar integration by parts combine to give

$$\int_{-\pi}^{\pi}\int_{0}^{\pi}(M_2^{22}\epsilon_2 + M_2^{23}\epsilon_3)\sin\eta'\ \mathrm{d}\eta'\mathrm{d}\xi' = c_2\int_{-\pi}^{\pi}\int_{0}^{\pi} g\left(\frac{1}{2}|\mathbf{v}|^2\right)(\mathbf{x}\cdot\mathbf{w})_{\eta}(\Delta_{\mathcal{S}^2}S^l)\mathrm{d}\mathcal{S}_2 = \\ -c_2 l(l+1)\int_{-\pi}^{\pi}\int_{0}^{\pi} g\left(\frac{1}{2}|\mathbf{v}|^2\right)(\mathbf{x}\cdot\mathbf{w})_{\eta}S^l(\mathbf{w})\sin\eta'\ \mathrm{d}\eta'\mathrm{d}\xi'.$$

Letting $g_3(s) = \int_0^{R^2(1-s)} g(z)\ \mathrm{d}z$, so that $g_3(\mathbf{x}\cdot\mathbf{w})_{\eta} = -R^2 g(\frac{1}{2}|\mathbf{v}|^2)(\mathbf{x}\cdot\mathbf{w})_{\eta}$, we pass the derivative through the integral and use the F-H theorem as before to arrive at

$$\int_{-\pi}^{\pi}\int_{0}^{\pi}(M_2^{22}\epsilon_2 + M_2^{23}\epsilon_3)\sin\eta'\ \mathrm{d}\eta'\mathrm{d}\xi' = \frac{c_2 l(l+1)\lambda_l(g_3)}{R^2}S^l_{\eta} \propto \epsilon_2.$$

Finally, the same argument on the remainder of the last row of M_2 gives

$$\int_{-\pi}^{\pi}\int_{0}^{\pi}(M_2^{32}\epsilon_2 + M_2^{33}\epsilon_3)\sin\eta'\,\mathrm{d}\eta'\mathrm{d}\xi' = \frac{c_2 l(l+1)\lambda_l(g_3)}{R^2\sin(\eta)}S_\xi^l \propto \epsilon_3.$$

Combining all of the above, we find

$$\int_{-\pi}^{\pi}\int_{0}^{\pi}M_2(\xi,\xi',\eta,\eta')\epsilon(\xi',\eta')\sin\eta'\,\mathrm{d}\eta'\mathrm{d}\xi' = \left(D^{11}S^l, D^{22}S_\eta^l, D^{33}\frac{S_\xi^l}{\sin(\eta)}\right)^t,$$

$$D^{11} = c_1\lambda_l(g_1) + c_2 l(l+1)\lambda_l(g_2) \quad D^{22} = D^{33} = c_1\lambda_l(g_2) + c_2\frac{l(l+1)}{R^2}\lambda_l(g_3),$$

so that D is linear in the coefficients as desired. Consequently, with this ansatz the linearized equations (2.9) become

$$\lambda\epsilon(\xi,\eta) = \left(\int_{\partial B(R\mathbf{e}_1,R)} G(\mathbf{x})\mathrm{d}S(\mathbf{x})\right)\epsilon(\xi,\eta) + D(c_1,c_2,l)\epsilon(\xi,\eta). \tag{2.19}$$

By symmetry, we see

$$\left(\int_{\partial B(R\mathbf{e}_1,R)} G(\mathbf{x})\mathrm{d}S(\mathbf{x})\right) = \mathrm{diag}(\alpha,\beta,\beta),$$

so that the second and third equations in (2.19) are identical. Consequently, solving the continuous linearized equations reduces to the 2×2 scalar eigenvalue problem determined by (2.19): $\lambda c_1 = \alpha c_1 + D^{11}(c_1,c_2,l)$ and $\lambda c_2 = \beta c_2 + D^{22}(c_1,c_2,l)$, just as in the two-dimensional case.

We can make one final simplification to the eigenvalue problem that comes from the steady-state equation for the sphere,

$$0 = \int_{\mathcal{S}^2} g\left(\frac{R^2}{2}|\mathbf{x}-\mathbf{w}|^2\right)(\mathbf{x}-\mathbf{w})\,\mathrm{d}\mathcal{S}_{\mathbf{w}}. \tag{2.20}$$

In particular, the sphere radius R satisfies (see Remark 2.1.2 below)

$$0 = \int_{\mathcal{S}^2} g(R^2(1-\mathbf{x}\cdot\mathbf{w}))(1-\mathbf{x}\cdot\mathbf{w})\,\mathrm{d}S_y \Leftrightarrow 0 = \int_{-1}^{1} g_2(s)\mathrm{d}s \tag{2.21}$$

by the F-H theorem with $l=0$. A simple calculation then gives $\beta = 0$.

To summarize the previous calculations, the decoupled sequence of eigenvalue problems

$$\lambda\begin{pmatrix}c_1\\c_2\end{pmatrix} = \begin{pmatrix}\alpha+\lambda_l(g_1) & l(l+1)\lambda_l(g_2)\\ \lambda_l(g_2) & \frac{l(l+1)}{R^2}\lambda_l(g_3)\end{pmatrix}\begin{pmatrix}c_1\\c_2\end{pmatrix} := \Omega_l\begin{pmatrix}c_1\\c_2\end{pmatrix} \tag{2.22}$$

determine the linear stability of the uniform sphere. To compute the entries of Ω_l, we recall that for a function $h \in L^1([-1,1])$ and $l \in \mathbb{N}$ we define $\lambda_l(h) = 2\pi \int_{-1}^{1} h(s)P_l(s)\mathrm{d}s$, with $P_l(s)$ denoting the Legendre polynomial of degree l normalized to $P_l(1) = 1$. The radius R of the sphere satisfies $0 = \int_{-1}^{1} g(R^2(1-s))(1-s)\mathrm{d}s$ and the coefficient $\alpha = 8\pi g(2R^2) + 2\pi \int_{-1}^{1} g(R^2(1-s))\mathrm{d}s$. Finally, we recall the definitions

$$\begin{aligned} g_1(s) &= R^2 g_s(R^2(1-s))(1-s)^2 - g(R^2(1-s))s, \\ g_2(s) &= g(R^2(1-s))(1-s), \quad (g_3)_s(s) = -R^2 g(R^2(1-s)). \end{aligned} \tag{2.23}$$

Remark 2.1.2. *For sufficiently smooth attractive-repulsive interaction kernels g, a uniform density, steady-state sphere solution to equation* (2.5) *exists if and only if $-\infty \leq \int_0^\infty sg(s)\ \mathrm{d}s < 0$. Indeed, projecting the equation of steady-state* (2.20) *onto the component normal to the sphere yields*

$$0 = \int_{\mathcal{S}^2} g(R^2(1-\mathbf{x}\cdot\mathbf{w}))(1-\mathbf{x}\cdot\mathbf{w})\ \mathrm{d}S_y \Leftrightarrow 0 = \int_{-1}^{1} g_2(s)\mathrm{d}s \tag{2.24}$$

by the F-H theorem with $l = 0$. Since $g > 0$ near zero, for R sufficiently small the integral on the RHS of (2.24) *is positive. Similarly, since $g < 0$ away from the origin, for R large enough the integral on the RHS decreases as $R \to \infty$. Thus when $\int_0^\infty sg(s)\ \mathrm{d}s < 0$ the RHS of* (2.24) *is negative for all sufficiently large radii. Therefore there exists an R which identically satisfies* (2.24)*. That the projection onto the tangential components satisfies* (2.20) *follows in a manner similar to the derivation of the tangential components of the ansatz. This applies regardless of the stability of the sphere, and regardless of whether the potential exhibits confinement.*

Remark 2.1.3. *In concordance with a local notion like linear stability, all equations only involve values of the potential V and its derivatives for values of $s \in [0, 2R^2]$. In particular, once we know the radius R of the sphere, we can assign arbitrary far-field behavior to the potential without affecting the validity or applicability of our analysis.*

2.1.2 Linearization of the Density

By solving the eigenvalue problem (2.22), our work in the previous section allows us to construct approximate solutions to the surface equations (2.4) with $f_0(\xi,\eta) = \sin(\eta)$, which correspond to small perturbations of the spherical solution. As we mentioned in §2, knowledge of the surface allows us to reconstruct the density of particles via $\rho_S(\xi,\eta,t)|\mathbf{X}_\xi \times \mathbf{X}_\eta|(t) = f_0(\xi,\eta)$. Therefore, a perturbation away from a sphere naturally induces a perturbation of the density away from uniform as well. Indeed, if we write our perturbation of the sphere as $u(\mathbf{x},t) = \Theta_1(\xi)\Theta_2(\eta)(R\mathbf{e}_1 + \epsilon(\mathbf{x})e^{\lambda t})$ for $\mathbf{x}(\xi,\eta) \in \mathcal{S}^2$ and $\epsilon(\mathbf{x})$ as in equation (2.18), we can linearize $\rho_S = \frac{\sin(\eta)}{|u_\xi \times u_\eta|}$ to find the leading order corrections to the density.

To this end, define $\mathcal{B}(\xi,\eta) := \Theta_1(\xi)\Theta_2(\eta)$. We can then compute $|u_\xi \times u_\eta|$ by using Lagrange's identity:

$$|u_\xi \times u_\eta|^2 = (u_\xi \cdot u_\xi)(u_\eta \cdot u_\eta) - (u_\xi \cdot u_\eta)^2.$$

Computing this directly, we find

$$\begin{aligned}
|u_\xi|^2 &= |\mathcal{B}_\xi R\mathbf{e}_1|^2 + 2R\mathcal{B}_\xi\mathbf{e}_1 \cdot \left(\mathcal{B}_\xi\epsilon(\mathbf{x}) + \mathcal{B}\epsilon(\mathbf{x})_\xi\right) e^{\lambda t} + \mathcal{O}(\epsilon^2) \\
|u_\eta|^2 &= |\mathcal{B}_\eta R\mathbf{e}_1|^2 + 2R\mathcal{B}_\eta\mathbf{e}_1 \cdot \left(\mathcal{B}_\eta\epsilon(\mathbf{x}) + \mathcal{B}\epsilon(\mathbf{x})_\eta\right) e^{\lambda t} + \mathcal{O}(\epsilon^2)
\end{aligned}$$

$$u_\xi \cdot u_\eta = R^2(\mathcal{B}_\eta^t\mathcal{B}_\xi)^{11} + \mathcal{O}(\epsilon). \tag{2.25}$$

Straightforward calculations yield the required derivatives of $\mathcal{B}$:

$$\mathcal{B}_\xi^t\mathcal{B}_\xi = \begin{pmatrix} \sin^2(\eta) & \sin(\eta)\cos(\eta) & 0 \\ \sin(\eta)\cos(\eta) & \cos^2(\eta) & 0 \\ 0 & 0 & 1 \end{pmatrix} \quad \mathcal{B}^t\mathcal{B}_\xi = \begin{pmatrix} 0 & 0 & -\sin(\eta) \\ 0 & 0 & -\cos(\eta) \\ \sin(\eta) & \cos(\eta) & 0 \end{pmatrix}$$

$$\mathcal{B}_\eta^t\mathcal{B}_\eta = \begin{pmatrix} 1 & 0 & 0 \\ 0 & 1 & 0 \\ 0 & 0 & 0 \end{pmatrix} \quad \mathcal{B}^t\mathcal{B}_\eta = \begin{pmatrix} 0 & -1 & 0 \\ 1 & 0 & 0 \\ 0 & 0 & 0 \end{pmatrix} \quad \mathcal{B}_\eta^t\mathcal{B}_\xi = \begin{pmatrix} 0 & 0 & -\cos(\eta) \\ 0 & 0 & \sin(\eta) \\ 0 & 0 & 0 \end{pmatrix}. \tag{2.26}$$

Using the relations (2.25) and (2.26) and the definition of the ansatz (2.18), we obtain

$$|u_\xi|^2 = \sin^2(\eta)\left\{R^2 + 2Rc_1e^{\lambda t}S^l + 2Rc_2e^{\lambda t}(\cot(\eta)S_\eta^l + \frac{S_{\xi\xi}^l}{\sin^2(\eta)})\right\} + \mathcal{O}(\epsilon^2)$$

$$|u_\eta|^2 = R^2 + 2Re^{\lambda t}\left\{c_1 S^l + c_2 S^l_{\eta\eta}\right\} + \mathcal{O}(\epsilon^2), (u_\xi \cdot u_\eta)^2 = \mathcal{O}(\epsilon^2).$$

Therefore, $|u_\xi \times u_\eta|^2 = \sin^2(\eta)\left\{R^4 + 4c_1 e^{\lambda t} R^3 S^l + 2c_2 e^{\lambda t} R^3 (\Delta_{\mathcal{S}^2} S^l)\right\} + \mathcal{O}(\epsilon^2)$, so that to leading order the perturbed density ρ_S obeys

$$\rho_S = \frac{1}{R^2}\left\{1 - \frac{e^{\lambda t}}{R}(2c_1 - c_2 l(l+1))S^l(\mathbf{x})\right\} + \mathcal{O}(\epsilon^2). \tag{2.27}$$

Additionally, we can determine the principal correction to the radius of the surface,

$$|u(\mathbf{x},t)| = \sqrt{R^2 + 2c_1 e^{\lambda t} R S^l(\mathbf{x}) + \mathcal{O}(\epsilon^2)} = R\left(1 + \frac{c_1 e^{\lambda t}}{R} S^l(\mathbf{x})\right) + \mathcal{O}(\epsilon^2). \tag{2.28}$$

We may therefore view the modes determined by the eigenvalue problems (2.22) as spheres of variable radius $R + c_1 e^{\lambda t} S^l(\mathbf{x})$, with the non-uniform particle density determined from (2.27).

2.2 Eigenvalue Problem in Arbitrary Dimensions

In this section, we extend our analysis of the linearization of the surface equation and the reduction to a scalar eigenvalue problem to an arbitrary $(d-1)$-sphere. Although the notation is more cumbersome, the argument proceeds exactly as in the three-dimensional case. Additionally, due to the tangential isotropy of the sphere, *the matrix associated to the eigenvalue problem remains* 2×2*, regardless of dimension.*

In the d–dimensional setting, the analogue of (2.5) becomes

$$\mathbf{X}_t(\eta_1, \ldots, \eta_{d-1}, t) = \int_{\mathcal{S}^{d-1}} g\left(\frac{1}{2}|\mathbf{X} - \mathbf{X}'|^2\right)(\mathbf{X} - \mathbf{X}')\, \mathrm{d}\mathcal{S}_{d-1} \tag{2.29}$$

$$\mathbf{X} = \mathbf{X}(\eta_1, \ldots, \eta_{d-1}, t) \in \mathbb{R}^d \quad \mathbf{X}' = \mathbf{X}(\eta_1', \ldots, \eta_{d-1}', t) \in \mathbb{R}^d,$$

so that a uniformly distributed steady-state sphere of radius R satisfies

$$0 = \int_{\mathcal{S}^{d-1}} g\left(\frac{R^2}{2}|\mathbf{x} - \mathbf{w}|^2\right)(\mathbf{x} - \mathbf{w})\, \mathrm{d}\mathcal{S}_{\mathbf{w}} \quad \forall \mathbf{x} \in \mathcal{S}^{d-1}.$$

We write the sphere of radius R in dimension d as $R\mathbf{x}$ for $\mathbf{x} \in \mathcal{S}^{d-1}$, and write a perturbation in the form $\delta\mathbf{x} = R\mathbf{x} + \mathcal{B}(\mathbf{x})\epsilon(\mathbf{x})e^{\lambda t}$. The matrix $\mathcal{B}$ plays the role of $\Theta_1(\xi)\Theta_2(\eta)$ from the

three dimensional calculation, i.e. a product of rotation matrices. We define the rows $\mathbf{b}_j$ of $\mathcal{B}(\mathbf{x})$ as follows: we take $\mathbf{b}_1 = \mathbf{x}$; next, define $\hat{\mathbf{b}}_j(\mathbf{x}) = \partial_{\eta_j}(\mathbf{x})$, where η_j denote any of the coordinates on $\mathcal{S}^{d-1}$; lastly, normalize $\mathbf{b}_j(\mathbf{x}) = \frac{\hat{\mathbf{b}}_j(\mathbf{x})}{|\hat{\mathbf{b}}_j(\mathbf{x})|}$. Then $\mathcal{B}^t\mathcal{B}(\mathbf{x}) = I$ for all $\mathbf{x} \in \mathcal{S}^{d-1}$. As for the ansatz, put $\epsilon_1(\mathbf{x}) = c_1 S^l(\mathbf{x})$ as before, and $\epsilon_{j+1}(\mathbf{x}) = c_2 \partial_{\eta_j}(S^l(\mathbf{x}))/|\hat{\mathbf{b}}_j(\mathbf{x})|$ for $1 \leq j \leq d-1$.

If we now expand to first order in ϵ and use the fact that the sphere is a steady-state, we obtain the continuous eigenvalue problem

$$\lambda\epsilon(\mathbf{x}) = \int_{\mathcal{S}^{d-1}} \left\{ g\left(\frac{1}{2}|\mathbf{v}|^2\right) I + g_s\left(\frac{1}{2}|\mathbf{v}|^2\right) \mathbf{v}\otimes\mathbf{v} \right\} \epsilon(\mathbf{x})\, \mathrm{d}\mathcal{S}_{\mathbf{w}} + \int_{\mathcal{S}^{d-1}} \left\{ g_s\left(\frac{1}{2}|\mathbf{v}|^2\right) \mathbf{v}\otimes\underline{\underline{\mathbf{v}}} - g\left(\frac{1}{2}|\mathbf{v}|^2\right) \mathcal{B}^t(\mathbf{x})\mathcal{B}(\mathbf{w}) \right\} \epsilon(\mathbf{w})\, \mathrm{d}\mathcal{S}_{\mathbf{w}}, \tag{2.30}$$

where $\mathbf{v} = R(\mathbf{e}_1 - \mathcal{B}^t(\mathbf{x})\mathbf{w})$ and $\underline{\underline{\mathbf{v}}} = R(\mathbf{e}_1 - \mathcal{B}^t(\mathbf{w})\mathbf{x})$. This generalizes (2.9) to any dimension. As in three dimensions, the reduction to a scalar eigenvalue problem follows from two claims. If we let M_1 denote the matrix in the first term of (2.30), we first claim that M_1 is diagonal of the form $M_1 = \mathrm{diag}(\alpha, 0, \cdots, 0)$ and independent of $\mathbf{x}$. Second, we claim that

$$\int_{\mathcal{S}^{d-1}} M_2(\mathbf{x},\mathbf{w})\epsilon(\mathbf{w})\, \mathrm{d}\mathcal{S}_{\mathbf{w}} = \left(D^{11}S^l, D^{22}\frac{S^l_{\eta_1}}{|\hat{\mathbf{b}}_1|}, \ldots, D^{22}\frac{S^l_{\eta_{d-1}}}{|\hat{\mathbf{b}}_{d-1}|} \right),$$

where M_2 denotes the matrix in the second term of (2.30), and $D^{ii} = D^{ii}(c_1, c_2, l)$ are linear in the coefficients. Combining this with the first claim again reduces (2.30) to the scalar eigenvalue problem

$$\lambda \begin{pmatrix} c_1 \\ c_2 \end{pmatrix} = \begin{pmatrix} \alpha c_1 + D^{11}(c_1, c_2, l) \\ D^{22}(c_1, c_2, l) \end{pmatrix}.$$

To establish the claims, we once again have as our main tool ([57]):

Theorem 2.2.1. *(Funk-Hecke Theorem in d-dimensions) Let $f(s)(1-s^2)^{\frac{d-3}{2}} \in L^1([-1,1])$. Then for any spherical harmonic of degree l and $\mathbf{x} \in \mathcal{S}^{d-1}$,*

$$\lambda S^l(\mathbf{x}) = \int_{\mathcal{S}^{d-1}} f(\mathbf{x}\cdot\mathbf{w}) S^l(\mathbf{w})\, \mathrm{d}\mathcal{S}_{\mathbf{w}}.$$

Again, the eigenvalue $\lambda = \lambda_l(f)$ depends only on the function f and the degree l of the harmonic, in that

$$\lambda_l(f) = \mathrm{vol}(\mathcal{S}^{d-2}) \int_{-1}^{1} f(s) P_{l,d}(s)(1-s^2)^{\frac{d-3}{2}}\, \mathrm{d}s,$$

where $\mathrm{vol}(\mathcal{S}^{d-2})$ denotes the surface area of the $d-2$ sphere. Also, $P_{l,d}(s)$ denotes the Gegenbauer polynomial $P_l^{(d/2-1)}(s)$ from [62], normalized so that $P_l(1)=1$. For $d=3$, these coincide the Legendre polynomials, whereas for $d=2$ we have $P_l(\cos(\eta))=\cos(l\eta)$. Under this change of variable, for $d=2$, we recover precisely the eigenvalue problem from [35]. We shall also need the following elementary lemma. For the proof, we denote by $\mathbf{w}(\eta_1,\dots,\eta_{d-1})$ a parameterization of $\mathcal{S}^{d-1}$ such that $\mathbf{w}=(\cos\eta_1,\sin\eta_1\tilde{\mathbf{w}})$ and $\tilde{\mathbf{w}}(\eta_2,\dots,\eta_{d-1})$ parametrizes $\mathcal{S}^{d-2}$. We also use Einstein notation for terms involving partial derivatives.

Lemma 2.2.2. *Let $f(\eta_1,\dots,\eta_{d-1})\in C^2$ with $(\eta_1,\dots,\eta_{d-1})$ denoting coordinates on $\mathcal{S}^{d-1}$ as above. Then $\partial_{\eta_j}\left(f_{\eta_j}\frac{\mathrm{d}\mathcal{S}_{\mathbf{w}}}{|\mathbf{w}_{\eta_j}|^2}\right)=\Delta_{\mathcal{S}^{d-1}}(f)\mathrm{d}\mathcal{S}_{\mathbf{w}}$.*

Proof. We induct on the dimension d. When $d=2$ this reads

$$\partial_\eta f_\eta \mathrm{d}\eta=\Delta_{\mathcal{S}^1}(f)\mathrm{d}\eta$$

so there is nothing to prove. Let us now write $\mathrm{d}\mathcal{S}_{\mathbf{w}}=\sin^{d-2}(\eta_1)\mathrm{d}\mathcal{S}^{d-2}$, where $\mathrm{d}\mathcal{S}^{d-2}$ depends only on $\eta_2,\dots,\eta_{d-1}$. As $|\mathbf{w}_{\eta_1}|=1$ and $|\mathbf{w}_{\eta_j}|=\sin\eta_1|\tilde{\mathbf{w}}_{\eta_j}|$ for $j>1$ we compute

$$\partial_{\eta_j}\left(f_{\eta_j}\frac{\mathrm{d}\mathcal{S}_{\mathbf{w}}}{|\mathbf{w}_{\eta_j}|^2}\right)=\partial_{\eta_1}\left(f_{\eta_1}\sin^{d-2}\eta_1\right)\mathrm{d}\mathcal{S}^{d-2}+\frac{\sin^{d-2}\eta_1}{\sin^2\eta_1}\partial_{\eta_j}\left(f_{\eta_j}\frac{\mathrm{d}\mathcal{S}^{d-2}}{|\tilde{\mathbf{w}}_{\eta_j}|^2}\right).$$

By the inductive hypothesis, it then follows that

$$\partial_{\eta_j}\left(f_{\eta_j}\frac{\mathrm{d}\mathcal{S}_{\mathbf{w}}}{|\mathbf{w}_{\eta_j}|^2}\right)=\partial_{\eta_1}\left(f_{\eta_1}\sin^{d-2}\eta_1\right)\mathrm{d}\mathcal{S}^{d-2}+\frac{\sin^{d-2}\Delta_{\mathcal{S}^{d-2}}(f)\mathrm{d}\mathcal{S}^{d-2}}{\sin^2\eta_1}.$$

However, $\mathrm{d}\mathcal{S}^{d-2}=\mathrm{d}\mathcal{S}_{\mathbf{w}}\sin^{2-d}\eta_1$ so that we obtain

$$\partial_{\eta_j}\left(f_{\eta_j}\frac{\mathrm{d}\mathcal{S}_{\mathbf{w}}}{|\mathbf{w}_{\eta_j}|^2}\right)=\left(\sin^{2-d}\eta_1\partial_{\eta_1}\left(f_{\eta_1}\sin^{d-2}\eta_1\right)+\frac{1}{\sin^2\eta_1}\Delta_{\mathcal{S}^{d-2}}(f)\right)\mathrm{d}\mathcal{S}_{\mathbf{w}}.$$

We recognize the expression in parentheses as $\Delta_{\mathcal{S}^{d-1}}(f)$. □

Claim 2.2.1. *In (2.30), $M_1=\mathrm{diag}(\alpha,0,\cdots,0)$ for some $\alpha\in\mathbb{R}$.*

By the orthogonality of $\mathcal{B}$ we recognize the vector $\underline{\underline{\mathbf{v}}}$ as a parameterization of $\partial B(R\mathbf{e}_1,R)$ in $\mathbb{R}^d$. Thus, the first term in (2.30) amounts to multiplying $\epsilon(\mathbf{x})$ by constant matrix

$$M_1=\int_{\partial B(R\mathbf{e}_1,R)}g\left(\frac{1}{2}|\mathbf{x}|^2\right)I+g_s\left(\frac{1}{2}|\mathbf{x}|^2\right)(\mathbf{x}\otimes\mathbf{x})\,\mathrm{d}\mathcal{S}_{\mathbf{x}}.$$

Parametrize $\partial B(R\mathbf{e}_1, R)$ by $\mathbf{x} = R(\mathbf{e}_1 - \mathbf{w})$, where $\mathbf{w} = (\cos(\eta_1), \sin(\eta_1)\tilde{\mathbf{w}})$ and $\tilde{\mathbf{w}} \in \mathbb{R}^{d-1}$ parametrizes $\mathcal{S}^{d-2}$. Then for $j, k \neq 1$ we have

$$\begin{aligned}
M_1^{jk} &= \int_0^\pi \int_{\mathcal{S}^{d-2}} g(R^2(1-\cos(\eta_1)))\delta_{jk}\sin(\eta_1)^{d-2}\,\mathrm{d}\eta_1 \mathrm{d}\mathcal{S}^{d-2} + \\
&\quad R^2 \int_0^\pi \int_{\mathcal{S}^{d-2}} g_s(R^2(1-\cos(\eta_1)))(\tilde{\mathbf{w}}\cdot\mathbf{e}_j)(\tilde{\mathbf{w}}\cdot\mathbf{e}_k)\sin(\eta_1)^{d}\,\mathrm{d}\eta_1 \mathrm{d}\mathcal{S}^{d-2} \\
&= \mathrm{vol}(\mathcal{S}^{d-2})\delta_{jk}\int_{-1}^1 g(R^2(1-s))(1-s^2)^{\frac{d-3}{2}}\mathrm{d}s + \\
&\quad \left(\int_{\mathcal{S}^{d-2}} \mathbf{x}_j\mathbf{x}_k\,\mathrm{d}\mathcal{S}^{d-2}\right)\int_{-1}^1 R^2 g_s(R^2(1-s))(1-s^2)^{\frac{d-1}{2}}\mathrm{d}s.
\end{aligned}$$

By symmetry, $\int_{\mathcal{S}^{d-2}} \mathbf{x}_j\mathbf{x}_k\,\mathrm{d}\mathcal{S}^{d-2} = \frac{\mathrm{vol}(\mathcal{S}^{d-2})}{d-1}\delta_{jk}$, so that

$$\frac{M_1^{jk}}{\mathrm{vol}(\mathcal{S}^{d-2})} = \delta_{jk}\int_{-1}^1 \left(g(R^2(1-s)) + \frac{R^2}{d-1}g_s(R^2(1-s))(1-s^2)\right)(1-s^2)^{\frac{d-3}{2}}\mathrm{d}s$$

whenever $j, k \neq 1$. Integrating the last term by parts, we arrive at

$$M_1^{jk} = \delta_{jk}\beta := \delta_{jk}\mathrm{vol}(\mathcal{S}^{d-2})\left(\int_{-1}^1 g(R^2(1-s))(1-s)(1-s^2)^{\frac{d-3}{2}}\mathrm{d}s\right) \tag{2.31}$$

for $j, k > 1$. Thus, the lower $(d-1)\times(d-1)$ block of M_1 takes the form $\mathrm{diag}(\beta, \ldots, \beta)$, with β as in (2.31). However, for $R\mathbf{x}$ to satisfy the equation of steady-state, we require $0 = \int_{\mathcal{S}^{d-1}} g(R^2(1-\mathbf{x}\cdot\mathbf{w}))(1-\mathbf{x}\cdot\mathbf{w})\mathrm{d}\mathcal{S}_{\mathbf{w}}$. Utilizing the F-H theorem with $l = 0$, this gives

$$0 = \int_{-1}^1 g(R^2(1-s))(1-s)(1-s^2)^{\frac{d-3}{2}}\mathrm{d}s, \tag{2.32}$$

so that in fact $\beta = 0$.

We now consider the remaining entries of M_1. If we now let $j = 1, k > 1$ we have

$$\begin{aligned}
&M_1^{1k} = M_1^{k1} = \\
&- R^2\int_0^\pi \int_{\mathcal{S}^{d-2}} g_s(R^2(1-\cos(\eta_1)))(1-\cos(\eta_1))(\tilde{\mathbf{w}}\cdot\mathbf{e}_k)\sin(\eta_1)^{d-1}\,\mathrm{d}\eta_1\mathrm{d}\mathcal{S}^{d-2} = \\
&- R^2\left(\int_{\mathcal{S}^{d-2}}\mathbf{x}_k\,\mathrm{d}\mathcal{S}^{d-2}\right)\int_{-1}^1 g_s(R^2(1-s))(1-s)(1-s^2)^{\frac{d-2}{2}}\mathrm{d}s = 0.
\end{aligned}$$

Thus, $M_1 = \mathrm{diag}(\alpha, 0, \ldots, 0)$ as claimed, where

$$\alpha = \mathrm{vol}(\mathcal{S}^{d-2})\int_{-1}^1 \left(g(R^2(1-s)) + R^2 g_s(R^2(1-s))(1-s)^2\right)(1-s^2)^{\frac{d-3}{2}}\mathrm{d}s. \tag{2.33}$$

♠

Claim 2.2.2. *In* (2.30),

$$\int_{\mathcal{S}^{d-1}} M_2(\mathbf{x},\mathbf{w})\epsilon(\mathbf{w})\,\mathrm{d}\mathcal{S}_{\mathbf{w}} = \left(D^{11}S^l, D^{22}\frac{S^l_{\eta_1}}{|\hat{\mathbf{b}}_1|}, \ldots, D^{22}\frac{S^l_{\eta_{d-1}}}{|\hat{\mathbf{b}}_{d-1}|} \right),$$

where $D^{ii} = D^{ii}(c_1, c_2, l)$ *are linear in* (c_1, c_2).

Let $\mathbf{x} = \mathbf{x}(\eta_1, \ldots, \eta_{d-1})$ and $\mathbf{w} = \mathbf{w}(\eta'_1, \ldots, \eta'_{d-1})$. We can then write the entries of $\mathbf{v}$ and $\underline{\underline{\mathbf{v}}}$ as

$$\frac{\mathbf{v}^1}{R} = (1 - \mathbf{x}\cdot\mathbf{w}), \quad \frac{\mathbf{v}^j}{R} = -\frac{\partial_{\eta_j}(\mathbf{x}\cdot\mathbf{w})}{|\hat{\mathbf{b}}_j|(\mathbf{x})}, \quad \frac{\underline{\underline{\mathbf{v}}}^1}{R} = (1 - \mathbf{x}\cdot\mathbf{w}), \quad \frac{\underline{\underline{\mathbf{v}}}^j}{R} = -\frac{\partial_{\eta'_j}(\mathbf{x}\cdot\mathbf{w})}{|\hat{\mathbf{b}}_j|(\mathbf{w})},$$

and the entries of $\mathcal{M}(\mathbf{x},\mathbf{w}) := \mathcal{B}^t(\mathbf{x})\mathcal{B}(\mathbf{w})$ as

$$\mathcal{M}^{11} = \mathbf{x}\cdot\mathbf{w}, \quad \mathcal{M}^{1j} = \frac{\partial_{\eta'_j}(\mathbf{x}\cdot\mathbf{w})}{|\hat{\mathbf{b}}_j(\mathbf{w})|}, \quad \mathcal{M}^{j1} = \frac{\partial_{\eta_j}(\mathbf{x}\cdot\mathbf{w})}{|\hat{\mathbf{b}}_j(\mathbf{x})|}, \quad \mathcal{M}^{jk} = \frac{\partial_{\eta_j}\partial_{\eta'_k}(\mathbf{x}\cdot\mathbf{w})}{|\hat{\mathbf{b}}_j(\mathbf{x})||\hat{\mathbf{b}}_j(\mathbf{w})|}.$$

We now demonstrate the claim row-by-row, and in doing so, we use Einstein summation notation. Based on the preceding definitions,

$$\int_{\mathcal{S}^{d-1}} M_2^{1j}\epsilon_j\,\mathrm{d}\mathcal{S}_{\mathbf{w}} = c_1\int_{\mathcal{S}^{d-1}} g_1(\mathbf{x}\cdot\mathbf{w})S^l(\mathbf{w})\,\mathrm{d}\mathcal{S}_{\mathbf{w}} + c_2\int_{\mathcal{S}^{d-1}} \partial_{\eta'_j}\left(g_2(\mathbf{x}\cdot\mathbf{w})\right)\partial^{\eta'_j}(S^l(\mathbf{w}))\frac{\mathrm{d}\mathcal{S}_{\mathbf{w}}}{|\hat{\mathbf{b}}_j(\mathbf{w})|^2}, \tag{2.34}$$

where $g_1(s) = R^2 g_s(R^2(1-s))(1-s)^2 - g(R^2(1-s))s$ and $g_2(s) = g(R^2(1-s))(1-s)$. For the first term in (2.34), we use a straightforward application of the F-H theorem to obtain

$$c_1\int_{\mathcal{S}^{d-1}} g_1(\mathbf{x}\cdot\mathbf{w})S^l(\mathbf{w})\,\mathrm{d}\mathcal{S}_{\mathbf{w}} = c_1\lambda_l(g_1)S^l(\mathbf{x}).$$

We then integrate the second term in (2.34) by parts to obtain

$$\int_{\mathcal{S}^{d-1}} M_2^{1j}\epsilon_j\,\mathrm{d}\mathcal{S}_{\mathbf{w}} = c_1\lambda_l(g_1)S^l(\mathbf{x}) - c_2\int_{\mathcal{S}^{d-1}} g_2(\mathbf{x}\cdot\mathbf{w})\partial_{\eta'_j}\left(\partial^{\eta'_j}(S^l(\mathbf{w}))\frac{\mathrm{d}\mathcal{S}_{\mathbf{w}}}{|\hat{\mathbf{b}}_j(\mathbf{w})|^2}\right). \tag{2.35}$$

Using the lemma with $f = S^l(\mathbf{w})$, (2.35) simplifies to

$$\int_{\mathcal{S}^{d-1}} M_2^{1j}\epsilon_j\,\mathrm{d}\mathcal{S}_{\mathbf{w}} = c_1\lambda_l(g_1)S^l(\mathbf{x}) - c_2\int_{\mathcal{S}^{d-1}} g_2(\mathbf{x}\cdot\mathbf{w})\Delta_{\mathcal{S}^{d-1}}(S^l(\mathbf{w}))\,\mathrm{d}\mathcal{S}_{\mathbf{w}} = (c_1\lambda_l(g_1) + c_2 l(l+d-2)\lambda_l(g_2))S^l(\mathbf{x}), \tag{2.36}$$

as S^l is an eigenfunction with eigenvalue $-l(l+d-2)$ and the F-H theorem. This establishes the claim for the first row with $D^{11}(c_1, c_2, l) = c_1\lambda_l(g_1) + c_2 l(l+d-2)\lambda_l(g_2)$.

Finally, we proceed to the remaining $d-1$ rows. We have

$$\int_{\mathcal{S}^{d-1}} M_2^{jk}\epsilon_k \, \mathrm{d}\mathcal{S}_{\mathbf{w}} = \frac{c_1}{|\hat{\mathbf{b}}_j(\mathbf{x})|}\int_{\mathcal{S}^{d-1}} \partial_{\eta_j}(g_2(\mathbf{x}\cdot\mathbf{w}))S^l(\mathbf{w}) \, \mathrm{d}\mathcal{S}_{\mathbf{w}} + \frac{c_2}{|\hat{\mathbf{b}}_j(\mathbf{x})|}\int_{\mathcal{S}^{d-1}} \big[-g(R^2(1-\mathbf{x}\cdot\mathbf{w}))_{\eta'_k}(\mathbf{x}\cdot\mathbf{w})_{\eta_j} - g(R^2(1-\mathbf{x}\cdot\mathbf{w}))(\mathbf{x}\cdot\mathbf{w})_{\eta_j\eta'_k}\big]\frac{\partial^{\eta'_k}S^l(\mathbf{w})}{|\hat{\mathbf{b}}_k(\mathbf{w})|^2} \, \mathrm{d}\mathcal{S}_{\mathbf{w}}. \tag{2.37}$$

In the first term of the RHS of (2.37), as the integral is in the η' variables, we may pass the derivative through the integral to obtain

$$\frac{c_1}{|\hat{\mathbf{b}}_j(\mathbf{x})|}\int_{\mathcal{S}^{d-1}} \partial_{\eta_j}(g_2(\mathbf{x}\cdot\mathbf{w}))S^l(\mathbf{w}) \, \mathrm{d}\mathcal{S}_{\mathbf{w}} = \frac{c_1\lambda_l(g_2)\partial_{\eta_j}S^l(\mathbf{x})}{|\hat{\mathbf{b}}_j(\mathbf{x})|}.$$

Integrating the second term of (2.37) by parts cancels the third term, leaving

$$\int_{\mathcal{S}^{d-1}} M_2^{jk}\epsilon_k \, \mathrm{d}\mathcal{S}_{\mathbf{w}} = \frac{c_1\lambda_l(g_2)\partial_{\eta_j}S^l(\mathbf{x})}{|\hat{\mathbf{b}}_j(\mathbf{x})|} + \frac{c_2}{|\hat{\mathbf{b}}_j(\mathbf{x})|}\int_{\mathcal{S}^{d-1}} g(R^2(1-\mathbf{x}\cdot\mathbf{w}))(\mathbf{x}\cdot\mathbf{w})_{\eta_j}\partial_{\eta'_k}\left(\frac{\partial^{\eta'_k}S^l(\mathbf{w})}{|\hat{\mathbf{b}}_k(\mathbf{w})|^2} \, \mathrm{d}\mathcal{S}_{\mathbf{w}}\right)$$

$$= \frac{c_1\lambda_l(g_2)\partial_{\eta_j}S^l(\mathbf{x})}{|\hat{\mathbf{b}}_j(\mathbf{x})|} - \frac{c_2 l(l+d-2)}{|\hat{\mathbf{b}}_j(\mathbf{x})|}\int_{\mathcal{S}^{d-1}} g(R^2(1-\mathbf{x}\cdot\mathbf{w}))(\mathbf{x}\cdot\mathbf{w})_{\eta_j}S^l(\mathbf{w}) \, \mathrm{d}\mathcal{S}_{\mathbf{w}}$$

using lemma 1 and the fact that S^l is an eigenfunction. If we once again let $g_3(s) = \int_0^{R^2(1-s)} g(z)\mathrm{d}z$, we may pass the derivative through the integral as before to obtain

$$\int_{\mathcal{S}^{d-1}} M_2^{jk}\epsilon_k \, \mathrm{d}\mathcal{S}_{\mathbf{w}} = \left(c_1\lambda_l(g_2) + \frac{c_2 l(l+d-2)}{R^2}\lambda_l(g_3)\right)\frac{\partial_{\eta_j}S^l(\mathbf{x})}{|\hat{\mathbf{b}}_j(\mathbf{x})|}.$$

This establishes the claim in the remaining rows with $D^{22}(c_1, c_2, l) = c_1\lambda_l(g_2) + \frac{c_2 l(l+d-2)}{R^2}\lambda_l(g_3)$.

♠

In summary, the continuous, d-dimensional eigenvalue problem (2.30) reduces to the 2×2 scalar eigenvalue problem

$$\lambda\begin{pmatrix} c_1 \\ c_2 \end{pmatrix} = \begin{pmatrix} \alpha + \lambda_l(g_1) & l(l+d-2)\lambda_l(g_2) \\ \lambda_l(g_2) & l(l+d-2)\frac{\lambda_l(g_3)}{R^2} \end{pmatrix}\begin{pmatrix} c_1 \\ c_2 \end{pmatrix} := \Omega_l\begin{pmatrix} c_1 \\ c_2 \end{pmatrix} \tag{2.38}$$

where the g_i remain as in the three dimensional case.

2.3 Linear Stability and Linear Well-Posedness

By reducing the linearized equations to a series of scalar problems, we can now readily identify the eigenvalues $\omega_l^{1,2}$ of the matrix Ω_l. This then allows us to characterize the linear stability of sphere solutions: we need $\omega_l^{1,2} < 0$ for all $l \geq 2$, together with $\omega_0^1 < 0,\ \omega_0^2 = 0,\ \omega_1^1 < 0$ and $\omega_1^2 = 0$ (rotation invariance manifests as a zero eigenvalue when $l = 0$, translation invariance manifests as a zero eigenvalue for $l = 1$). Therefore, the sphere is linearly stable if $\mathrm{tr}(\Omega_l) < 0$ and $\det(\Omega_l) > 0$ for all $l \geq 2$. Due to the form of Ω_l, we see $\det(\Omega_l) > 0$ can happen only if $\alpha + \lambda_l(g_1)$ and $\lambda_l(g_3)$ have the same sign. The condition $\mathrm{tr}(\Omega_l)$ then forces the negativity of both, so that we deduce the stability of mode l occurs when

$$\text{(i)}\ \ \alpha + \lambda_l(g_1) < 0 \quad \text{(ii)}\ \ \lambda_l(g_3) < 0 \tag{2.39}$$

$$\text{(iii)}\ \ (\alpha + \lambda_l(g_1))\lambda_l(g_3) > R^2[\lambda_l(g_2)]^2. \tag{2.40}$$

This characterization of stability proves most useful in our analysis, and provides some additional insights. Indeed, from the relation for the perturbed density (2.27) and the perturbed radius (2.28), we see that a perturbation for which $c_1 = 0$ corresponds to a perturbation of density along the sphere, and not of the sphere itself. Condition (ii) therefore has a natural interpretation in terms of stability of the sphere with respect to perturbations of the density away from uniform. More specifically, as $(g_3)_s(s) = -R^2 g(R^2(1-s))$, the function $V(s) := -g_3(1 - s/R^2)$ gives the potential that governs the pairwise interaction. We can then consider the potential energy $E(\rho_S)$ of the system as a function of the density,

$$E(\rho_S) = \int_{\mathcal{S}^2 \times \mathcal{S}^2} V\left(\frac{1}{2}|\mathbf{x} - \mathbf{w}|^2\right) \rho_S(\mathbf{x})\rho_S(\mathbf{w})\, \mathrm{d}\mathcal{S}_{\mathbf{x}}\mathrm{d}\mathcal{S}_{\mathbf{w}}, \tag{2.41}$$

and ask when $\rho_S \equiv 1$ corresponds to a minimum of (2.41). Using the F-H theorem as in §2.1.1 we find that this happens precisely when (ii) holds for all $l \geq 1$. Conversely, perturbations for which $c_2 = 0$ have no component tangential to the sphere. This happens when $l = 0$ for instance. In this case (2.40) reduces to $\alpha + \lambda_0(g_1) < 0$, which gives stability of the sphere

with respect to pure dilations. Condition (i), then, enforces stability of the sphere with respect to purely normal modes.

Having characterized stability for finite l, we now wish to investigate the behavior of the spectrum as $l \to \infty$. The most classical question concerns the *linear well-posedness* of sphere solutions, i.e. when the eigenvalues remain bounded as $l \to \infty$. In practice, however, we primarily concern ourselves with a stronger notion: we wish to characterize when the sphere is *eventually stable*, that is, when $\omega_l^{1,2} < 0$ for all l sufficiently large. With eventually stable potentials we find that the finite number of unstable modes completely characterizes the ground state. We now address both issues using theorem 2.3.1, which furnishes asymptotic formulae for $\omega_l^{1,2}$ for sufficiently regular potentials.

To include the types of potentials that frequently occur in applications, we will assume $V \in C^2((0,\infty))$, but allow growth in V as $s \to 0$. Specifically, we assume $V, V_s = o(s^{\frac{1-d}{2}})$ as $s \to 0$. Additionally, to guarantee that $\lambda_l(g_i)$ are well-defined and to satisfy the hypothesis in the F-H theorem, we must require $g_i(s)(1-s^2)^{\frac{d-3}{2}} \in L^1([-1,1])$. Recalling from (3.2) that

$$\begin{aligned} g_1(s) &= R^2 g_s(R^2(1-s))(1-s)^2 - s g(R^2(1-s)), \\ g_2(s) &= g(R^2(1-s))(1-s), \;\; (g_3)_s(s) = -R^2 g(R^2(1-s)), \end{aligned}$$

we should at least require $g_s(R^2(1-s))(1-s)^2(1-s^2)^{\frac{d-3}{2}},\; g(R^2(1-s))(1-s^2)^{\frac{d-3}{2}} \in L^1$. We shall actually assume slightly more, namely that

$$g_s(R^2(1-s))(1-s)(1-s^2)^{\frac{d-3}{2}} \in L^1, g(R^2(1-s))(1-s^2)^{\frac{d-3}{2}} \in L^1. \tag{2.42}$$

Under these hypotheses, we have the following:

Theorem 2.3.1. *Let $V \in C^2((0,\infty))$ and $V, V_s = o(s^{\frac{1-d}{2}})$ as $s \downarrow 0$. Assume also (2.42). Then we have*

(i) $tr(\Omega_l) \sim \alpha$ and $det(\Omega_l) \sim R^2 l(l+d-2)\alpha\lambda_l(g_3) = o(1)$ as $l \to \infty$.

(ii) The sphere solution of radius R given by (2.24) is linearly well-posed, i.e. $\exists C$ such that $\omega_l^{1,2} < C$ for all $l \geq 0$.

(iii) Suppose $g(s)$ has a generalized power series expansion

$$g(s) = \sum_{i=1}^{\infty} c_i s^{p_i}, \qquad p_1 < p_2 < \cdots \quad \textit{with} \quad c_1 > 0, \tag{2.43}$$

that converges sufficiently rapidly. If the following conditions hold

$$(1)\ \ \alpha < 0 \quad \text{and} \quad (2)\ \ p_1 \in \left(-\frac{d-1}{2}, 0\right) \cup \bigcup_{n=0}^{\infty} (2n+1, 2n+2), \tag{2.44}$$

then the sphere is eventually stable i.e. (ii) holds for $C = 0$.

Remark 2.3.2. *The condition $\alpha < 0$ enforces stability with respect to high-mode normal perturbations. Indeed, when $\alpha > 0$ then all sufficiently high modes have a positive eigenvalue uniformly bounded away from zero, and the corresponding eigenfunction tends to a purely normal perturbation. Additionally, while the generalized power series (2.43) covers many potentials that occur in practice, such as the Morse potential, Gaussian potentials and power-law potentials, the conclusion of part (iii) holds for other classes of potentials without such an expansion. For instance, if the interaction kernel grows sufficiently rapidly near the origin while remaining smooth otherwise, part (iii) still holds. We conjecture (iii) still holds even if an expansion* (2.43) *only holds locally near zero, such as with the interaction* (1.6)*.*

Proof. To show (i), we need to estimate rate of decay of $\lambda_l(g_i)$. We recall that

$$\lambda_l(g_i) = C(d) \int_{-1}^{1} g_i(s) P_{l,d}(s) (1-s^2)^{\frac{d-3}{2}} \, \mathrm{d}s,$$

where the constant $C(d)$ depends only on the dimension of space, d, and that the polynomial $P_{l,d}(s)$ satisfies the Gegenbauer equation

$$(1-s^2)P''_{l,d} - (d-1)sP'_{l,d} + l(l+d-2)P_{l,d} = 0 \tag{2.45}$$

together with the normalization $P_{l,d}(1) = 1$. From these definitions, we have that $f(s)(1-s^2)^{\frac{d-3}{2}} \in L^1([-1,1])$ guarantees $\lambda_l(f) = o(1)$ (c.f. [29]).

Consider first $\lambda_l(g_1)$. The assumptions in (2.42) then suffice to have $g_1(s)(1-s^2)^{\frac{d-3}{2}} \in L^1$, so that $\lambda_l(g_1) = o(1)$. Proceeding now to $\lambda_l(g_2)$, we have,

$$l(l+d-2)\lambda_l(g_2) = \int_{-1}^{1} g_2(s)(1-s^2)^{\frac{d-3}{2}} l(l+d-2) P_l(s) \, \mathrm{d}s =$$

$$-\int_{-1}^{1} g_2(s)(1-s^2)^{\frac{d-1}{2}} P''_{l,d}\,\mathrm{d}s + (d-1)\int_{-1}^{1} sP'_{l,d}(s)(1-s^2)^{\frac{d-3}{2}} g_2(s)\,\mathrm{d}s$$

as $P_{l,d}$ satisfies the Gegenbauer equation (2.45). We integrate by parts in the first term, where the boundary terms vanish due to the growth assumption on $g = -V_s$. The identity $(s^2-1)P'_{l,d} = l\left[sP_{l,d}(s) - P_{l-1,d}(s)\right]$ (equation (4.7.27) in [62]) then yields

$$l(l+d-2)\lambda_l(g_2) = \int_{-1}^{1} (g_2)_s(s)(1-s^2)^{\frac{d-1}{2}} P'_{l,d}(s)\,\mathrm{d}s = \\ l\int_{-1}^{1} (g_2)_s(s)(1-s^2)^{\frac{d-3}{2}}\left[P_{l-1,d}(s) - sP_{l,d}(s)\right]\,\mathrm{d}s.$$

As $(g_2)_s(s) = -R^2 g_s(R^2(1-s))(1-s) - g(R^2(1-s))$, once again (2.42) suffices to have $(l+d-2)\lambda_l(g_2) = o(1)$, so that $\lambda_l(g_2) = o(l^{-1})$. Similarly, for $\lambda_l(g_3)$ we compute

$$l(l+d-2)\lambda_l(g_3) = \int_{-1}^{1} g_3(s)(1-s^2)^{\frac{d-3}{2}} l(l+d-2)P_{l,d}(s)\,\mathrm{d}s = \\ -\int_{-1}^{1} g_3(s)(1-s^2)^{\frac{d-1}{2}} P''_{l,d}\,\mathrm{d}s + (d-1)\int_{-1}^{1} sP'_{l,d}(s)(1-s^2)^{\frac{d-3}{2}} g_3(s)\,\mathrm{d}s.$$

We integrate by parts twice, where the boundary terms vanish as before, and use that $(g_3)_s(s) = -R^2 g(R^2(1-s))$ to discover

$$\frac{1}{R^2} l(l+d-2)\lambda_l(g_3) = \int_{-1}^{1} \frac{\mathrm{d}}{\mathrm{d}s}\left\{g(R^2(1-s))(1-s^2)^{\frac{d-1}{2}}\right\} P_{l,d}(s)\,\mathrm{d}s.$$

Expanding the right hand side,

$$\frac{1}{R^2} l(l+d-2)\lambda_l(g_3) = -\int_{-1}^{1} \left\{R^2 g_s(R^2(1-s))(1-s^2) + \right. \\ \left. (d-1)sg(R^2(1-s))\right\}(1-s^2)^{\frac{d-3}{2}} P_{l,d}(s)\,\mathrm{d}s.$$

Again (2.42) allows us to conclude that the first and second terms vanish as $l \to \infty$. Therefore, $\lambda_l(g_3) = o(l^{-2})$.

As $\lambda_l(g_1) = o(1)$, $\lambda_l(g_3) = o(l^{-2})$ and $\mathrm{tr}(\Omega_l) = \alpha + \lambda_l(g_1) + l(l+d-2)\lambda_l(g_3)R^{-2}$ from (2.38), we have $\mathrm{tr}(\Omega_l) \to \alpha$. As for $\det(\Omega_l)$, we have $\frac{\det(\Omega_l)}{R^2 l(l+d-2)} = \alpha\lambda_l(g_3) + \lambda_l(g_3)\lambda_l(g_1) - \left[\lambda_l(g_2)\right]^2$. To discover the principal term, we note first that $\lambda_l(g_3)\lambda_l(g_1)$ clearly vanishes faster than $\alpha\lambda_l(g_3)$. Returning to $\lambda_l(g_3)$, we integrate by parts once and again use the identity $(s^2-1)P'_{l,d} = l\left[sP_{l,d}(s) - P_{l-1,d}(s)\right]$ to find

$$(l+d-2)\lambda_l(g_3) = \int_{-1}^{1} g(R^2(1-s))(1-s^2)^{\frac{d-3}{2}}\left[sP_{l,d}(s) - P_{l-1,d}(s)\right]\,\mathrm{d}s.$$

As $g_2(s) = g(R^2(1-s))(1-s)$, this reads

$$(l+d-2)\lambda_l(g_3) = -\lambda_l(g_2) - \lambda_{l-1}(g_2) + \int_{-1}^{1} g(R^2(1-s))(1-s^2)^{\frac{d-3}{2}} \left[P_{l,d}(s) - sP_{l-1,d}(s)\right] \, \mathrm{d}s.$$

In particular, $\lambda_l(g_3)$ decays no faster than $\lambda_l(g_2)/(l+d-2)$. Since $\lambda_l(g_2) = o(l^{-1})$, $[\lambda_l(g_2)]^2$ decays faster. In other words,

$$\frac{\det(\Omega_l)}{R^2 l(l+d-2)} = \alpha\lambda_l(g_3) + \text{higher order terms.} \tag{2.46}$$

This concludes the proof of (i) and (ii). To show (iii), note that $(g_3)_s(s) = -R^2 g(R^2(1-s))$. By lemma 2.3.3 shown below, we then obtain

$$\lambda_l(g_3) \sim C(p_1, d, R)\frac{\sin(\pi p_1)c_1}{1+p_1}\Gamma(2+p_1)l^{-(2p_1+d+1)} \quad \text{as} \quad l \to \infty$$

where C denotes a positive constant. Thus $\lambda_l(g_3) < 0$ for sufficiently large l as long as p_1 satisfies (2.44). In conjunction with $\alpha < 0$ and (2.46), it then immediately follows $\mathrm{tr}(\Omega_l) < 0$ and $\det(\Omega_l) > 0$ for all l sufficiently large, so the sphere is eventually stable. This concludes the proof. □

Finally, we provide the lemma which was key in deriving part (iii) of Theorem 2.3.1; it will also prove useful in §2.4 for constructing potentials with specified instabilities.

Lemma 2.3.3. *Let $p + \frac{d-1}{2} > 0$. Then we have*

$$\lambda_l((1-s)^p) = -2^{p+d-2}\frac{\mathrm{vol}(\mathcal{S}^{d-2})\sin(\pi p)\Gamma(p+\frac{d-1}{2})\Gamma(p+1)\Gamma(\frac{d-1}{2})\Gamma(l-p)}{\pi\Gamma(l+p+d-1)},$$

$$\lambda_l((1-s)^p) \sim -\frac{2^{p+d-2}}{\pi}\mathrm{vol}(\mathcal{S}^{d-2})\sin(\pi p)\Gamma(p+\frac{d-1}{2})\Gamma(p+1)\Gamma(\frac{d-1}{2})l^{-2p-d+1}$$

as $l \to \infty$.

Proof. Using the expression of Gegenbauer polynomials in terms of hypergeometric functions

[62], we may write

$$\frac{\lambda_l((1-s)^p)}{\mathrm{vol}(\mathcal{S}^{d-2})} =$$
$$\int_{-1}^{1}(1-s)^{p+(d-3)/2}(1+s)^{(d-3)/2}\ {}_2F_1\left(-l,l+d-2;\frac{d-1}{2};\frac{1-s}{2}\right)\mathrm{d}s =$$
$$2^{p+d-2}\int_0^1 t^{p+(d-3)/2}(1-t)^{(d-3)/2}\ {}_2F_1\left(-l,l+d-2;\frac{d-1}{2};t\right)\ \mathrm{d}t$$

after the change of variables $t = \frac{1-s}{2}$. The generalized Euler transform for hypergeometric functions [58] then gives

$$\frac{\lambda_l((1-s)^p)}{\mathrm{vol}(\mathcal{S}^{d-2})} =$$
$$2^{p+d-2}\mathrm{B}(p+\frac{d-1}{2},\frac{d-1}{2})\ {}_3F_2\left(-l,l+d-2,p+\frac{d-1}{2};\frac{d-1}{2},p+d-1;1\right).$$

Using Saalschütz's theorem [12] to evaluate the hypergeometric term, we obtain

$$\frac{\lambda_l((1-s)^p)}{\mathrm{vol}(\mathcal{S}^{d-2})} = 2^{p+d-2}\mathrm{B}(p+\frac{d-1}{2},\frac{d-1}{2})\frac{\Gamma(l-p)\Gamma(p+d-1)}{\Gamma(-p)\Gamma(l+p+d-1)}.$$

Using the identity $\Gamma(1-z)\Gamma(z) = \pi/\sin(\pi z)$ and expanding the beta function, we arrive at the stated expression,

$$\pi\frac{\lambda_l((1-s)^p)}{\mathrm{vol}(\mathcal{S}^{d-2})} = -2^{p+d-2}\sin(\pi p)\Gamma(p+\frac{d-1}{2})\Gamma(p+1)\Gamma(\frac{d-1}{2})\frac{\Gamma(l-p)}{\Gamma(l+p+d-1)}.$$

For the asymptotics as $l \to \infty$, we note that Stirling's approximation gives $\Gamma(l-p)/\Gamma(l+p+d-1) \sim l^{-2p-d+1}$. □

2.4 Numerical Examples

In this section, we provide numerical examples to illustrate how the different types of instability manifest as different qualitative behaviors of the ground states. We compute steady-state solutions to (1.2) for several different interactions g using a fourth-order Adams-Bashforth scheme, with the number of particles $N = 1000$. We take random initial conditions in all cases, and simulate until the l_∞ norm of (1.2) falls below $.001/N$.

We begin by considering a generalized Lennard-Jones interaction, $g(s) = s^{-p} - s^{-q}$ for $0 < p, q < 1$. To ensure a physically realistic potential consisting of short-range repulsion

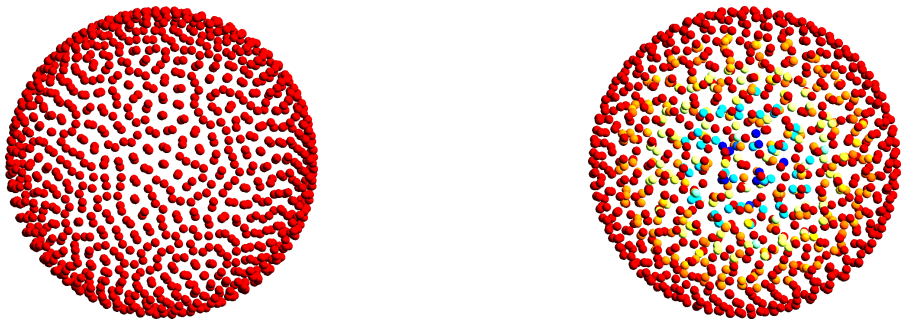

(a) (b)

Figure 2.1: Equilibrium state of (1.2) with $N = 1000$ particles and g given by the generalized Lennard-Jones interaction $g(s) = s^{-p} - s^{-q}$. (a) $(p, q) = (1/3, 1/6)$. Particles concentrate uniformly on a surface of the sphere, with no particles in the interior. (b) $(p, q) = (1/2, 1/4)$. Particles fill the interior of a ball. The color-coding indicates the distance of a particle to their common center of mass.

and far-field attraction, we must demand $p > q$. We then find, by (2.44) (ii), that $\lambda_l(g_3) < 0$ for all but finitely many l with no further restriction. The sign of α, then, completely determines the high-mode behavior. Direct computation shows that $(2R^2)^{p-q} = \frac{2-q}{2-p}$, so that the condition $q < \frac{2p-1}{2p-2}$ determines when $\alpha < 0$, and thus the eventual stability of the sphere. To illustrate both cases, we first select $(p, q) = (\frac{1}{3}, \frac{1}{6})$ so that $\alpha < 0$. By repeatedly using lemma 2.3.3, we additionally verify that for all l the stability conditions (2.40) hold. We therefore expect to accurately describe the solution as a sphere of radius $R = 2^{-1/2}(\frac{11}{10})^3$. Figure 2.1 (a) shows the resulting particle simulation. We next select $(p, q) = (1/2, 1/4)$, so that $\alpha > 0$ and we no longer expect the solution to concentrate on a co-dimension one manifold. As figure 2.1 (b) indicates, the solution instead fills a ball surrounding the origin; the color of a particle indicates its distance to the origin.

A more interesting picture begins to emerge when the sphere destabilizes yet remains eventually stable. As our examples will illustrate, the low mode instabilities fully describe the ground state. Due to the intricate steady-states it produces, cf. figure (1.1), we illustrate this phenomenon with the interaction $g(s) = \frac{\tanh(a(1-\sqrt{2s}))+b}{\sqrt{2s}}$ introduced in [35]. The top of figure

2.2(a) depicts a computed steady-state of (1.2) with $(a, b) = (7, -.9)$. These parameters result in a mode $l = 3$ instability. We then compute the eigenvector (c_1, c_2) of Ω_3, and use the result to construct the resulting surface from equation (2.28) and its corresponding density from equation (2.27), shown in the bottom of figure 2.2(a). This suggests that the linearized density echoes the overall shape of the full nonlinear problem in the vicinity of the bifurcation point. We perform the same computation for the parameter values $(a, b) = (9, 0)$, which yields a mode $l = 4$ instability, as shown in figure 2.2(b). Our theory and the experiments have excellent agreement.

The observation that particles align themselves with low-mode instabilities furnishes us with an avenue to construct potentials with intricate ground-states. Indeed, if we design an eventually stable interaction $g(s)$ with a single unstable mode, the resulting steady-state should resemble a spherical harmonic of that degree. To illustrate this procedure, we give an explicit construction of an interaction with a pure mode 5 instability.

First, we destabilize mode 5. We accomplish this by enforcing $\lambda_5(g_3) > 0$, which suffices due to the characterization (2.40). Using the identity

$$s^n = \sum_{l=n,n-2,\dots} \frac{(2l+1)n!}{2^{\frac{n-l}{2}}(.5(n-l))!(l+n+1)!!} P_l(s), \tag{2.47}$$

we can take $g_3(s) = \frac{s^5}{5} + p_4(s)$, where $p_m(s)$ denotes a polynomial of degree no more than m. Next, we choose $p_3(s)$ to stabilize modes $l \leq 4$. As $\lambda_l(p_4) = 0$ whenever $l > 4$, this choice does not affect the instability of mode 5. Indeed, taking $p_3 = -3s^2 - 4s^3$ we obtain $R^2 g(R^2(1-s)) = 3s^2 + 4s^3 - s^4$, where from (2.24) we see $R = 1$. This yields an interaction $g(s) = 3(1-s)^2 + 4(1-s)^3 - (1-s)^4$ with a pure mode 5 instability, while all modes $l \geq 6$ contain exactly one zero eigenvalue. Lastly, we stabilize the remaining modes by adding a negative definite perturbation, $\tilde{g}(s) = g(s) + \epsilon f(s)$ for $f(s) = \frac{1}{\sqrt{s}}$. Using lemma 2.3.3 we find that

$$R\lambda_l(f_3) = -\frac{2^{2+3/2}}{8l^3 + 12l^2 - 2l - 3}, \qquad R\lambda_l(f_2) = \frac{\lambda_l(f_3)}{2},$$
$$R\lambda_l(f_1) = -2^{3/2}\frac{4l^2 + 4l - 2}{8l^3 + 12l^2 - 2l - 3}, \qquad R\alpha_f = \frac{2^{5/2}}{3}.$$

Therefore, for $\epsilon > 0$ sufficiently small, $\tilde{g}$ has mode 5 unstable with all other modes stable. Figure 2.2(c) shows the resulting ground-state and spherical harmonic.

2.5 Discussion

This chapter addressed the fundamental question of understanding how the structure of particle potentials predict the types of patterns that can emerge. An analysis of the linear stability of uniform sphere solutions aided in achieving this goal. The d-dimensional eigenvalue problems reduced into a decoupled series of 2×2 scalar problem involving a single spherical harmonic. This reduction aided in providing a formulation of stability and linear well-posedness conditions that have natural physical interpretations. These conditions then provided the means to predict the co-dimension and the types of symmetries that emerged in the resulting patterns. Using this predictive ability, we explicitly constructed a potential to yield a desired particle distribution, thereby addressing a particular case of the inverse statistical mechanics problem for self-assembly. In the subsequent chapter, we extend this construction to arbitrary instabilities. Also, we note that our theory currently allows us to predict only the degree of a spherical harmonic that appears in the ground state. In dimensions $d \geq 3$, it remains an open issue to determine which spherical harmonic of a particular degree will arise.

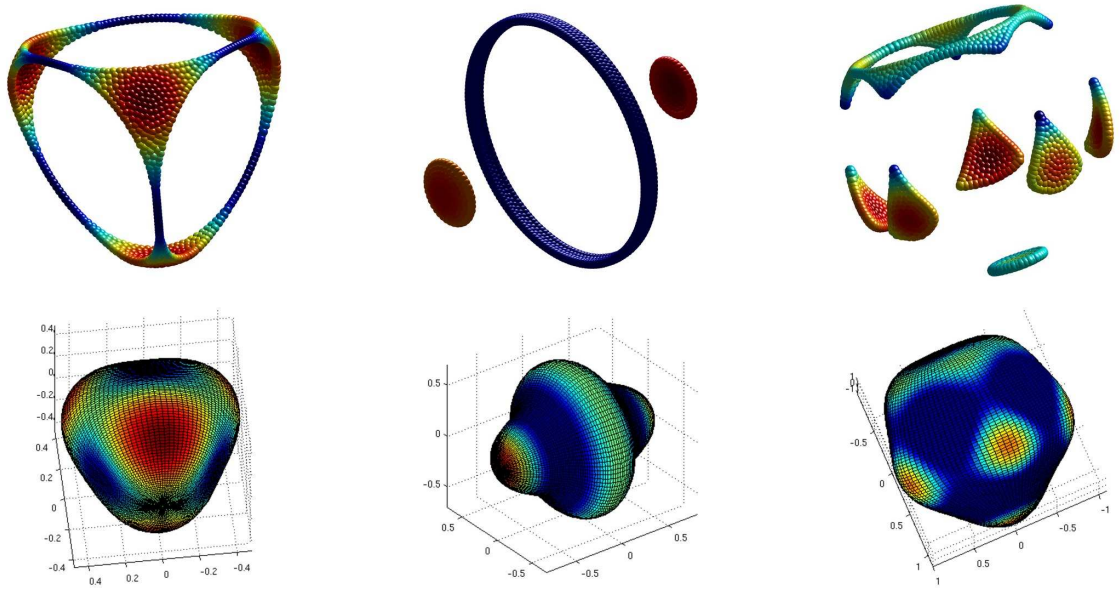

(a) (b) (c)

Figure 2.2: Top row: The result of the simulation of the gradient flow (1.2) with $N = 1000$ particles for three different force laws. Bottom row: linearized solution corresponding to the instability mode as computed from (2.22). (a) Top: force law (1.6) with $(a, b) = (7, -.9)$. Bottom: Perturbation of a sphere using the spherical harmonic of mode $l = 3, m = 2$. (b) Top: Same as (a) but with $(a, b) = (9, 0)$. Bottom: Perturbation of a sphere using the spherical harmonic of mode $l = 4, m = 0$. (c) Top: $g(s) = 3(1-s)^2+4(1-s)^3-(1-s)^4+\varepsilon s^{-1/2}$ with $\varepsilon = 2^{-3/2}$. Sphere perturbed by a linear combination of the modes $l = 5, m = 5$ and $l = 5, m = 0$. The figures are color-coded according to the distance from the origin.

CHAPTER 3

Linearized Inverse Statistical Mechanics

As the previous chapter observed, the linear instability of the uniform sphere results in the formation of complex, spherical harmonic patters in the nonlinear ground state. This chapter leverages this observation to address the issue of inverse statistical mechanics, i.e. constructing a potential to yield a desired pattern. More precisely, we pose the linearized inverse statistical mechanics question: given a finite set of spherical harmonics, can we construct an interaction potential that possesses exactly these instabilities? The main result of this chapter provides a simple, closed form solution to this problem. Figure 3.1 illustrates the success of this approach to produce intricate, self-organized patterns: a true soccer ball results from the instability of a mode 6 spherical harmonic that we explicitly build into the interaction potential.

The rest of the chapter proceeds as follows: we review the stability conditions from chapter 2 and other necessary background material in § 3.1; we construct potentials that possess a single instability of odd degree in § 3.2 and of even degree in § 3.3; in § 3.4 we combine the previous two sections to construct potentials that exhibit any arbitrary specified number of instabilities; we conclude by providing several numerical examples of simulated ground states from our constructed potentials in § 3.5.

3.1 Preliminaries

Before addressing our main task, we first recall the relevant aspects from the linear theory. We shall refer to the function $g : \mathbb{R}^+ \to \mathbb{R}$ as the **interaction kernel** that governs the motion of the particles. Formally, a given interaction kernel admits a uniform density 2-sphere of

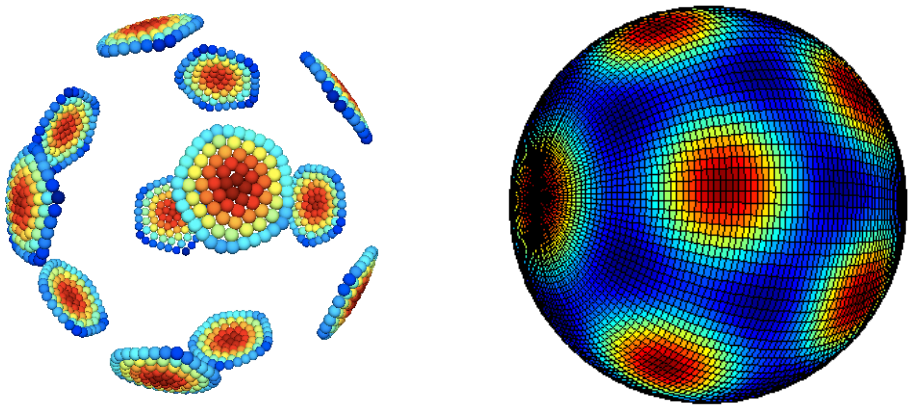

Figure 3.1: Left: a "soccer ball" minimizer to the discrete minimization (1.1), computed by solving (1.2) directly to steady state. Right: approximation of the steady state using the linear theory [71] for spherical solutions to the continuum model (1.3).

radius $R > 0$ as a steady state solution to (1.3) if and only if R satisfies the following **radius condition**:

$$0 = \int_{-1}^{1} g(R^2(1-s))(1-s)\,\mathrm{d}s. \tag{3.1}$$

For a given R satisfying (3.1), we showed in the previous chapter that one can determine the linear stability of the corresponding spherical solution by examining a countable sequence of decoupled, scalar eigenvalue problems. For notational convenience in stating the eigenvalue problems, we shall frequently refer to the following **auxiliary quantities** that R, g and its derivative $g_s(s) = \frac{\mathrm{d}g}{\mathrm{d}s}$ fully determine:

$$g_1(s) := R^2 g_s(R^2(1-s))(1-s)^2 - g(R^2(1-s))s,$$

$$g_2(s) := g(R^2(1-s))(1-s)$$

$$\frac{\mathrm{d}g_3}{\mathrm{d}s}(s) := -R^2 g(R^2(1-s))$$

$$\alpha := \int_{-1}^{1} \left[g(R^2(1-s)) + R^2 g_s(R^2(1-s))(1-s)^2\right] \mathrm{d}s \tag{3.2}$$

Additionally, for an integer $l \geq 0$ and a function $f \in L^1([-1,1])$, we shall need to reference the quantity

$$\lambda_l(f) := \int_{-1}^{1} f(s) P_l(s)\, \mathrm{d}s, \tag{3.3}$$

where $P_l(s)$ denotes the Legendre polynomial of degree l normalized to $P_l(1) = 1$; the quantity $\lambda_l(f)$ is closely related to the expansion of f in terms of Legendre polynomials. With these definitions in hand, the decoupled series of scalar eigenvalue problems

$$\lambda \begin{pmatrix} c_1 \\ c_2 \end{pmatrix} = \begin{pmatrix} \alpha + \lambda_l(g_1) & l(l+1)\lambda_l(g_2) \\ \lambda_l(g_2) & \frac{l(l+1)}{R^2}\lambda_l(g_3) \end{pmatrix} \begin{pmatrix} c_1 \\ c_2 \end{pmatrix} := \Omega_l(g) \begin{pmatrix} c_1 \\ c_2 \end{pmatrix} \tag{3.4}$$

completely characterize the local stability of a uniform sphere solution; all that remains is to verify that the eigenvalues of $\Omega_l(g)$ have the appropriate sign.

To simplify this task, we make two observations that come immediately from (3.4). First is that the two modes $l = 0$ and $l = 1$ necessarily have a zero eigenvalue. Indeed, for $l = 0$ we find that

$$\lambda_0(g_2) = \int_{-1}^{1} g(R^2(1-s))(1-s)\, \mathrm{d}s = 0$$

by the radius condition (3.1), so that

$$\Omega_0(g) = \begin{pmatrix} \alpha + \lambda_0(g_1) & 0 \\ 0 & 0 \end{pmatrix}.$$

We therefore demand negativity of the remaining non-zero eigenvalue, $\alpha + \lambda_0(g_1)$, to ensure stability with respect to mode-zero perturbations. For this, we substitute directly from the definition of g_1 to compute

$$\alpha + \lambda_0(g_1) = \int_{-1}^{1} [g\left(R^2(1-s)\right)(1-s) - \frac{\mathrm{d}}{\mathrm{d}s}\left(g(R^2(1-s))\right)(1-s)^2]\mathrm{d}s = 4g(2R^2),$$

which follows from integration by parts and the radius condition. We conclude the sphere is stable with respect to mode-zero perturbations when $g(2R^2) < 0$. For $l = 1$, we have from the definitions above that $\lambda_1(g_2) = \int_{-1}^{1} g(R^2(1-s))(s-s^2)\mathrm{d}s$. By applying the radius condition, $\int_{-1}^{1} g(R^2(1-s))\mathrm{d}s = \int_{-1}^{1} g(R^2(1-s))s\mathrm{d}s$, so in fact $\lambda_1(g_2) = \int_{-1}^{1} g(R^2(1-s))(1-s^2)\mathrm{d}s$. An

integration by parts and another application of the radius condition then combine to show

$$\alpha + \lambda_1(g_1) = \int_{-1}^{1} \left[g(R^2(1-s))(1-s^2) - \frac{\mathrm{d}}{\mathrm{d}s}(g(R^2(1-s)))(1-s)^2(1+s)\mathrm{d}s \right] = -2\int_{-1}^{1} g(R^2(1-s))(1-s^2)\mathrm{d}s.$$

Also, as $\lambda_1(g_3) = -\int_{-1}^{1} g_3(s)\frac{\mathrm{d}}{\mathrm{d}s}(\frac{1-s^2}{2})\mathrm{d}s$ we integrate by parts to find $\lambda_1(g_3) = -\frac{R^2}{2}\int_{-1}^{1} g(R^2(1-s))(1-s^2)\mathrm{d}s$. Combining these calculations shows that

$$\Omega_1(g) = \begin{pmatrix} -2C & 2C \\ C & -C \end{pmatrix},$$

where $C := \int_{-1}^{1} g(1-s)(1-s^2)\mathrm{d}s$. Therefore, the sphere is stable with respect to mode-one perturbations when $C > 0$. Second, while modes $l \geq 2$ do not necessarily have zero eigenvalues, we observe that the form of $\Omega_l(g)$ dictates the sphere is stable to mode-l perturbations when the following **stability conditions**

$$\text{(i) } \lambda_l(g_3) < 0 \qquad \text{(ii) } \alpha + \lambda_l(g_1) < 0$$

$$\text{(iii) } \lambda_l(g_3)(\alpha + \lambda_l(g_1)) > R^2\left[\lambda_l(g_2)\right]^2 \tag{3.5}$$

simultaneously hold for all $l \geq 2$. We summarize these results in theorem 3.1.1.

Theorem 3.1.1. *Consider an interaction kernel $g(s) : \mathbb{R}^+ \to \mathbb{R}$ and a radius R satisfying* (3.1). (a) *If $g(2R^2) < 0$, $\int_{-1}^{1} g(R^2(1-s))(1-s^2)\,\mathrm{d}s > 0$ and* (i − iii) *in* (3.5) *hold $\forall\, l \geq 2$, then the sphere of radius R is stable;* (b) *if* (i), (ii) *or* (iii) *fails with strict inequality for some $l \geq 2$, then mode l is unstable.*

This characterization of stability furnishes a straightforward path to construct interaction kernels with arbitrary instabilities. We shall ensure (iii) fails for the desired modes, while ensuring that part (a) continues to hold for all remaining modes. The genesis of our construction lies with a useful identity that expresses powers in terms of positive sums of Legendre polynomials. For integers $n \geq 0$, we have

$$s^{2n} = \sum_{l=0}^{n} \left\{ 2^{2l+1} \frac{(2n)!(n+l)!}{(n-l)!(2(n+l)+1)!} \right\} \frac{P_{2l}(s)}{||P_{2l}||_0^2},$$

$$s^{2n+1} = \sum_{l=0}^{n} \left\{ 2^{2l+2} \frac{(2n+1)!(n+l+1)!}{(n-l)!(2(n+l+1)+1)!} \right\} \frac{P_{2l+1}(s)}{||P_{2l+1}||_0^2}. \tag{3.6}$$

Here, $||f||_0^2$ denotes the $L^2([-1,1])$ norm of f, so that we may read off $\lambda_{2l}(s^{2n})$ and $\lambda_{2l+1}(s^{2n+1})$ directly from (3.6) as the quantities between braces. To destabilize exactly one mode, the formula (3.6) suggests an interaction kernel of the form $g(s) = p_{n-1}(1-s) - (1-s)^n$, where $p_{n-1}(1-s)$ denotes a polynomial of degree $n-1$ in the variable $(1-s)$. Provided $R = 1$, we can then calculate using (3.2) and the fact that $\lambda_{n+1}(s^m) = 0$, for $m \leq n$ at least, that $(n+1)\lambda_{n+1}(g_3) = \lambda_{n+1}(s^{n+1}) > 0$. From theorem 3.1.1 (b), mode $n+1$ is unstable for any choice of p_{n-1}. In particular, we can choose p_{n-1} so that $R = 1$ and all modes $l \leq n$ are stable. For modes $l \geq n+2$, we again conclude from the definition of Ω_l and the fact that $\lambda_l(s^m) = 0$ for $l > m$ that

$$\Omega_l(g) = \mathrm{diag}(\alpha, 0).$$

If we also choose p_{n-1} so that $\alpha < 0$, we may simply add any arbitrarily small, negative-definite perturbation to stabilize the remaining modes $l > m$.

The main difficulty lies in choosing $p_{n-1}(s)$ appropriately to meet these two requirements. This is the content of theorems 3.2.1 and 3.3.1; sections 3 and 4 provide their respective proofs. In the construction, we shall make great use of the ratios of the coefficients (3.6). For consecutive values of n, if $n \geq 1$ and $l \leq n-1$ then

$$\begin{aligned} R_{2n,2l} &:= \frac{\lambda_{2l}(s^{2n})}{\lambda_{2l}(s^{2n-2})} = \frac{n(2n-1)}{(n-l)(2n+2l+1)}, \\ R_{2n+1,2l+1} &:= \frac{\lambda_{2l+1}(s^{2n+1})}{\lambda_{2l+1}(s^{2n-1})} = \frac{n(2n+1)}{(n-l)(2n+2l+3)}. \end{aligned} \tag{3.7}$$

On the other hand, for consecutive values of l, if $1 \leq l \leq n$ then

$$\begin{aligned} \frac{\lambda_{2l}(s^{2n})}{\lambda_{2l-2}(s^{2n})} &= \frac{n-l+1}{n+l+1/2} \\ \frac{\lambda_{2l+1}(s^{2n+1})}{\lambda_{2l-1}(s^{2n+1})} &= \frac{n-l+1}{n+l+3/2}. \end{aligned} \tag{3.8}$$

Therefore, from (3.8) we have that

$$\begin{aligned} \lambda_{2l}(s^{2n}) &= \lambda_{2l-2}(s^{2n}) \left[1 - \frac{4l-1}{2n+2l+1}\right] \\ \lambda_{2l+1}(s^{2n+1}) &= \lambda_{2l-1}(s^{2n+1}) \left[1 - \frac{4l+1}{2n+2l+3}\right], \end{aligned} \tag{3.9}$$

so λ_{2l} and λ_{2l+1} decrease as l increases. We also need explicit bounds for specific values of l, in particular that

$$\begin{aligned}\lambda_{2l}(s^{2n}) \leq \lambda_2(s^{2n}) &= \frac{4n}{(2n+1)(2n+3)},\\ \lambda_{2l+1}(s^{2n+1}) \leq \lambda_3(s^{2n+1}) &= \frac{4n}{(2n+3)(2n+5)}.\end{aligned} \tag{3.10}$$

By greatly leveraging these formulas, we will prove that a simple choice for $p_{n-1}(1-s)$ has the desired properties.

Theorem 3.1.3 provides the last ingredient in our construction, in that it furnishes a family of the required negative-definite perturbations. The family of interaction kernels take the form of shifted inverse powers, $g(s) = s^{-p} - \mu$ for $0 < p \leq \frac{1}{2}$. To yield the unit sphere as a steady state we find μ must satisfy

$$2\mu = \int_{-1}^{1} (1-s)^{1-p}\, \mathrm{d}s = \frac{2^{2-p}}{2-p}. \tag{3.11}$$

After recalling a useful lemma from the previous chapter that allows us to calculate coefficients for inverse powers, we proceed to state and prove theorem 3.1.3.

Lemma 3.1.2. *Let $p > -1$. Then*

$$\lambda_l((1-s)^p) = -2^{p+1}\frac{\sin(\pi p)\Gamma^2(p+1)\Gamma(l-p)}{\pi\Gamma(l+p+2)}.$$

Theorem 3.1.3. *Let $g(s) = s^{-p} - \mu$ with $0 < p \leq \frac{1}{2}$ and μ satisfy (3.11). Then the unit sphere solution is stable.*

Proof. For $l = 0$ we require $g(2) < 0$, which holds as $g(2) = 2^{-p} - 2^{1-p}(2-p)^{-1}$ and $p > 0$. For $l = 1$ we require $\int_{-1}^{1} g(1-s)(1-s^2)\, \mathrm{d}s > 0$. By direct computation,

$$\int_{-1}^{1} g(1-s)(1-s^2)\, \mathrm{d}s = 2^{3-p}\left(\frac{2}{3(2-p)} - \frac{1}{3-p}\right) > 0$$

as desired. For $l \geq 2$, we first compute the auxiliary quantities

$$\begin{aligned} g_1(s) &= (1-p)(1-s)^{1-p} - (1-s)^{-p} + \mu s, & g_2(s) &= (1-s)^{1-p} - \mu(1-s),\\ \alpha &= 2^{1-p}\left(2 + \frac{1}{1-p} - \frac{6}{2-p}\right), & g_3(s) &= \frac{(1-s)^{1-p}}{1-p} + \mu s.\end{aligned}$$

By lemma 3.1.2, when $l \geq 2$ we have

$$\lambda_l(g_3) = -\frac{2^{2-p}\sin(\pi(1-p))\Gamma^2(2-p)\Gamma(l+p-1)}{\pi(1-p)\Gamma(l+3-p)}$$
$$\lambda_l(g_1) = (1-p)^2\lambda_l(g_3) - \frac{2^{1-p}\sin(\pi p)\Gamma^2(1-p)\Gamma(l+p)}{\pi\Gamma(l+2-p)},$$

and $\lambda_l(g_2) = (1-p)\lambda_l(g_3)$. Clearly, (i) holds. As $\alpha \leq 0$, (ii) holds as well. Finally, from the fact $(\alpha + \lambda_l(g_1))(\lambda_l(g_3)) > (1-p)^2[\lambda_l(g_3)]^2 = [\lambda_l(g_2)]^2$, we see (iii) holds and the sphere is therefore stable. □

The next two sections constitute the most difficult aspect of our solution to the linearized inverse statistical mechanics problem. The tedious, technical proofs of theorems 3.2.1 and 3.3.1 do not provide any new insight outside of the statement of the theorems themselves. The uninterested reader may comfortably skip them, and proceed directly to § 3.4.

3.2 An Unstable Odd Mode

We address first the problem of destabilizing a single odd mode $2n+1$ for $n \geq 1$. We shall use an interaction kernel of the form $g(1-s) = c_0(1+3s) + c_{-2}s^{2n-2} + c_{-1}s^{2n-1} - s^{2n}$. First, we enforce that $R = 1$. From (3.1) we need $\int_{-1}^{1} g(1-s)(1-s)\mathrm{d}s = 0$, which necessitates $c_{-2} = \frac{2n-1}{2n+1}(1+c_{-1})$. We then have that

$$\lambda_{2n+1}(g_3) = \frac{\lambda_{2n+1}(s^{2n+1})}{2n+1} > 0$$

by (3.6). Therefore, mode $2n+1$ is unstable as claimed, independent of c_0 and c_{-1}.

The difficulty now lies in choosing the coefficients c_0 and c_{-1} to stabilize all modes $l \leq 2n$. We therefore devote the remainder of this section to proving

Theorem 3.2.1. *Let* $g(s) = c_0(1+3(1-s)) + \frac{2n-1}{2n+1}(1+c_{-1})(1-s)^{2n-2} + c_{-1}(1-s)^{2n-1} - (1-s)^{2n}$ *for* $n \geq 1$. *Then for any* c_0, c_{-1} *satisfying*

$$c_{-1} > n - \frac{1}{2}, \qquad\qquad c_0 > \frac{3c_{-1}}{2n+1}, \tag{3.12}$$

$g(s)$ *exhibits a pure mode* $2n+1$ *instability: all modes* $l \leq 2n$ *are stable, while* $\Omega_l(g) = diag(\alpha, 0)$ *for* $\alpha < 0$ *and all* $l > 2n+1$.

s^m	α	g_1	g_2	g_3
$m=0$	$-6c_0-\frac{8+6c_{-1}}{2n+1}$	$-3c_0$	c_0	0
$m=1$	0	$5c_0$	$2c_0$	$-c_0$
$m=2$	0	$-6c_0$	$-3c_0$	$-\frac{3c_0}{2}$
$m=2n-3$	0	$-c_{-2}(2n-2)$	0	0
$m=2n-2$	0	$\frac{2(2n-1)(2n-2)+c_{-1}(2n-1)(2n-5)}{2n+1}$	c_{-2}	0
$m=2n-1$	0	$\frac{6n-1-c_{-1}(2n-1)(2n+3)}{2n+1}$	$\frac{2c_{-1}-(2n-1)}{2n+1}$	$-\frac{1+c_{-1}}{2n+1}$
$m=2n$	0	$-4n-2nc_{-1}$	$-(1+c_{-1})$	$-\frac{c_{-1}}{2n}$
$m=2n+1$	0	$2n+1$	1	$\frac{1}{2n+1}$

Table 3.1: Coefficients of the auxiliary quantities (3.2) when using a kernel of the form in theorem 3.2.1.

For $l=0$, the stability condition reads $g(2)<0$. This gives $-2c_0-\frac{2(1+c_{-1})}{2n+1}<0$, which holds due to positivity of the coefficients c_0 and c_{-1}. For $l=1$, we verify $\int_{-1}^{1} g(1-s)(1-s^2)\mathrm{d}s>0$ directly. After simplifying, this reads

$$\frac{2c_0}{3}+\frac{(1+c_{-1})}{2n+1}\left(1-\frac{2n-1}{2n+1}\right)>\left(\frac{1}{2n+1}-\frac{1}{2n+3}\right)$$

which again holds due to the positivity of c_0 and c_{-1}. For $l\geq 2$, we first compute the auxiliary quantities in terms of powers s^m for $0\leq m\leq 2n+1$. Table 3.1 summarizes the coefficients. Next, we verify conditions (i-iii) in (3.5) hold under the requirements (3.12).

Condition (i)

For even modes $2\leq 2l\leq 2n$, we check $\lambda_{2l}(g_3)\leq -\frac{c_{-1}}{2n}\lambda_{2l}(s^{2n})<0$ due to the positivity of the coefficients in (3.6) and as $c_{-1}>0$. For odd modes $3\leq 2l+1\leq 2n-1$, $\forall l\leq n-1$ we must have

$$(1+c_{-1})\lambda_{2l+1}(s^{2n-1})>\lambda_{2l+1}(s^{2n+1})\Leftrightarrow\frac{n(2n+1)}{(n-l)(2n+2l+3)}<(1+c_{-1})$$

by using (3.7). As $l = n-1$ is the most restrictive case, c_{-1} must therefore satisfy

$$(1 + c_{-1}) > \frac{n(2n+1)}{4n+1},$$

which holds due to (3.12).

Condition (ii)

To show that (ii) holds for all $l \geq 2$ under the hypothesis (3.12), we first prove two lemmas that establish bounds from above on $\lambda_{2l}(g_1)$ and $\lambda_{2l+1}(g_1)$.

Lemma 3.2.2. *Let* $3 \leq 2l+1 \leq 2n-1$ *and* c_0, c_{-1} *satisfy* (3.12). *Then* $\lambda_{2l+1}(g_1) \leq \frac{6c_{-1}+8}{2n+1}$.

Proof. Write $(2n+1)\lambda_{2l+1}(g_1) = c_{-1}I_{2l+1} + J_{2l+1}$, where from Table 3.1

$$\begin{aligned}
I_{2l+1} &= (2n-1)(2n+3)\lambda_{2l+1}(s^{2n-1}) - (2n-1)(2n-2)\lambda_{2l+1}(s^{2n-3}),\\
J_{2l+1} &= (2n+1)^2\lambda_{2l+1}(s^{2n+1}) + (6n-1)\lambda_{2l+1}(s^{2n-1}) -\\
&\quad (2n-1)(2n-2)\lambda_{2l+1}(s^{2n-3}),
\end{aligned}$$

for $1 \leq l \leq n-2$, whereas

$$\begin{aligned}
I_{2n-1} &= (2n-1)(2n+3)\lambda_{2n-1}(s^{2n-1}),\\
J_{2n-1} &= (2n+1)^2\lambda_{2n-1}(s^{2n+1}) + (6n-1)\lambda_{2n-1}(s^{2n-1}).
\end{aligned}$$

Using (3.9) gives that, for $3 \leq 2l-1 \leq 2n-3$,

$$\begin{aligned}
I_{2l+1} =& (2n-1)(2n+3)\lambda_{2l-1}(s^{2n-1})\left[1 - \frac{4l+1}{2n+2l+1}\right] -\\
& (2n-1)(2n-2)\lambda_{2l-1}(s^{2n-3})\left[1 - \frac{4l+1}{2n+2l-1}\right]
\end{aligned}$$

$$\begin{aligned}
\Rightarrow I_{2l+1} = I_{2l-1} &- \frac{(2n-1)(2n+3)(4l+1)}{2n+2l+1}\lambda_{2l-1}(s^{2n-1}) +\\
&\frac{(2n-1)(2n-2)(4l+1)}{2n+2l-1}\lambda_{2l-1}(s^{2n-3}).
\end{aligned}$$

Recalling (3.7),

$$I_{2l+1} = I_{2l-1} - (2n-1)(4l+1)\lambda_{2l-1}(s^{2n-3})\left[\frac{\lambda_{2l-1}(s^{2n-1})(2n+3)}{\lambda_{2l-1}(s^{2n-3})(2n+2l+1)} - \frac{(2n-2)}{2n+2l-1}\right] =$$

$$I_{2l-1} - \frac{(2n-1)(4l+1)}{(2n+2l-1)}\lambda_{2l-1}(s^{2n-3})\left[\frac{(n-1)(2n-1)(2n+3)}{(n-l)(2n+2l+1)} - (2n-2)\right].$$

As $(n-l)(2n+2l+1)$ decreases in l, $I_{2l+1} < I_{2l-1} \leq I_3$ when $l \geq 2$ if $(n-1)(2n-1)(2n+3) \geq (2n-2)(n-2)(2n+5)$, which holds for the non-vacuous values $n \geq 4$.

In a similar fashion, using (3.8)

$$J_{2l+1} = J_{2l-1} + (4l+1)\left[\frac{(2n-1)(2n-2)\lambda_{2l-1}(s^{2n-3})}{2n+2l-1} - \frac{(2n+1)^2\lambda_{2l-1}(s^{2n+1})}{2n+2l+3} - \frac{(6n-1)\lambda_{2l-1}(s^{2n-1})}{2n+2l+1}\right].$$

Substituting from (3.7),

$$J_{2l+1} = J_{2l-1} + \frac{(4l+1)(n-1)(2n-1)\lambda_{2l-1}(s^{2n-3})}{(2n+2l-1)(2n+2l+1)}\left[2(2n+2l+1) - \frac{n(2n+1)^3}{(n-l)(n-l+1)(2n+2l+3)} - \frac{(6n-1)}{(n-l)}\right].$$

Therefore, we may conclude $J_{2l+1} < J_{2l-1} \leq J_3$ if $2 < \frac{n(2n+1)^3}{(n-l)(n-l+1)(2n+2l+3)(2n+2l+1)} + \frac{(6n-1)}{(n-l)(2n+2l+1)}$ for all $l \geq 2$. We once again have that the right hand side increases with l, so that setting $l = 2$ we find it necessary that $2 < \frac{n(2n+1)^3}{(n-2)(n-1)(2n+7)(2n+5)} + \frac{(6n-1)}{(n-2)(2n+5)}$, which holds as well when $n \geq 4$.

Consequently, $(2n+1)\lambda_{2l+1}(g_1) \leq (2n+1)\lambda_3(g_1)$ when $3 \leq 2l+1 \leq 2n-3$. Computing I_3 from (3.10) gives

$$I_3 = (2n-1)(2n+3)\lambda_3(s^{2n-1}) - (2n-1)(2n-2)\lambda_3(s^{2n-3}) = -\frac{4(n-1)}{2n+1}[2(n-2) - (2n-1)] = \frac{12(n-1)}{2n+1} < 6.$$

Similarly, $J_3 = \frac{4n(2n+1)^2}{(2n+3)(2n+5)} + \frac{4(n-1)(6n-1)}{(2n+1)(2n+3)} - \frac{2(n-1)4(n-2)}{(2n+1)}$, so that $J_3 > 8 \Leftrightarrow 98n + 85 > 0$. This demonstrates the claim for the cases $3 \leq 2l+1 \leq 2n-3$. For the remaining case

$2l+1 = 2n-1 \geq 3$, using (3.6) the requirements $I_{2n-1} < 6$ and $J_{2n-1} < 8$ read

$$6 > 2^{1-2n}\frac{\sqrt{\pi}\Gamma(2n)(2n-1)(2n+3)}{\Gamma(2n+\frac{1}{2})},$$
$$8 > 2^{1-2n}\frac{\sqrt{\pi}\Gamma(2n)}{\Gamma(2n+\frac{1}{2})}\left[n(2n+1)^3(4n+1)^{-1}+(6n-1)\right]$$

respectively. As $n \geq 2$, I_{2n-1} and J_{2n-1} decrease with n, it suffices to calculate that

$$6 > 2^{-3}\frac{21\sqrt{\pi}\Gamma(4)}{\Gamma(\frac{9}{2})}, \quad 8 > 2^{-3}\frac{\sqrt{\pi}\Gamma(4)}{\Gamma(\frac{9}{2})}\left[\frac{349}{9}\right].$$

□

Lemma 3.2.3. *Let $2 \leq l \leq 2n$ and c_0, c_{-1} satisfy (3.12). Then $\lambda_{2l}(g_1) < 0$.*

Proof. Decompose $(2n+1)\lambda_{2l}(g_1) = J_{2l} + c_{-1}I_{2l} - 6c_0\lambda_{2l}(s^2)$, where for $1 \leq l \leq n-1$

$$I_{2l} = (2n-1)(2n-5)\lambda_{2l}(s^{2n-2}) - 2n(2n+1)\lambda_{2l}(s^{2n}),$$
$$J_{2l} = 2(2n-1)(2n-2)\lambda_{2l}(s^{2n-2}) - 4n(2n+1)\lambda_{2l}(s^{2n})$$

while

$$I_{2n} = -2n(2n+1)\lambda_{2n}(s^{2n}), \qquad J_{2n} = -4n(2n+1)\lambda_{2n}(s^{2n}).$$

Using (3.7), $J_{2l} < 0$ and $I_{2l} < 0$ when $2 \leq l \leq 2n$ follows from a straightforward verification.

□

To complete the task at hand for odd modes, as $\alpha = -6c_0 - \frac{8+6c_{-1}}{2n+1}$, by lemma 3.2.2 $\alpha + \lambda_{2l+1}(g_1) < -6c_0$. For the even modes, lemma 3.2.3 shows $\alpha + \lambda_{2l}(g_1) < \alpha < 0$ holds under (3.12).

Condition (iii)

To verify (iii) for the odd modes $3 \leq 2l+1 \leq 2n-1$, by lemma 3.2.2 we have $\alpha + \lambda_{2l+1}(g_1) < -6c_0$. From Table 3.1,

$$\lambda_{2l+1}(g_2) = \lambda_{2l+1}(s^{2n-1})(R_{2n+1,2l+1} + \frac{2c_{-1}-(2n-1)}{2n+1}),$$
$$\lambda_{2l+1}(g_3) = \frac{\lambda_{2l+1}(s^{2n-1})}{2n+1}(R_{2n+1,2l+1} - (1+c_{-1})),$$

with $R_{2n+1,2l+1}$ denoting the ratio (3.7). For $3 \leq 2l+1 \leq 2n-1$ it therefore suffices to demonstrate

$$6c_0\left((1+c_{-1}) - R_{2n+1,2l+1}\right) > \lambda_{2l+1}(s^{2n-1})(2n+1)\left(R_{2n+1,2l+1} + \frac{2c_{-1}-(2n-1)}{2n+1}\right)^2. \tag{3.13}$$

Under the hypothesis (3.12), the quantity in parentheses on the left hand side dominates the quantity in parentheses on the right hand side. Therefore, the inequality

$$6c_0 > \lambda_{2l+1}(s^{2n-1})(2n+1)\left(R_{2n+1,2l+1} + \frac{2c_{-1}-(2n-1)}{2n+1}\right)$$

implies (3.13). Simplifying the right hand side then gives

$$6c_0 > (2n+1)(\lambda_{2l+1}(s^{2n+1}) + \frac{2c_{-1}-(2n-1)}{2n+1}\lambda_{2l+1}(s^{2n-1})).$$

As the right hand side increases with l, we set $l=1$ to discover a sufficient bound on c_0, that

$$6c_0 > (2n+1)(\lambda_3(s^{2n+1}) + \frac{2c_{-1}-(2n-1)}{2n+1}\lambda_3(s^{2n-1})).$$

Computing this directly using (3.10) shows that, due to (3.12),

$$(2n+1)(\lambda_3(s^{2n+1}) + \frac{2c_{-1}-(2n-1)}{2n+1}\lambda_3(s^{2n-1})) < \frac{18c_{-1}}{2n+1} < 6c_0 \tag{3.14}$$

as desired.

For the even modes $2 \leq 2l \leq 2n-2$, by lemma 3.2.3 $\alpha + \lambda_{2l}(g_1) \leq \alpha = -(6c_0 + \frac{8+6c_{-1}}{2n+1})$. From Table 3.1, compute

$$\lambda_{2l}(g_2) = (1+c_{-1})\left(\frac{2n-1}{2n+1}\lambda_{2l}(s^{2n-2}) - \lambda_{2l}(s^{2n})\right)$$
$$\lambda_{2l}(g_3) = -\frac{c_{-1}\lambda_{2l}(s^{2n})}{2n}.$$

It is enough therefore to show

$$\frac{c_{-1}(8+6c_{-1}+6(2n+1)c_0)}{2n(2n+1)} > (1+c_{-1})^2\left(\frac{2n-1}{2n+1}R^{-1}_{2n,2l} - 1\right)^2\lambda_{2l}(s^{2n}). \tag{3.15}$$

As $|\frac{2n-1}{2n+1}R^{-1}_{2n,2l} - 1| \leq 1$ for $n \geq 1$, the inequality

$$\frac{c_{-1}(8+6c_{-1}+6(2n+1)c_0)}{2n(2n+1)} > (1+c_{-1})^2\left|\frac{2n-1}{2n+1}\lambda_{2l}(s^{2n-2}) - \lambda_{2l}(s^{2n})\right|$$

in fact implies (3.15). As

$$\frac{2n+3}{2n}\lambda_{2l}(s^{2n}) - \frac{2n-1}{2n+1}\lambda_{2l}(s^{2n-2}) > \lambda_{2l}(s^{2n}) - \frac{2n-1}{2n+1}\lambda_{2l}(s^{2n-2}) > 0$$

and decreases with l, we again set $l = 1$ to discover a sufficient bound, that

$$\begin{aligned}&\frac{c_{-1}(8 + 6c_{-1} + 6(2n+1)c_0)}{2n(2n+1)} > \\ &(1+c_{-1})^2\left(\frac{2n+3}{2n}\lambda_2(s^{2n}) - \frac{2n-1}{2n+1}\lambda_2(s^{2n-2})\right) = \frac{6(1+c_{-1})^2}{(2n+1)^2}.\end{aligned} \tag{3.16}$$

After simplifying, we find that (3.16) holds when (3.12) does. For the remaining even mode $l = 2n$, as $\lambda_{2n}(g_1) < 0$ it suffices to demonstrate

$$\frac{c_{-1}(8 + 6c_{-1} + 6(2n+1)c_0)}{2n(2n+1)} > (1+c_{-1})^2\lambda_{2n}(s^{2n}).$$

As $\lambda_{2n}(s^{2n}) \leq \frac{2}{2n(2n+1)}$ when $n \geq 1$, this holds under the hypothesis (3.12). This completes the proof of theorem 3.2.1.

3.3 An Unstable Even Mode

We now turn to the problem of destabilizing an even mode $2n+2$ for $n \in \mathbb{N}$. We utilize an interaction kernel of the form $g(1-s) = c_0(1+3s) + c_{-2}s^{2n-1} + c_{-1}s^{2n} - \frac{2n+3}{2n+1}s^{2n+1}$. Enforcing $R = 1$ shows $c_{-2} = 1 + c_{-1}$. We then have

$$\lambda_{2n+2}(g_3) = \frac{2n+3}{(2n+1)(2n+2)}\lambda_{2n+2}(s^{2n+2}) > 0$$

by (3.6). As before, mode $2n+2$ is unstable independently of the choices of c_0, c_{-1}.

We now turn our attention to establishing

Theorem 3.3.1. *Let* $g(s) = c_0(1+3(1-s)) + (1+c_{-1})(1-s)^{2n-1} + c_{-1}(1-s)^{2n} - \frac{2n+3}{2n+1}(1-s)^{2n+1}$ *for* $n \geq 1$. *Then for all* c_0, c_{-1} *such that*

$$c_{-1} > n + \frac{1}{2}, \qquad\qquad c_0 > \frac{4c_{-1}}{2n+1}, \tag{3.17}$$

$g(s)$ *exhibits a pure mode* $2n+2$ *instability.*

s^m	α	g_1	g_2	g_3
$m=0$	$-6c_0+\frac{8+2c_{-1}}{2n+1}$	$-3c_0$	c_0	0
$m=1$	0	$5c_0$	$2c_0$	$-c_0$
$m=2$	0	$-6c_0$	$-3c_0$	$-\frac{3c_0}{2}$
$m=2n-2$	0	$-c_{-2}(2n-1)$	0	0
$m=2n-1$	0	$(2n-2)c_{-1}+2(2n-1)$	c_{-2}	0
$m=2n$	0	$2nc_{-1}+3$	-1	$-\frac{1+c_{-1}}{2n}$
$m=2n+1$	0	$-2(2n+3)-(2n+1)c_{-1}$	$-c_{-1}-\frac{2n+3}{2n+1}$	$-\frac{c_{-1}}{2n+1}$
$m=2n+2$	0	$\frac{(2n+2)(2n+3)}{2n+1}$	$\frac{2n+3}{2n+1}$	$\frac{2n+3}{(2n+1)(2n+2)}$

Table 3.2: Coefficients of the auxiliary quantities (3.2) when using a kernel of the form in theorem 3.3.1.

For $l=0$, as $g(2)=-2c_0+\frac{2}{2n+1}$ and $c_0>\frac{1}{2n+1}$ we have stability of mode $l=0$. For $l=1$, we need $0<\int_{-1}^{1} g(1-s)(1-s^2)\,\mathrm{d}s = c_0\int_{-1}^{1}(1-s^2)\mathrm{d}s + c_{-1}\int_{-1}^{1} s^{2n}(1-s^2)$, which holds trivially as $c_0, c_{-1}>0$. For $l\geq 2$, we compute the auxiliary quantities in terms of powers s^m for $0\leq m\leq 2n+2$ and summarize the results in Table 3.2. We now verify that (i-iii) in (3.5) hold for $l\geq 2$ under the requirement (3.17).

Condition (i)

For odd modes $3\leq 2l+1\leq 2n+1$ we check $\lambda_{2l+1}(g_3)=-\frac{c_{-1}}{2n+1}\lambda_{2l+1}(s^{2n+1})<0$ as $c_{-1}>0$. Because $l=n$ is the most restrictive case for the even modes $2\leq 2l\leq 2n$, it suffices to have

$$\frac{2n+3}{(2n+1)(2n+2)}\lambda_{2l}(s^{2n+2}) < \frac{1+c_{-1}}{2n}\lambda_{2l}(s^{2n}) \quad \Leftrightarrow (1+c_{-1}) > \frac{n(2n+3)}{4n+3},$$

by using (3.7), which holds due to (3.17).

Condition (ii)

To demonstrate (ii), as in the odd case, we first establish two lemmas that provide upper bounds for $\lambda_{2l}(g_1)$ and $\lambda_{2l+1}(g_1)$.

Lemma 3.3.2. *Let $2 \leq 2l \leq 2n$ and c_0, c_{-1} satisfy (3.17). Then $\lambda_{2l}(g_1) \leq \frac{4c_{-1}+8}{2n+1}$.*

Proof. Write $\lambda_{2l}(g_1) + 3c_{-1}\lambda_{2l}(s^{2n}) = c_{-1}I_{2l} + J_{2l}$, where $I_{2l} = (2n+3)\lambda_{2l}(s^{2n}) - (2n-1)\lambda_{2l}(s^{2n-2})$ and $J_{2l} = \frac{(2n+3)(2n+2)}{(2n+1)}\lambda_{2l}(s^{2n+2}) + 3\lambda_{2l}(s^{2n}) - (2n-1)\lambda_{2l}(s^{2n-2})$. Using (3.8), when $2 \leq 2l-2 \leq 2n-2$

$$I_{2l} = I_{2l-2} + (4l-1)\left[\frac{(2n-1)\lambda_{2l-2}(s^{2n-2})}{2n+2l-1} - \frac{(2n+3)\lambda_{2l-2}(s^{2n})}{2n+2l+1}\right].$$

By (3.7), the quantity in brackets is negative in the relevant cases, so that $I_{2l} < I_{2l-2} \leq I_2$. Similarly, we have that

$$J_{2l} = J_{2l-2} + (4l-1)\left[\frac{(2n-1)\lambda_{2l-2}(s^{2n-2})}{2n+2l-1} - \frac{3\lambda_{2l-2}(s^{2n})}{2n+2l+1} - \frac{(2n+2)(2n+3)\lambda_{2l-2}(s^{2n+2})}{(2n+1)(2n+2l+3)}\right].$$

To have $J_{2l} < J_{2l-2} \leq J_2$ in the relevant cases, we therefore require that

$$1 < \frac{3n}{(n-l+1)(2n+2l+1)} + \frac{n(n+1)(2n+2)(2n+3)}{(n-l+1)(n-l+2)(2n+2l+1)(2n+2l+3)}.$$

As the right hand side increases with l, we set $l=2$ and ask that $(n-1)(2n+5)(2n+7) < 3n(2n+7) + (n+1)(2n+2)(2n+3)$, or equivalently $26n + 41 > 0$.

Consequently, $\lambda_{2l}(g_1) \leq J_2 + c_{-1}I_2$ when $2 \leq 2l \leq 2n-2$. By direct computation from (3.10), $I_2 = \frac{4}{2n+1}$ and $J_2 = \frac{32(n+2)^2-44}{(2n+1)(2n+3)(2n+5)} \leq \frac{8}{2n+1}$, which demonstrates the claim for the cases $2 \leq 2l \leq 2n-2$. For the remaining case $2l = 2n \geq 2$, $\lambda_{2n}(g_1) = J_{2n} + c_{-1}I_{2n}$ where

$$I_{2n} = 2n\lambda_{2n}(s^{2n}) \qquad J_{2n} = \left[\frac{(2n+2)(2n+3)}{2n+1}R_{2n+2,2n} + 3\right]\lambda_{2n}(s^{2n}).$$

Maximizing these quantities over integers at $n=1$ yields $\lambda_{2n}(g_1) \leq \frac{2c_{-1}+8}{2n+1}$. □

Lemma 3.3.3. *Let $3 \leq 2l+1 \leq 2n+1$ and $c_{-1} > 0$. Then $\lambda_{2l+1}(g_1) < 0$.*

Proof. This follows exactly as in the proof of lemma 3.2.3. □

To complete the task at hand for even modes $2 \leq 2l \leq 2n$. As $\alpha = -6c_0 + \frac{8+2c_{-1}}{2n+1}$ it suffices to take $6c_0 \geq \frac{16+6c_{-1}}{2n+1}$, which proves less restrictive than (3.17). By lemma 3.3.3, $\lambda_{2l+1}(g_1) \leq 0$, so this suffices for the odd modes as well.

Condition (iii)

Lastly, we move to (iii). For the even modes $2 \leq 2l \leq 2n$, by lemma 3.3.2 and Table 3.2

$$\begin{aligned}
\alpha + \lambda_{2l}(g_1) &\leq -6c_0 + \frac{6c_{-1}+16}{2n+1} \\
\lambda_{2l}(g_3) &= \lambda_{2l}(s^{2n}) \left[\frac{(2n+3)R_{2n+2,2l}}{(2n+2)(2n+1)} - \frac{1+c_{-1}}{2n} \right] \\
\lambda_{2l}(g_2) &= \lambda_{2l}(s^{2n}) \left[\frac{(2n+3)R_{2n+2,2l}}{2n+1} - 1 \right].
\end{aligned}$$

It is therefore adequate to show

$$\begin{aligned}
(6c_0 - \frac{6c_{-1}+16}{2n+1}) \left[(1+c_{-1}) - \frac{2n(2n+3)R_{2n+2,2l}}{(2n+2)(2n+1)} \right] \geq \\
2n\lambda_{2l}(s^{2n}) \left[\frac{(2n+3)R_{2n+2,2l}}{2n+1} - 1 \right]^2. \qquad (3.18)
\end{aligned}$$

Due to (3.17), the quantity in brackets on the left hand dominates the (positive) quantity in brackets on the right hand side. Therefore, the inequality

$$(6c_0 - \frac{6c_{-1}+16}{2n+1}) \geq 2n\lambda_{2l}(s^{2n}) \left[\frac{(2n+5)R_{2n+2,2l}}{2n+1} - 1 \right]$$

certainly implies (3.18). As the right hand side decreases with l, we set $l = 1$ to discover a sufficient bound on c_0, that

$$6c_0 > \frac{6c_{-1}+16}{2n+1} + 2n\lambda_2(s^{2n}) \left[\frac{(2n+5)R_{2n+2,2}}{2n+1} - 1 \right].$$

Computing this directly from (3.10) shows that indeed

$$6c_0 > \frac{24c_{-1}}{2n+1} > \frac{6c_{-1}+16}{2n+1} + \frac{8n}{(2n+1)(2n+3)}$$

as desired.

For the odd modes $3 \leq 2l+1 \leq 2n-1$, by lemma 3.3.3 $\alpha+\lambda_{2l+1}(g_1) \leq \alpha = -6c_0+\frac{8+2c_{-1}}{2n+1}$. From Table 3.2,

$$\lambda_{2l+1}(g_2) = \lambda_{2l+1}(s^{2n+1})\left[c_{-1}(R^{-1}_{2n+1,2l+1}-1)+R^{-1}_{2n+1,2l+1}-\frac{2n+3}{2n+1}\right],$$
$$\lambda_{2l+1}(g_3) = -\frac{c_{-1}\lambda_{2l+1}(s^{2n+1})}{2n+1},$$

so it suffices to demonstrate

$$(6c_0-\frac{8+2c_{-1}}{2n+1})\frac{c_{-1}}{2n+1} \geq \lambda_{2l+1}(s^{2n+1})\left[c_{-1}(R^{-1}_{2n+1,2l+1}-1)+R^{-1}_{2n+1,2l+1}-\frac{2n+3}{2n+1}\right]^2. \tag{3.19}$$

As $\left|c_{-1}(R^{-1}_{2n+1,2l+1}-1)+R^{-1}_{2n+1,2l+1}-\frac{2n+3}{2n+1}\right| \leq 1+c_{-1}$, the inequality

$$(6c_0-\frac{8+2c_{-1}}{2n+1})\frac{c_{-1}}{2n+1} \geq (1+c_{-1})\left|(1+c_{-1})\lambda_{2l+1}(s^{2n-1})-(\frac{2n+3}{2n+1}+c_{-1})\lambda_{2l+1}(s^{2n+1})\right|.$$

implies (3.19). We have

$$\left|(1+c_{-1})\lambda_{2l+1}(s^{2n-1})-(\frac{2n+3}{2n+1}+c_{-1})\lambda_{2l+1}(s^{2n+1})\right| < (1+c_{-1})\left(\frac{2n+5}{2n+1}\lambda_{2l+1}(s^{2n+1})-\lambda_{2l+1}(s^{2n-1})\right),$$

where the right hand side decreases with l. Setting $l=1$, we discover a sufficient requirement on c_0, that

$$(6c_0-\frac{8+2c_{-1}}{2n+1})\frac{c_{-1}}{2n+1} \geq (1+c_{-1})^2\left(\frac{2n+5}{2n+1}\lambda_3(s^{2n+1})-\lambda_3(s^{2n-1})\right) = \frac{4(1+c_{-1})^2}{(2n+1)(2n+3)}.$$

After simplification, we obtain

$$6c_0 \geq \frac{6c_{-1}+16}{2n+1}+(8+4c_{-1})\left(\frac{1}{2n+3}-\frac{1}{2n+1}\right)+\frac{4}{(2n+3)c_{-1}},$$

which proves less restrictive than (3.17). For the remaining odd mode $l=2n+1$ we have

$$\alpha+\lambda_{2n+1}(g_1) \leq -6c_0+\frac{2c_{-1}+8}{2n+1}$$
$$\lambda_{2n+1}(g_2) = -\lambda_{2n+1}(s^{2n+1})\left[c_{-1}+\frac{2n+3}{2n+1}\right],$$
$$\lambda_{2n+1}(g_3) = -\frac{c_{-1}\lambda_{2l+1}(s^{2n+1})}{2n+1},$$

so that we demonstrate

$$(6c_0 - \frac{8+2c_{-1}}{2n+1})\frac{c_{-1}}{2n+1} \geq \lambda_{2n+1}(s^{2n+1})\left(c_{-1} + \frac{2n+3}{2n+1}\right)^2.$$

But, if $n \geq 1$ then $\lambda_{2n+1}(s^{2n+1}) \leq \frac{2}{(2n+1)^2}$. Therefore, we conclude the proof of theorem 3.3.1 if

$$6c_0 \geq \frac{4c_{-1} + 8 + 4(\frac{2n+3}{2n+1}) + \frac{2}{c_{-1}}\left(\frac{2n+3}{2n+1}\right)^2}{2n+1}.$$

We find this holds due to (3.17).

3.4 Potentials with Arbitrary Instabilities

With theorems 3.1.3,3.2.1 and 3.3.1 established, we now have all the necessary ingredients to construct interaction kernels that exhibit arbitrary instabilities. To illustrate the general procedure, we first construct an interaction kernel with a single unstable mode. We take an interaction kernel of the form $g(s) = g^{2n+1}(s) + \epsilon_1 g^p(s)$ for a single odd mode $2n+1$. Here $g^{2n+1}(s)$ denotes any degree $2n$ polynomial satisfying the hypotheses of theorem 3.2.1 and $g^p(s)$ denotes any interaction kernel satisfying the hypotheses of theorem 3.1.3. The stability condition for $l = 0$ reads $g(2) < 0$, which holds trivially when $\epsilon_1 > 0$ as both $g^{2n+1}(2) < 0$ and $g^p(2) < 0$. The stability condition for $l = 1$ holds trivially as well. Due to the linearity of $\Omega_l(g)$ in g, we find

$$\Omega_l(g) := \Omega_l(g^{2n+1} + \epsilon_1 g^p) = \Omega_l(g^{2n+1}) + \epsilon_1 \Omega_l(g^p). \tag{3.20}$$

As a consequence of theorem 3.2.1, $\Omega_l(g^{2n+1})$ has non-positive eigenvalues when $l \geq 2$ and $l \neq 2n+1$, while $\Omega_l(g^p)$ has strictly negative eigenvalues as a consequence of theorem 3.1.3. Due to the column-scaled structure of $\Omega_l(f)$ from (3.4), for any function f there exists an orthonormal basis for $\mathbb{R}^2$ with respect to the inner product $\langle \vec{c_1}, \vec{c_2} \rangle_D = \langle D\vec{c_1}, \vec{c_2} \rangle$. Here $D = \text{diag}(1, l(l+1))$ and $\langle , \rangle$ denotes the Euclidean inner-product on $\mathbb{R}^2$. Therefore $\Omega_l(f)$ has negative eigenvalues if and only if $\langle D\vec{c}, \Omega_l(f)\vec{c} \rangle < 0$ for all $\vec{c} \in \mathbb{R}^2$. Taking the inner product $\langle , \rangle_D$ of (3.20) shows that $\Omega_l(g)$ has only negative eigenvalues whenever $2 \leq l$ and $l \neq 2n+1$, provided $\epsilon_1 > 0$. Thus, the interaction kernel $g(s) := g^{2n+1}(s) + \epsilon_1 g^p(s)$ has all

modes $l \neq 2n+1$ stable. To preserve the instability of mode $2n+1$, we take ϵ_1 small enough to ensure the instability condition $\lambda_{2n+1}(g_3) > 0$. From the definitions of g^{2n+1}, g^p and g_3 this reads as

$$\epsilon_1 < \frac{(1-p)\lambda_{2n+1}(s^{2n+1})}{|(2n+1)\lambda_{2n+1}((1-s)^{1-p})|} = \frac{(1-p)2^{2n+p}\pi\Gamma^2(2n+2)\Gamma(2n+4-p)}{(2n+1)\sin(\pi(1-p))\Gamma^2(2-p)\Gamma(2n+p)\Gamma(4n+4)}, \tag{3.21}$$

by a direct computation using (3.6) and lemma 3.1.2. Similarly, for an even mode the interaction kernel $g(s) = g^{2n+2}(s) + \epsilon_1 g^p(s)$ yields a single unstable mode $2n+2$ provided

$$\epsilon_1 < \frac{(2n+3)(1-p)2^{2n+p+1}\pi\Gamma^2(2n+3)\Gamma(2n+5-p)}{(2n+1)(2n+2)\sin(\pi(1-p))\Gamma^2(2-p)\Gamma(2n+p+1)\Gamma(4n+6)}. \tag{3.22}$$

To create an interaction kernel with precisely two unstable modes, say n_1 and n_2 with $n_1 < n_2$, we let $g(s) := \frac{1}{\epsilon_1} g^{n_1}(s) + \frac{1}{\epsilon_2} g^{n_2}(s) + g^p(s)$ and attempt to choose $\epsilon_1, \epsilon_2 > 0$ in a manner that preserves the instability of the modes n_1 and n_2. As before, $g^{n_i}(s)$ denotes the appropriate degree $n_i - 1$ polynomial from theorem 3.2.1 or theorem 3.3.1, and $g^p(s)$ denotes a stable sphere furnished from theorem 3.1.3. By linearity, $g_3(s) = \frac{1}{\epsilon_1} g_3^{n_1}(s) + \frac{1}{\epsilon_2} g_3^{n_2}(s) + g_3^p(s)$. As the auxiliary quantity $g_3^{n_1}$ is a polynomial of degree $n_1 < n_2$, the coefficient $\lambda_{n_2}(g_3^{n_1})$ vanishes so the instability condition $\lambda_{n_2}(g_3) > 0$ reads as

$$\epsilon_2 < \frac{(1-p)\lambda_{n_2}(g_3^{n_2})}{|\lambda_{n_2}((1-s)^{1-p})|}.$$

This takes the same form as (3.21) and (3.22). Therefore, for ϵ_2 sufficiently small $g(s)$ exhibits a mode n_2 instability. Having chosen ϵ_2, we then select ϵ_1 to satisfy the instability condition for mode n_1, i.e. that $\lambda_{n_1}(g_3) > 0$. This places the restriction on ϵ_1 that

$$\epsilon_1 < \frac{(1-p)\lambda_{n_1}(g_3^{n_1})}{|\lambda_{n_1}((1-s)^{1-p})| + (1-p)\frac{1}{\epsilon_2}|\lambda_{n_1}(g_3^{n_2})|}.$$

For any such $\epsilon_1, \epsilon_2 > 0$, all modes $l \in \mathbb{N} \setminus \{n_1, n_2\}$ are stable by the same inner product argument as in the single mode case.

Creating an interaction kernel with any finite number of unstable modes $n_1 < n_2 < \ldots < n_k$ follows the exact same procedure: we choose a positive linear combination of $g^{n_i}, 1 \leq i \leq k$

and g^p in a manner that preserves the instability conditions $\lambda_{n_i}(g_3) > 0$ for all $1 \leq i \leq k$. The interaction kernel takes the form

$$g(s) = \sum_{i=1}^{k} \frac{1}{\epsilon_i} g^{n_i}(s) + g^p(s).$$

Beginning with ϵ_1, we then inductively choose the coefficients to maintain $\lambda_{n_i}(g_3) > 0$:

$$\epsilon_i < \frac{(1-p)\lambda_{n_i}(g^{n_i})}{|\lambda_{n_i}((1-s)^{1-p})| + (1-p)\sum_{j=i+1}^{k} \frac{1}{\epsilon_j} |\lambda_{n_i}(g^{n_j})|}.$$

This solves our linearized inverse statistical mechanics problem, yielding an interaction kernel with exactly the specified instabilities.

3.5 Numerical Examples

The analytical framework provided by theorem 3.2.1, 3.3.1 and the construction in § 3.4 allows us to create pairwise potentials with arbitrary instabilities. This framework serves as a powerful tool for investigating the minimizers of (1.1), and in this section we provide several numerical examples of these constructions. In each of our simulations we compute steady states of (1.2) using gradient descent, and end the simulation when the l^∞ norm of (1.2) falls below $.001/N$. Unless stated otherwise, initial conditions were randomly distributed on the unit sphere. Also, as the maximal distance between any two particles in a computed steady state does not exceed 2.1 and the conditions for stability only require values of the potential $V(s)$ for $s \in [0, 2]$, we could redefine $V(s)$ for $s > 2.1$ without affecting the validity of our conclusions. While we do not do so here, this observation may prove useful for simulating higher order even modes where the potential becomes repulsive in the far-field.

We begin with a numerical study of the kernels with a single unstable mode,

$$\begin{aligned} g^{2n+1}(s) =& c_0(1 + 3(1-s)) + \frac{2n-1}{2n+1}(1 + c_{-1})(1-s)^{2n-2} + \\ & c_{-1}(1-s)^{2n-1} - (1-s)^{2n} + \epsilon \left(s^{-p} - \frac{2^{1-p}}{2-p} \right), \\ g^{2n+2}(s) =& c_0(1 + 3(1-s)) + (1 + c_{-1})(1-s)^{2n-1} + \\ & c_{-1}(1-s)^{2n} - \frac{2n+3}{2n+1}(1-s)^{2n+1} + \epsilon \left(s^{-p} - \frac{2^{1-p}}{2-p} \right), \end{aligned}$$

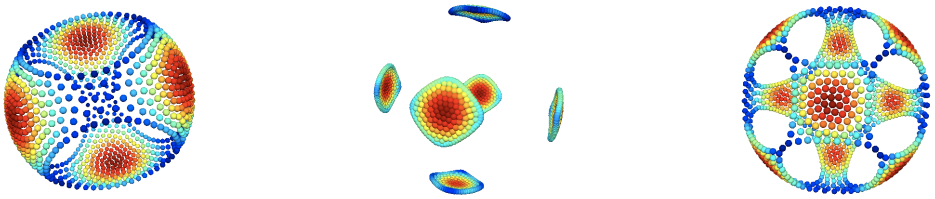

(a) Steady state with a mode 3 instability

(b) Steady state with a mode 4 instability

(c) Steady state with a mode 5 instability

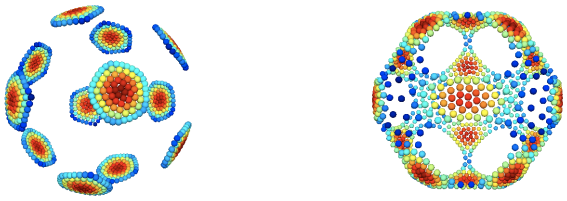

(d) Steady state with a mode 6 instability

(e) Steady state with a mode 7 instability

Figure 3.2: Steady states for potentials with a single unstable mode. The number of particles $N = 1000$, and the color of a particle indicates its distance to the center of mass, i.e. the origin.

for modes 3 through 7 with varying choices of the parameters $(c_0, c_{-1}, p, \epsilon)$. Figure 3.2 shows the results for $N = 1000$; the color of a particle indicates its distance from the origin. We plot the corresponding potentials $\frac{\mathrm{d}V}{\mathrm{d}s} := -g(s)$ themselves in figure 3.3. We normalize each potential to $V(0) = 1$ and plot the resulting function for $s \in [0, \frac{5}{2}]$, as the distance between any two particles in a given steady state falls well within this range. After normalization, the potentials have some commonality: each is convex over the entire interval and possess a single local minimum. However, as figure 3.2 demonstrates, the potentials produce vastly different ground states despite this superficial similarity. Thus it is the linear theory from [71] that provides a means of making rather subtle yet meaningful distinctions between potentials.

Next, we fix a particular unstable mode 6 potential with parameters $(c_0, c_{-1}, p) = (2.5, 4, .25)$

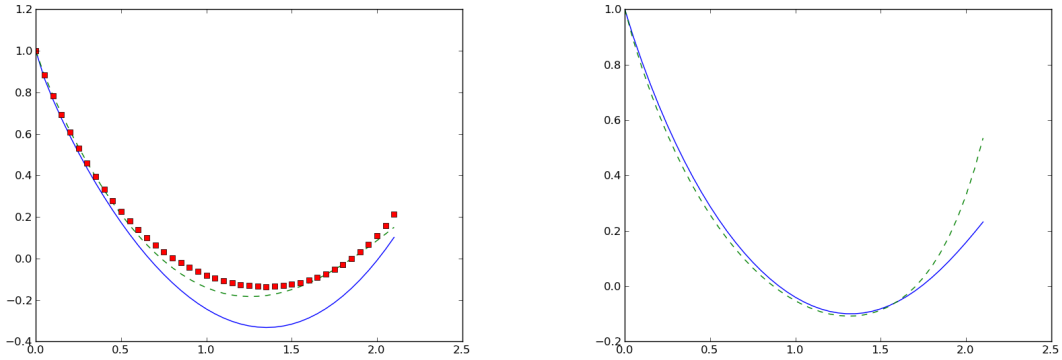

Figure 3.3: Unstable mode 3-7 potentials $V(s)$, plotted for $s \in [0, \frac{5}{2}]$ and normalized to $V(0) = 1$. Left— blue is the unstable mode 3 potential, green is the unstable mode 4 and red is the unstable mode 5. Right— blue is the unstable mode 6 potential and green is the unstable mode 7.

and investigate how the steady states vary with the parameter ϵ. We begin by taking the previous value $\epsilon = 1.75$ with random initial conditions as before, and solve (1.2) to steady state with $N = 300$. We decrease ϵ by .1, begin the simulation again with the previous steady state as an initial condition, and then repeat. Figure 3.4 displays the results after iterating this procedure three times. The steady states for $\epsilon = 1.75$ and $\epsilon = 1.65$ appear similar: particles concentrate along the same 5^{th} degree spherical harmonic, and the particle density increases when ϵ decreases. An **i**ntramode bifurcation occurs as ϵ continues to decrease; for $\epsilon = 1.55$, a different spherical harmonic of the same degree appears. It persists for $\epsilon = 1.45$ with slightly denser groups of particles. The linear theory indicates that, in principle, any 5^{th} degree spherical harmonic could appear. However, this numerical study suggests that this does not happen: when $\epsilon = 1.55$, we begin with a given spherical harmonic as an initial condition and find a different harmonic as the steady state. Instead, for a fixed potential it appears that the steady state lies near the same 5^{th} degree spherical harmonic regardless of initial conditions. We find this behavior characterizes potentials with a single unstable mode, in that intramode bifurcations occur as ϵ varies. The linear theory provides no indication for which harmonic gets selected, and this remains an open problem.

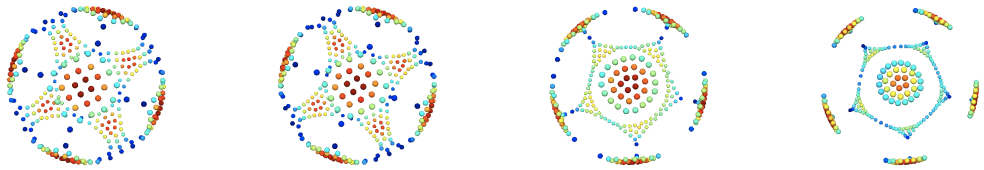

(a) $\epsilon = 1.75$ (b) $\epsilon = 1.65$ (c) $\epsilon = 1.55$ (d) $\epsilon = 1.45$

Figure 3.4: An unstable mode 5 potential for varying values of the ϵ parameter. An intramode bifurcation occurs between figures (b) and (c).

Lastly, using the construction in § 3.4 we provide some examples of interaction kernels that have multiple unstable modes. Specifically, we investigate a linear combination of the mode 3 kernel and the mode 5 kernel from before,

$$\begin{aligned} g(s) &= \frac{1}{\epsilon} g^3(s) + g^5(s) + 1.75 \left(s^{-1/4} - \frac{2^{3/4}}{1.75} \right), \\ g^3(s) &= \frac{13}{6} + \frac{11}{2}(1-s) - (1-s)^2, \\ g^5(s) &= 2.5(1 + 3(1-s)) + 3(1-s)^2 + 4(1-s)^3 - (1-s)^4. \end{aligned}$$

Following § 3.4, for all $\epsilon > 0$ we know that $g(s)$ exhibits a mode 5 instability and a mode 3 instability as well for all ϵ sufficiently small. Furthermore, $g(s)$ exhibits only these instabilities. We simulate as before: beginning with $\frac{1}{\epsilon} = 3.3$, we allow the particles to reach steady state, decrease $\frac{1}{\epsilon}$ by .1, and use the previous steady state as the new initial condition. Figure 3.5 shows the resulting steady states for $N = 300$. Particles begin by concentrating along a 3^{rd} degree spherical harmonic. In a similar fashion to the previous example, at first $\lambda_3(g_3) > 0$. As $\frac{1}{\epsilon}$ decreases $\lambda_3(g_3)$ remains positive, yet an intramode bifurcation occurs at $\frac{1}{\epsilon} = 3.2$. Particles then continue to concentrate along this harmonic with decreasing density until we observe another intramode bifurcation at $\frac{1}{\epsilon} = 2.8$. In this case $\lambda_3(g_3)$ becomes negative but condition (iii) in theorem 3.1.1 fails, so the mode 3 instability persists. Eventually an **intermode bifurcation** occurs at $\frac{1}{\epsilon} = 2.7$, when mode 3 stabilizes. In these remaining cases, a 5^{th} degree spherical harmonic now visually dominates in the steady state as opposed to a 3^{rd} degree spherical harmonic.

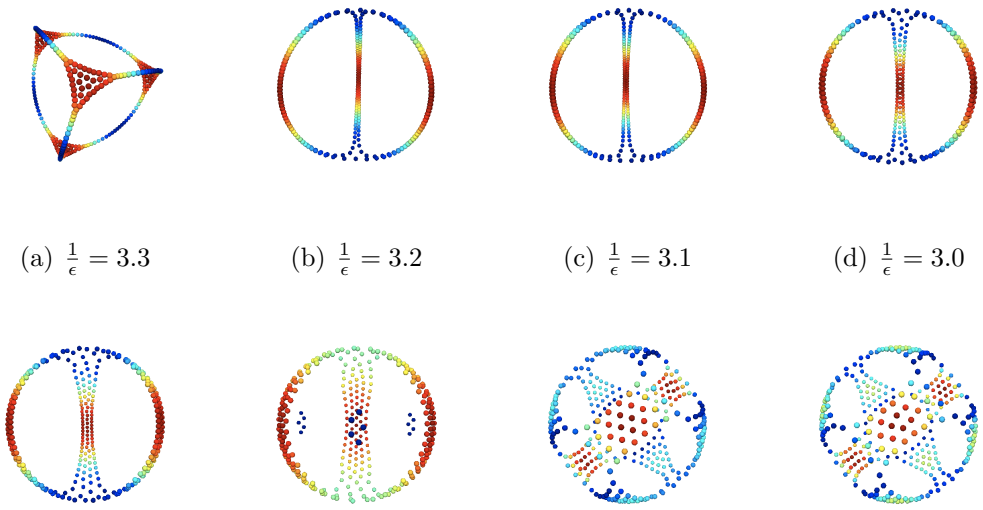

(a) $\frac{1}{\epsilon} = 3.3$ (b) $\frac{1}{\epsilon} = 3.2$ (c) $\frac{1}{\epsilon} = 3.1$ (d) $\frac{1}{\epsilon} = 3.0$

(e) $\frac{1}{\epsilon} = 2.9$ (f) $\frac{1}{\epsilon} = 2.8$ (g) $\frac{1}{\epsilon} = 2.7$ (h) $\frac{1}{\epsilon} = 2.6$

Figure 3.5: An unstable $3-5$ mixed mode potential for varying values of the $\frac{1}{\epsilon}$ parameter. Intramode bifurcations occur between figures (a) and (b), then also between figures (e) and (f). An intermode bifurcation occurs between figures (f) and (g).

3.6 Discussion

This chapter both posed and solved the linearized inverse statistical mechanics problem: given a finite number of instabilities, we provided explicit formulas for potentials with precisely those instabilities. This construction allowed us to design complex, spherical formations of particles that minimize the fully nonlinear problem (1.1). The patterns form as the particles concentrate along one of the unstable spherical harmonics in the potential. In this regard, our work here provides further support for the connection between linear instability and pattern formation first uncovered in [71]. As the single mode examples indicate, the linear theory proves capable of drawing subtle distinctions between potentials (see figure 3.3) that result in readily observable consequences for the steady states (see figure 3.2), such as intermode bifurcations. Moreover, the precise control over the instabilities afforded by § 3.4 allowed us to explore aspects of this connection that the linear theory leaves unanswered. Principally, we gave numerical evidence that indicates only a single harmonic of the unstable degree will appear for a given potential despite the fact that all harmonics of the same degree are unstable. In other words, the linear theory does not provide a means for predicting intramode bifurcations. The route to understanding these bifurcations therefore probably lies in a weakly nonlinear analysis of spherical solutions. This remains an unanswered question and a subject for future research.

CHAPTER 4

Well-Posedness Theory

Whereas the previous chapters applied linear techniques to address nonlinear questions, this chapter begins the extension of the linear theory to a nonlinear one. The most basic aspects of the nonlinear theory concern the issues of existence and uniqueness for distribution solutions to the aggregation equation

$$\begin{aligned} &\frac{\partial \rho}{\partial t}(\mathbf{y},t) + \operatorname{div}(\rho(\mathbf{y},t)\mathbf{u}(\mathbf{y},t)) = 0, \quad \mathbf{y} \in \mathbb{R}^d, \quad t \geq 0, \\ &\mathbf{u}(\mathbf{y},t) = \int_{\mathbb{R}^d} g\left(\frac{1}{2}|\mathbf{y}-\mathbf{z}|^2\right)(\mathbf{y}-\mathbf{z})\,\rho(\mathbf{z},t)\,\mathrm{d}\mathbf{z}, \end{aligned} \tag{4.1}$$

where the density ρ concentrates on a co-dimension one manifold. We refer to these solutions aggregation sheets. Our main aim lies in extending the linear well-posedness theory from chapter 2 to the fully nonlinear problem. We therefore show that when the equation for the sheet is linearly well-posed then the fully non-linear evolution is also well-posed locally in time for the class of bi-Lipschitz surfaces. In other words, when the initial data $\Phi_0(\mathbf{x})$ defines a Lipschitz homeomorphism the fully non-linear problem is well-posed across the full range of linearly well-posed kernels. Moreover, we show that if the initial sheet is in fact C^1 then the solution itself remains C^1 as long as it remains Lipschitz. We then address issues regarding continuation and global existence of solutions. We prove that a unique continutation exists provided Φ and its inverse remain Lipschitz, and by explicit construction we show that finite time singularities of each type of may occur. For kernels with an attractive singularity at the origin, we generalize the results for $L^\infty(\mathbb{R}^d)$ [7] and general $L^p(\mathbb{R}^d)$ solutions [8] to (4.1) that show finite time singularity occurs if and only if the kernel is Osgood. Finally, for a subclass of the natural potentials studied in [14] [8] [7] we show that the solution exists globally when the kernel has a repulsive singularity at the origin.

To make our hypotheses on the interaction kernel $g(s)$ for these results precise, we recall that the linear theory from [71, 35] shows the solution $\Phi(\mathbf{x}) \equiv R\mathbf{x}$ is linearly well-posed only if

$$g\left(R^2(1-s)\right)(1-s^2)^{\frac{d-3}{2}} \in L^1([-1,1]). \tag{4.2}$$

For simplicity, we assume the kernel behaves as a power law, $g(s) = \mathcal{O}(s^p)$, near the origin, although our arguments apply in a more general context. The linear well-posedness condition then enforces

$$p > \frac{1-d}{2}. \tag{4.3}$$

This suggests the following assumptions on the interaction kernel:

Definition 4.0.1. *Let $g(s) : \mathbb{R}^+ \to \mathbb{R}$. Then $g(s)$ defines an **admissible interaction kernel** if $g \in C^1(\mathbb{R}^+ \setminus \{0\})$, and there exist constants $C > 0, \delta > 0, p > \frac{1-d}{2}$ such that*

$$\max\{|g(s)|, |sg'(s)|\} \leq Cs^p \quad \forall\, s \in (0,\delta). \tag{4.4}$$

We shall demonstrate well-posedness of the IDE in the space $C^{0,1}(\mathcal{S}^{d-1})$ of Lipschitz functions over the sphere $\mathcal{S}^{d-1}$, where $C^{0,1}(\mathcal{S}^{d-1})$ has the usual norm

$$||\Phi||_{C^{0,1}} := \max_{\mathcal{S}^{d-1}} |\Phi(\mathbf{x})| + \mathrm{Lip}[\Phi], \quad \mathrm{Lip}[\Phi] := \sup_{\mathbf{x}\neq\mathbf{w}} \frac{|\Phi(\mathbf{x}) - \Phi(\mathbf{w})|}{|\mathbf{x}-\mathbf{w}|}. \tag{4.5}$$

To allow for the singularity in $g(s)$ at zero, we restrict attention to initial data $\Phi_0(\mathbf{x})$ lying in the subset $\mathcal{O}_M \subset C^{0,1}(\mathcal{S}^{d-1})$ of all functions where both $\mathrm{Lip}[\Phi] \leq M$ and $\mathrm{Lip}[\Phi^{-1}] \leq M$,

$$\mathcal{O}_M := \left\{ \Phi \in C^{0,1}(\mathcal{S}^{d-1}) : \frac{1}{M} \leq \inf_{\mathbf{x}\neq\mathbf{w}} \frac{|\Phi(\mathbf{x}) - \Phi(\mathbf{w})|}{|\mathbf{x}-\mathbf{w}|} \leq \mathrm{Lip}[\Phi] \leq M \right\}. \tag{4.6}$$

This class of initial data proves less restrictive than the requirements on initial data that appear in related problems. As we enforce regularity in the kernel $g(s)$ this allows us to relax the regularity requirements on the initial sheet itself, and this makes our task somewhat easier. In particular, we need not assume any regularity in addition to boundedness of derivatives along the sheet. Similar results for vortex patches [43, 44] require Hölder regularity in derivatives, and results for the Birkhoff-Rott equation typically require analyticity [60] or other additional regularity hypotheses [73]. Proving an existence result for more singular

kernels, such as the Newtonian potential, would therefore require a different approach than we adopt here, so we make no effort in this direction. Also in contrast to many studies on the Birkhoff-Rott equation, we consider compact sheets instead of sheets homeomorphic to the real line. This also causes our approach to demonstrating existence to differ to a large extent.

The remainder of this chapter proceeds as follows: in section 2 we first establish the necessary estimates on the nonlocal term in the IDE, and this allows us derive local existence in section 3 using a modified version of simple Picard iteration; subsection 3.1 addresses issues regarding differentiability of solutions and the final section addresses questions regarding the long term behavior of solutions; we finish with some concluding remarks.

4.1 Elementary Properties and A-Priori Estimates

Like its co-dimension zero counterpart (4.1), solutions to the IDE (1.13) exhibit several conserved quantities. Foremost, it formally expresses conservation of mass in that

$$M_\rho := \int_{\mathbb{R}^d} \rho(\mathbf{x}, t) \equiv \int_{\mathcal{S}^{d-1}} f_0(\mathbf{x}) \, \mathrm{d}\mathcal{S}^{d-1}(\mathbf{x}) \tag{4.7}$$

for all time. Moreover, we have conservation of center of mass

$$\int_{\mathbb{R}^d} \mathbf{x}\rho(\mathbf{x}, t) = \int_{\mathcal{S}^{d-1}} \Phi(\mathbf{x}, t) \equiv \int_{\mathcal{S}^{d-1}} \Phi_0(\mathbf{x}), \tag{4.8}$$

which we assume equals zero throughout the remainder of the chapter. Potential energy also dissipates along solutions. Indeed, let $V(s)$ denote a potential for the evolution, i.e. that $\frac{\mathrm{d}V}{\mathrm{d}s} = -g(s)$, and define

$$E_\Phi(t) := \frac{1}{2} \int_{\mathcal{S}^{d-1} \times \mathcal{S}^{d-1}} V\left(\frac{1}{2}|\Phi(\mathbf{x}, t) - \Phi(\mathbf{z}, t)|^2\right) f_0(\mathbf{x}) f_0(\mathbf{z}) \, \mathrm{d}\mathcal{S}^{d-1}(\mathbf{x}) \mathrm{d}\mathcal{S}^{d-1}(\mathbf{z})$$

A simple calculation then formally yields

$$\frac{\mathrm{d}}{\mathrm{d}t} E_\Phi(t) = -\int_{\mathcal{S}^{d-1}} \left|\frac{\partial \Phi}{\partial t}\right|^2. \tag{4.9}$$

These statements can be readily justified using the arguments that follow.

We begin by recalling a standard theorem that will prove useful on several occasions, i.e. the Funk-Hecke formula for spherical harmonics [57]. Our desire to satisfying the integrability hypothesis for the formula further motivates for the growth rate (4.3) on $g(s)$ near the origin.

Theorem 4.1.1. *(Funk-Hecke Theorem)*

Let $h(s)(1-s^2)^{\frac{d-3}{2}} \in L^1([-1,1])$. *Then for any* $\mathbf{x} \in \mathcal{S}^{d-1}$ *and any spherical harmonic* $S^l(\mathbf{x})$ *of degree* l,

$$\int_{\mathcal{S}^{d-1}} h(\langle \mathbf{x}, \mathbf{w} \rangle) S^l(\mathbf{w}) \, \mathrm{d}\mathcal{S}^{d-1}(\mathbf{w}) = \\ \mathrm{vol}(\mathcal{S}^{d-2}) \left(\int_{-1}^{1} h(s)(1-s^2)^{\frac{d-3}{2}} P_{l,d}(s) \, \mathrm{d}s \right) S^l(\mathbf{x}),$$

where $P_{l,d}(s)$ *denotes the Gegenbauer polynomial* $P_l^{(\frac{d}{2}-1)}(s)$ *from [62] normalized to* $P_{l,d}(1) = 1$.

Before turning our attention to estimating the nonlocality in (1.13), we first illustrate utilize theorem 4.1.1 to construct the simple but important class of exact spherical solutions to (1.13). These solutions will later prove useful in determing how solutions to (1.13) behave for large times.

Example 4.1.2. *(Spherical Solutions) Let* $\Phi(\mathbf{x}, t) = R(t)\mathbf{x}$ *for* $R(t) > 0$ *and* $f_0(\mathbf{w}) \equiv 1$. *Substituting this expression into* (1.13) *yields*

$$\frac{\mathrm{d}R}{\mathrm{d}t}\mathbf{x} = R(t) \int_{\mathcal{S}^{d-1}} g\left(\frac{R(t)^2}{2} |\mathbf{x} - \mathbf{w}|^2 \right) (\mathbf{x} - \mathbf{w}) \, \mathrm{d}\mathcal{S}^{d-1}(\mathbf{w}).$$

The facts that $\mathbf{w}$ *is a spherical harmonic of degree one and that* $P_{l,d}(s) = s$ *combine with the Funk-Hecke theorem for* $l = 0, 1$ *to show*

$$\frac{\mathrm{d}R}{\mathrm{d}t}\mathbf{x} = \mathrm{vol}(\mathcal{S}^{d-2}) R(t) \left[\int_{-1}^{1} g\left(R(t)^2(1-s) \right) (1-s)(1-s^2)^{\frac{d-3}{2}} \, \mathrm{d}s \right] \mathbf{x}.$$

Therefore $\Phi(\mathbf{x}, t) = R(t)\mathbf{x}$ *defines a solution to* (1.13) *if* $R(t)$ *solves the ordinary differential equation*

$$\frac{\mathrm{d}R}{\mathrm{d}t} = \mathrm{vol}(\mathcal{S}^{d-2}) R(t) \int_{-1}^{1} g\left(R(t)^2(1-s) \right) (1-s)(1-s^2)^{\frac{d-3}{2}} \, \mathrm{d}s. \tag{4.10}$$

The case $l = 0$ of theorem 4.1.1 also proves useful in establishing the following two technical lemmas. Their proof constitutes the majority of the effort needed to establish theorem 4.2.1, as they suffice to show the right hand side of (1.13) is locally Lipschitz in $C^0(\mathcal{S}^{d-1})$. A combination of Picard iteration and a-posteriori estimates then yields the theorem. The first lemma estimates expressions of the form

$$H(\mathbf{y}) := \int_{\mathcal{S}^{d-1}} h\left(\frac{1}{2}|\mathbf{y} - \Phi(\mathbf{w})|^2\right) f_0(\mathbf{w}) \, \mathrm{d}\mathcal{S}^{d-1}(\mathbf{w}) \tag{4.11}$$

for all $\mathbf{y} \in \mathbb{R}^d$, where we envision $h(s) = g(s)$ or $h(s) = sg'(s)$ so that h satisfies a hypothesis similar to (4.4).

Lemma 4.1.3. *Let $h(s) : \mathbb{R}^+ \to \mathbb{R}$ be locally bounded away from zero, and suppose $\exists K > 0, \sigma > 0, q > \frac{1-d}{2}$ with $|h(s)| \leq Ks^q$ for all $s \in (0, \sigma)$. If $\Phi(\mathbf{x}) \in \mathcal{O}_M$ then*

$$|H(\mathbf{y})| \leq C(h, d_{\mathbf{y}}, M)||f_0||_{L^\infty}.$$

The constant C depends only on h, M and $d_{\mathbf{y}} := \min_{\mathbf{x}\in\mathcal{S}^{d-1}} |\mathbf{y} - \Phi(\mathbf{x})|$, and increases with both $d_{\mathbf{y}}$ and M.

Proof. Fix $\mathbf{y} \in \mathbb{R}^d$ and decompose

$$H(\mathbf{y}) = \int_{|\mathbf{y}-\Phi(\mathbf{w})|\geq\sqrt{2\sigma}} + \int_{|\mathbf{y}-\Phi(\mathbf{w})|<\sqrt{2\sigma}} := \mathrm{I} + \mathrm{II}.$$

Let $\mathbf{x}_0$ denote a minimizer of $|\mathbf{y} - \Phi(\mathbf{x})|$ over $\mathbf{x} \in \mathcal{S}^{d-1}$, so that $d_{\mathbf{y}} = |\mathbf{y} - \Phi(\mathbf{x}_0)|$. Due to the boundedness of h away from zero,

$$|\mathrm{I}| \leq \mathrm{vol}(\mathcal{S}^{d-1})||h||_{L^\infty([\sigma, 2M^2+d_{\mathbf{y}}^2])}||f_0||_{L^\infty(\mathcal{S}^{d-1})}.$$

As for the second integral, the growth hypothesis on h near zero implies that

$$|\mathrm{II}| \leq K2^{-q}||f_0||_{L^\infty(\mathcal{S}^{d-1})} \int_{\mathcal{S}^{d-1}} |\mathbf{y} - \Phi(\mathbf{w})|^{2q} \, \mathrm{d}\mathcal{S}^{d-1}(\mathbf{w}).$$

If $q \geq 0$ then $|\mathrm{II}| \leq K2^{-q}||f_0||_{L^\infty(\mathcal{S}^{d-1})}(d_{\mathbf{y}} + 2M)^{2q}\mathrm{vol}(\mathcal{S}^{d-1})$, so assume that $q < 0$. The facts that $|\mathbf{y} - \Phi(\mathbf{w})| \geq \frac{1}{2}|\Phi(\mathbf{x}_0) - \Phi(\mathbf{w})|$ and that Φ^{-1} is Lipschitz with constant M suffice to show

$$|\mathrm{II}| \leq K2^{-2q}||f_0||_{L^\infty(\mathcal{S}^{d-1})}M^{-2q} \int_{\mathcal{S}^{d-1}} (1 - \langle \mathbf{x}_0, \mathbf{w}\rangle)^q \, \mathrm{d}\mathcal{S}^{d-1}(\mathbf{w}).$$

As $q + \frac{d-3}{2} > -1$, the case $l = 0$ of theorem 4.1.1 allows us to compute the last term,

$$\int_{\mathcal{S}^{d-1}} (1 - \langle \mathbf{x}_0, \mathbf{w} \rangle)^q \, \mathrm{d}\mathcal{S}^{d-1}(\mathbf{w}) = \mathrm{vol}(\mathcal{S}^{d-2}) \int_{-1}^{1} (1-s)^q (1-s^2)^{\frac{d-3}{2}} \, \mathrm{d}s < \infty.$$

□

The second lemma allows us to differentiate expressions of the form

$$\mathbf{v}^i_\Phi(\mathbf{y}) := \int_{\mathcal{S}^{d-1}} g\left(\frac{1}{2}|\mathbf{y} - \Phi(\mathbf{w})|^2\right) (\mathbf{y}^i - \Phi^i(\mathbf{w})) f_0(\mathbf{w}) \, \mathrm{d}\mathcal{S}^{d-1}(\mathbf{w}), \tag{4.12}$$

for any $\mathbf{y} = (\mathbf{y}^1, \mathbf{y}^2, \ldots, \mathbf{y}^d)^t \in \mathbb{R}^d$, where the subscript notation $\mathbf{v}^i_\Phi(\mathbf{y})$ indicates the possibly changing dependence on $\Phi(\mathbf{x})$. A combination of both lemmas then establishes the required properties of the right hand side of (1.13) as corollaries.

Lemma 4.1.4. *Suppose $g(s)$ defines an admissible kernel and $f_0 \in L^\infty(\mathcal{S}^{d-1})$. If $\Phi(\mathbf{x}) \in \mathcal{O}_M$ and $\Psi(\mathbf{x}) \in C^{0,1}(\mathcal{S}^{d-1})$, then for fixed $\mathbf{y} \in \mathbb{R}^d$*

$$\frac{\mathrm{d}}{\mathrm{d}\epsilon} \int_{\mathcal{S}^{d-1}} g\left(\frac{1}{2}|\mathbf{y} - \Phi(\mathbf{w}) - \epsilon\Psi(\mathbf{w})|^2\right) (\mathbf{y}^i - \Phi^i(\mathbf{w}) - \epsilon\Psi^i(\mathbf{w})) f_0(\mathbf{w}) \, \mathrm{d}\mathcal{S}^{d-1}(\mathbf{w}) \mid_{\epsilon=0}$$

$$= -\int_{\mathcal{S}^{d-1}} \Bigg[g\left(\frac{1}{2}|\mathbf{y} - \Phi(\mathbf{w})|^2\right) \Psi^i(\mathbf{w}) + g'\left(\frac{1}{2}|\mathbf{y} - \Phi(\mathbf{w})|^2\right) \langle \mathbf{y} - \Phi(\mathbf{w}), \Psi(\mathbf{w}) \rangle \, (\mathbf{y}^i - \Phi^i(\mathbf{w})) \Bigg] f_0(\mathbf{w}) \, \mathrm{d}\mathcal{S}^{d-1}(\mathbf{w}).$$

Proof. For fixed $1 \leq i \leq d$ and $\mathbf{y} \in \mathbb{R}^d$ consider the quantity

$$\frac{\mathbf{v}^i_{\Phi+\epsilon\Psi}(\mathbf{y}) - \mathbf{v}^i_\Phi(\mathbf{y})}{\epsilon} =$$
$$\frac{1}{\epsilon} \int_{\mathcal{S}^{d-1}} g\left(\frac{1}{2}|\mathbf{y} - \Phi(\mathbf{w}) - \epsilon\Psi(\mathbf{w})|^2\right) (\mathbf{y}^i - \Phi^i(\mathbf{w}) - \epsilon\Psi^i(\mathbf{w})) f_0(\mathbf{w}) \, \mathrm{d}\mathcal{S}^{d-1}(\mathbf{w}) -$$
$$\frac{1}{\epsilon} \int_{\mathcal{S}^{d-1}} g\left(\frac{1}{2}|\mathbf{y} - \Phi(\mathbf{w})|^2\right) (\mathbf{y}^i - \Phi^i(\mathbf{w})) f_0(\mathbf{w}) \, \mathrm{d}\mathcal{S}^{d-1}(\mathbf{w}).$$

Let g_ϵ denote the integrand. As g is differentiable away from zero and Φ is one-to-one it follows that

$$g_\epsilon \to -\Bigg[g\left(\frac{1}{2}|\mathbf{y} - \Phi(\mathbf{w})|^2\right) \Psi^i(\mathbf{w}) + g'\left(\frac{1}{2}|\mathbf{y} - \Phi(\mathbf{w})|^2\right) \langle \mathbf{y} - \Phi(\mathbf{w}), \Psi(\mathbf{w}) \rangle \, (\mathbf{y}^i - \Phi^i(\mathbf{w})) \Bigg] f_0(\mathbf{w})$$

for almost every $\mathbf{w} \in \mathcal{S}^{d-1}$. The aim thus becomes to conclude that in fact

$$\int_{\mathcal{S}^{d-1}} g_\epsilon \to -\int_{\mathcal{S}^{d-1}} \left[g\left(\frac{1}{2}|\mathbf{y}-\Phi(\mathbf{w})|^2\right)\Psi^i(\mathbf{w}) + \right.$$
$$\left. g'\left(\frac{1}{2}|\mathbf{y}-\Phi(\mathbf{w})|^2\right)\langle \mathbf{y}-\Phi(\mathbf{w}), \Psi(\mathbf{w})\rangle\,(\mathbf{y}^i - \Phi^i(\mathbf{w}))\right] f_0(\mathbf{w}). \tag{4.13}$$

If $d_{\mathbf{y}} = \min_{\mathcal{S}^{d-1}} |\mathbf{y}-\Phi(\mathbf{w})| > 0$, this immediately follows as $g \in C^1(\mathbb{R}^+ \setminus \{0\})$ and the dominated convergence theorem. The difficulty comes when $\mathbf{y} = \Phi(\mathbf{x}_0)$ for some $\mathbf{x}_0 \in \mathcal{S}^{d-1}$. In this case, it suffices show that the g_ϵ are uniformly integrable: for any $\gamma > 0$ there exists $N > 0$ so that

$$\sup_\epsilon \int_{\mathcal{S}^{d-1}} |g_\epsilon| \mathbf{1}_{\{|g^\epsilon|>N\}} < \gamma.$$

The Vitali convergence theorem then yields the desired result.

To show uniform integrability, let $\mathbf{z}^\epsilon := \Phi(\mathbf{x}_0) - \Phi(\mathbf{w}) - \epsilon\Psi(\mathbf{w})$ and $\mathbf{z} := \Phi(\mathbf{x}_0) - \Phi(\mathbf{w})$. For fixed ϵ let $A := \{||\epsilon\Psi||_\infty \leq \frac{|\mathbf{z}|}{2}\}$ and write

$$g_\epsilon = g_\epsilon \mathbf{1}_A + g_\epsilon \mathbf{1}_{\mathcal{S}^{d-1}\setminus A} := g_\epsilon^1 + g_\epsilon^2$$
$$g_\epsilon = \left[-g\left(\frac{1}{2}|\mathbf{z}^\epsilon|^2\right)\Psi^i(\mathbf{w}) + \frac{g\left(\frac{1}{2}|\mathbf{z}^\epsilon|^2\right) - g\left(\frac{1}{2}|\mathbf{z}|^2\right)}{\epsilon}\mathbf{z}^i \right] f_0(\mathbf{w}).$$

If $\mathbf{w} \in A$ then $|\mathbf{z}| \leq 2|\mathbf{z}^\epsilon|$. To estimate g_ϵ^1, the mean value theorem furnishes $s_0 \in (\frac{|\mathbf{z}|^2}{8}, \frac{9|\mathbf{z}|^2}{8})$ with $g\left(\frac{1}{2}|\mathbf{z}^\epsilon|^2\right) - g\left(\frac{1}{2}|\mathbf{z}|^2\right) = \frac{1}{2}g'(s_0)(|\mathbf{z}^\epsilon|^2 - |\mathbf{z}|^2)$. Therefore

$$|g_\epsilon^1| \leq ||f_0||_{L^\infty(\mathcal{S}^{d-1})}||\Psi||_{L^\infty(\mathcal{S}^{d-1})}\left(\left|g\left(\frac{1}{2}|\mathbf{z}^\epsilon|^2\right)\right| + |g'(s_0)|\frac{5|\mathbf{z}|^2}{4}\right).$$

To estimate g_ϵ^2, since $\mathbf{w} \notin A$ then $\frac{|\mathbf{z}|}{|\epsilon|} \leq 2||\Psi||_\infty$, so that

$$|g_\epsilon^2| \leq ||f_0||_{L^\infty(\mathcal{S}^{d-1})}\left(\left|g\left(\frac{1}{2}|\mathbf{z}^\epsilon|^2\right)\right| ||\Psi||_\infty + \left|g\left(\frac{1}{2}|\mathbf{z}^h|^2\right)\right| \frac{|\mathbf{z}|}{|\epsilon|} + \left|g\left(\frac{1}{2}|\mathbf{z}|^2\right)\right| \frac{|\mathbf{z}|}{|\epsilon|}\right)$$
$$\leq 3||f_0||_{L^\infty(\mathcal{S}^{d-1})}||\Psi||_{L^\infty(\mathcal{S}^{d-1})}\left(\left|g\left(\frac{1}{2}|\mathbf{z}^h|^2\right)\right| + \left|g\left(\frac{1}{2}|\mathbf{z}|^2\right)\right|\right).$$

Combining these estimates yields

$$|g_\epsilon| \leq C_1\left(\left|g\left(\frac{1}{2}|\mathbf{z}^\epsilon|^2\right)\right| + \left|g\left(\frac{1}{2}|\mathbf{z}|^2\right)\right| + |g'(s_0)||\mathbf{z}|^2\right) := \mathrm{I} + \mathrm{II} + \mathrm{III}.$$

for some absolute constant C_1 that depends only on $||f_0||_{L^\infty(\mathcal{S}^{d-1})}$,$||\Psi||_{L^\infty(\mathcal{S}^{d-1})}$. As a linear combination of uniformly integrable functions is uniformly integrable, it suffices to show the uniform of $\mathrm{I} - \mathrm{III}$ individually.

To show the uniform integrability of I, as in the proof of lemma 4.1.3 let $\mathbf{x}_0^\epsilon$ denote a minimizer of $|\Phi(\mathbf{x}_0) - \Phi(\mathbf{w}) - \epsilon\Psi(\mathbf{w})|$ over $\mathbf{w} \in \mathcal{S}^{d-1}$, and decompose

$$\int_{\{\mathrm{I}>N\}} \mathrm{I}\, \mathrm{d}\mathcal{S}^{d-1}(\mathbf{w}) \leq \int_{\{\mathrm{I}>N\}\cap\{|\mathbf{z}^\epsilon|\geq\sqrt{2\delta}\}} + \int_{\{\mathrm{I}>N\}\cap\{|\mathbf{z}^\epsilon|\leq\sqrt{2\delta}\}}$$

If $|\mathbf{z}^\epsilon| \geq \sqrt{2\delta}$ then $\mathrm{I} \leq ||g||_{L^\infty([\delta,(2M+||\Psi||_\infty)^2])} := K(M, ||\Psi||_\infty)$ whenever $|\epsilon| \leq 1$. When $|\mathbf{z}^\epsilon| < \sqrt{2\delta}$, the growth rate of $g(s)$ near zero demonstrates

$$\mathrm{I} \leq C2^{-p}|\mathbf{z}^\epsilon|^{2p}.$$

If $p \geq 0$ the dominated convergence theorem gives the desired result. If $p < 0$, the fact that $|\mathbf{z}^\epsilon| \geq \frac{1}{2}|\Phi(\mathbf{x}_0^\epsilon) + \epsilon\Psi(\mathbf{x}_0^\epsilon) - \Phi(\mathbf{w}) - \epsilon\Psi(\mathbf{w})|$ yields

$$\mathrm{I} \leq C2^{-3p}|\Phi(\mathbf{x}_0^\epsilon) + \epsilon\Psi(\mathbf{x}_0^\epsilon) - \Phi(\mathbf{w}) - \epsilon\Psi(\mathbf{w})|^{2p}.$$

Now, as $\Psi \in C^{0,1}(\mathcal{S}^{d-1})$ and $\Phi(\mathbf{x}) \in \mathcal{O}_M$, for all ϵ sufficiently small $\Phi(\mathbf{x}) + \epsilon\Psi(\mathbf{x}) \in \mathcal{O}_{2M}$ as well. Therefore, for $|\mathbf{z}^\epsilon| < \sqrt{2\delta}$

$$\mathrm{I} \leq C2^{-3p}(2M)^{-2p}|\mathbf{x}_0^\epsilon - \mathbf{w}|^{2p} = C2^{-4p}M^{-2p}(1 - \langle\mathbf{x}_0^\epsilon, \mathbf{w}\rangle)^p := f_M(\langle\mathbf{x}_0^\epsilon, \mathbf{w}\rangle).$$

Summarizing the preceding, when $N > 0$

$$\begin{aligned}\int_{\{\mathrm{I}>N\}} \mathrm{I} &\leq \int_{\{\mathrm{I}>N\}\cap\{|\mathbf{z}^\epsilon|\geq\sqrt{2\delta}\}} + \int_{\{\mathrm{I}>N\}\cap\{|\mathbf{z}^\epsilon|\leq\sqrt{2\delta}\}} \\ &\leq K(M, ||\Psi||_\infty)\int_{\{K>N\}} + \int_{\{f_M>N\}} f_M.\end{aligned}$$

By the case $l = 0$ of theorem 4.1.1,

$$\int_{\{f_M>N\}} f_M = C2^{-4p}M^{-2p}\mathrm{vol}(\mathcal{S}^{d-2})\int_{-1}^{1}(1-s)^p(1-s^2)^{\frac{d-3}{2}}\mathbf{1}_{\{(1-s)^p>N\}}\,\mathrm{d}s.$$

Taking N sufficiently large, independently of ϵ, shows that

$$\sup_\epsilon \int_{\mathcal{S}^{d-1}} \left| g\left(\frac{1}{2}|\mathbf{z}^\epsilon|^2\right)\right| \mathbf{1}_{\{\mathrm{I}>N\}} < \gamma$$

as desired. For II, as $\Phi(\mathbf{x}) \in \mathcal{O}_M$, by lemma 4.1.3 $\int_{\mathcal{S}^{d-1}} \mathrm{II} \leq C(g, 0, M) < \infty$. By the dominated convergence theorem,

$$\int_{\mathcal{S}^{d-1}} \mathrm{II}\mathbf{1}_{\{\mathrm{II}>N\}} \to 0$$

uniformly in ϵ as well. For III, again decompose

$$\int_{\{\text{III}>N\}} \text{III}\, \mathrm{d}\mathcal{S}^{d-1}(\mathbf{w}) \leq \int_{\{\text{III}>N\}\cap\{|s_0|\geq\sqrt{2\delta}\}} + \int_{\{\text{III}>N\}\cap\{|s_0|\leq\sqrt{2\delta}\}},$$

and recall that $s_0 \in (\frac{|\mathbf{z}|^2}{8}, \frac{9|\mathbf{z}|^2}{8})$. As in lemma 4.1.3, each term can be dominated by an integrable function that does not depend on ϵ, so III is uniformly integrable as well. $\square$

Now, let $\mathbf{v}_\Phi(\mathbf{y}) : \mathbb{R}^d \to \mathbb{R}^d$ denote the right hand side of (1.13) evaluated at an arbitrary point $\mathbf{y} \in \mathbb{R}^d$,

$$\mathbf{v}_\Phi(\mathbf{y}) := (\mathbf{v}^1_\Phi(\mathbf{y}), \ldots, \mathbf{v}^d_\Phi(\mathbf{y}))^t$$

with $\mathbf{v}^i_\Phi(\mathbf{y})$ given by (4.12). By taking $\Psi(\mathbf{x}) \equiv -\mathbf{e}_j$ for $1 \leq j \leq d$ in lemma 4.1.4, we conclude

$$\begin{aligned}[\nabla \mathbf{v}_\Phi](\mathbf{y}) = \int_{\mathcal{S}^{d-1}} \Bigg[& g\left(\frac{1}{2}|\mathbf{y}-\Phi(\mathbf{w})|^2\right) \mathrm{Id} + \\ & g'\left(\frac{1}{2}|\mathbf{y}-\Phi(\mathbf{w})|^2\right)(\mathbf{y}-\Phi(\mathbf{w}))(\mathbf{y}-\Phi(\mathbf{w}))^t\Bigg] f_0(\mathbf{w})\, \mathrm{d}\mathcal{S}^{d-1}(\mathbf{w}), \end{aligned} \tag{4.14}$$

where Id denotes the $d \times d$ identity matrix. Applying lemma 4.1.3 then shows the matrix norm $||\nabla \mathbf{v}_\Phi||_2(\mathbf{y}) \leq C(g, g', d_\mathbf{y}, M)||f_0||_\infty$, for some constant C that increases with $d_\mathbf{y}$. The mean value theorem then yields

Corollary 4.1.5. *Let $\Phi(\mathbf{x}) \in \mathcal{O}_M$. Then for any two points $\mathbf{y}_1, \mathbf{y}_2 \in \mathbb{R}^d$*

$$|\mathbf{v}_\Phi(\mathbf{y}_1) - \mathbf{v}_\Phi(\mathbf{y}_2)| \leq C(g, g', \max\{d_{\mathbf{y}_1}, d_{\mathbf{y}_2}\}, M)||f_0||_\infty |\mathbf{y}_1 - \mathbf{y}_2|. \tag{4.15}$$

Similarly, fix $\mathbf{y} \in \mathbb{R}^d, \Phi, \Psi \in C^{0,1}(\mathcal{S}^{d-1})$ and suppose that for $0 \leq \epsilon \leq 1$ the line $L_\epsilon := \epsilon\Psi + (1-\epsilon)\Phi \in \mathcal{O}_M$. We can then use lemma 4.1.4 to deduce

$$\begin{aligned}\frac{\mathrm{d}}{\mathrm{d}\epsilon}\mathbf{v}^i_{L_\epsilon}(\mathbf{y}) = -\int_{\mathcal{S}^{d-1}} \Bigg[& g\left(\frac{1}{2}|\mathbf{y}-L_\epsilon(\mathbf{w})|^2\right)(\Psi^i(\mathbf{w}) - \Phi^i(\mathbf{w})) + \\ & g'\left(\frac{1}{2}|\mathbf{y}-L_\epsilon(\mathbf{w})|^2\right)\langle \mathbf{y}-L_\epsilon(\mathbf{w}), \Psi(\mathbf{w})-\Phi(\mathbf{w})\rangle\,(\mathbf{y}^i - L^i_\epsilon(\mathbf{w}))\Bigg] f_0(\mathbf{w})\, \mathrm{d}\mathcal{S}^{d-1}(\mathbf{w}) \end{aligned}$$

An application of lemma 4.1.3 then shows

$$\left|\frac{\mathrm{d}}{\mathrm{d}\epsilon}\mathbf{v}^i_{L_\epsilon}\right| \leq C(g, g', d_\mathbf{y}, M)||f_0||_\infty \max_{\mathcal{S}^{d-1}} |\Psi(\mathbf{x}) - \Phi(\mathbf{x})|,$$

where $d_{\mathbf{y}} = \min_{\mathcal{S}^{d-1}} |\mathbf{y} - L_\epsilon|$ and the constant C depends only on L_ϵ through M. For $\mathbf{y} \in \mathbb{R}^d$ fixed, the fundamental theorem of calculus then shows

$$|\mathbf{v}^i_\Psi(\mathbf{y}) - \mathbf{v}^i_\Phi(\mathbf{y})| = \left| \int_0^1 \frac{\mathrm{d}}{\mathrm{d}\epsilon} \mathbf{v}^i_{L_\epsilon}(y) \, \mathrm{d}\epsilon \right| \leq C(g, g', d_{\mathbf{y}}, M) ||f_0||_\infty \max_{\mathcal{S}^{d-1}} |\Psi(\mathbf{x}) - \Phi(\mathbf{x})|.$$

We therefore get the following corollary

Corollary 4.1.6. *Let $\Phi, \Psi \in C^{0,1}$ be such that the line $L_\epsilon := \epsilon\Psi + (1-\epsilon)\Phi \in \mathcal{O}_M$ for all $0 \leq \epsilon \leq 1$. Then for any $\mathbf{y} \in \mathbb{R}^d$,*

$$|\mathbf{v}_\Psi(\mathbf{y}) - \mathbf{v}_\Phi(\mathbf{y})| \leq C(g, g', d_{\mathbf{y}}, M) ||f_0||_\infty \max_{\mathcal{S}^{d-1}} |\Psi(\mathbf{x}) - \Phi(\mathbf{x})|. \tag{4.16}$$

The arguments in the proof of 4.1.4 also establish the following lemma that demonstrates continuity of the gradient $[\nabla \mathbf{v}_\Phi](\mathbf{y})$ of the Eulerian velocity field. To avoid redundancy, we leave the proof as an exercise for the reader.

Lemma 4.1.7. *Suppose $g(s)$ defines an admissible kernel and $f_0 \in L^\infty(\mathcal{S}^{d-1})$. If $\Phi(\mathbf{x}) \in \mathcal{O}_M$, then the matrix $[\nabla \mathbf{v}_\Phi](\mathbf{y})$ given by (4.14) is continuous as a function on $\mathbb{R}^d$.*

4.2 Local Well-Posedness

We may now proceed to demonstrate our main result, i.e. local existence for the IDE (1.13)—

Theorem 4.2.1. *(Local Well-Posedness for the IDE) Let $g(s)$ define an admissible kernel, $f_0 \in L^\infty$ and $\Phi_0(\mathbf{x}) \in \mathcal{O}_{M/2}$. Then there exists $T = T(g, g', M, ||f_0||_\infty)$ such that the IDE (1.13) has a solution*

$$\Phi(\mathbf{x}, t) \in C^1([-T, T]; C^0(\mathcal{S}^{d-1})) \cap C([-T, T]; C^{0,1}(\mathcal{S}^{d-1}) \cap \mathcal{O}_M).$$

If $\Psi(\mathbf{x}, t) \in C([-T', T']; C^{0,1}(\mathcal{S}^{d-1}))$ denotes another solution for any $T' \leq T$, then $\Phi(\mathbf{x}, t) \equiv \Psi(\mathbf{x}, t)$ on $[-T', T']$.

Fix an initial datum $\Phi_0(\mathbf{x}) \in \mathcal{O}_{M/2}$ and let $\Phi(\mathbf{x},t) \in C([0,T];C^{0,1}(\mathcal{S}^{d-1}))$. In the usual manner, define a mapping $A[\Phi]$ by

$$\Phi(\mathbf{x},t) \to A[\Phi](\mathbf{x},t) := \Phi_0(\mathbf{x}) + \int_0^t \int_{\mathcal{S}^{d-1}} g\left(\frac{1}{2}|\Phi(\mathbf{x},s)-\Phi(\mathbf{w},s)|^2\right)(\Phi(\mathbf{x},s)-\Phi(\mathbf{w},s))f_0(\mathbf{w})\,\mathrm{d}\mathcal{S}^{d-1}(\mathbf{w})\mathrm{d}s,$$

so that it suffices to show this mapping has a fixed point. To this end, we need to prove the following three propositions regarding the mapping, and may then proceed to apply straightforward Picard iteration.

Proposition 4.2.2. *Let $\Phi_0(\mathbf{x}) \in \mathcal{O}_{M/2}$ and $\mathrm{Lip}[\Phi-\Phi_0](t) \le \min\left\{\frac{M}{2}, \frac{1}{M}\right\}$ for all $t \in [0,T]$. Then $\Phi(\mathbf{x},t) \in \mathcal{O}_M$ for all $t \in [0,T]$.*

Proof. By the triangle inequality, $|\Phi(\mathbf{x},t)-\Phi(\mathbf{w},t)| = |\Phi(\mathbf{x},t)-\Phi_0(\mathbf{x})-(\Phi(\mathbf{w},t)-\Phi_0(\mathbf{w}))+\Phi_0(\mathbf{x})-\Phi_0(\mathbf{w})| \le \mathrm{Lip}[\Phi-\Phi_0](t)|\mathbf{x}-\mathbf{w}| + |\Phi_0(\mathbf{x})-\Phi_0(\mathbf{w})| \le M|\mathbf{x}-\mathbf{w}|$. By the reverse triangle inequality, $|\Phi(\mathbf{x},t)-\Phi(\mathbf{w},t)| \ge |\Phi_0(\mathbf{x})-\Phi_0(\mathbf{w})||\mathbf{x}-\mathbf{w}| - \mathrm{Lip}[\Phi-\Phi_0](t)|\mathbf{x}-\mathbf{w}| \ge (\frac{2}{M} - \mathrm{Lip}[\Phi-\Phi_0](t))|\mathbf{x}-\mathbf{w}| \ge \frac{1}{M}|\mathbf{x}-\mathbf{w}|$. □

Proposition 4.2.3. *Let $\Phi(\mathbf{x},t) \in \mathcal{O}_M$ for all $t \in [0,T]$. If $T = T(g,g',M,||f_0||_\infty)$ is sufficiently small, then*

$$||A[\Phi]-\Phi_0||_{C^{0,1}}(t) < \min\left\{\frac{M}{2}, \frac{1}{M}\right\}.$$

for all $t \in [0,T]$.

Proof. Set $h(\mathbf{x},t) := A[\Phi](\mathbf{x},t)-\Phi_0(\mathbf{x}) = \int_0^t \mathbf{v}_\Phi(\Phi(\mathbf{x},s))\,\mathrm{d}s$. By lemma 4.1.3, $|\mathbf{v}_\Phi(\Phi(\mathbf{x},s))| \le C(g,0,M)||f_0||_\infty$, so that $||h||_\infty(t) \le TC(g,0,M)||f_0||_\infty$. By corollary 4.1.5,

$$\begin{aligned}
|h(\mathbf{x},t)-h(\mathbf{w},t)| &\le \int_0^t |\mathbf{v}_\Phi(\Phi(\mathbf{x},s))-\mathbf{v}_\Phi(\Phi(\mathbf{w},s))|\,\mathrm{d}s \\
&\le C(g,g',2M,M)||f_0||_\infty \int_0^t |\Phi(\mathbf{x},s)-\Phi(\mathbf{w},s)|\,\mathrm{d}s \\
&\le C(g,g',2M,M)||f_0||_\infty MT|\mathbf{x}-\mathbf{w}|.
\end{aligned}$$

Taking $T = T(g,g',M,||f_0||_\infty)$ sufficiently small yields the desired bound for $\max_{\mathcal{S}^{d-1}}|h(\mathbf{x},t)|$ and $\mathrm{Lip}[h](t)$ for all $t \in [0,T]$. □

Proposition 4.2.4. *Suppose that* $||\Phi - \Phi_0||_{C^{0,1}} < \min\left\{\frac{M}{2}, \frac{1}{M}\right\}$ *and* $||\Psi - \Phi_0||_{C^{0,1}} < \min\left\{\frac{M}{2}, \frac{1}{M}\right\}$ *. Then for* T *sufficiently small depending only on* M*,*

$$\sup_{t\in[0,T]} \max_{\mathcal{S}^{d-1}} |A[\Psi](\mathbf{x},t) - A[\Phi](\mathbf{x},t)| \leq K \sup_{t\in[0,T]} \max_{\mathcal{S}^{d-1}} |\Psi(\mathbf{x},t) - \Phi(\mathbf{x},t)|$$

for some $K < 1$*.*

Proof. We have

$$\begin{aligned}
&|A[\Psi](\mathbf{x},t) - A[\Phi](\mathbf{x},t)| = \\
&\left| \int_0^t \mathbf{v}_\Psi(\Psi(\mathbf{x},s)) - \mathbf{v}_\Psi(\Phi(\mathbf{x},s)) + \mathbf{v}_\Psi(\Phi(\mathbf{x},s)) - \mathbf{v}_\Phi(\Phi(\mathbf{x},s))\, \mathrm{d}s \right| \leq \\
&\int_0^t |\mathbf{v}_\Psi(\Psi(\mathbf{x},s)) - \mathbf{v}_\Psi(\Phi(\mathbf{x},s))|\, \mathrm{d}s + \int_0^t |\mathbf{v}_\Psi(\Phi(\mathbf{x},s)) - \mathbf{v}_\Phi(\Phi(\mathbf{x},s))|\, \mathrm{d}s.
\end{aligned}$$

As $\mathrm{Lip}[\epsilon\Psi + (1-\epsilon)\Phi - \Phi_0](t) \leq \min\left\{\frac{M}{2}, \frac{1}{M}\right\}$ for all $0 \leq \epsilon \leq 1$, proposition 4.2.2 shows that the line $L_\epsilon := \epsilon\Psi(\cdot,t) + (1-\epsilon)\Phi \in \mathcal{O}_M$. Corollary 4.1.5 provides a sufficient estimate for the first term,

$$\begin{aligned}
&\int_0^t |\mathbf{v}_\Psi(\Psi(\mathbf{x},s)) - \mathbf{v}_\Psi(\Phi(\mathbf{x},s))|\, \mathrm{d}s \leq \\
&\qquad\qquad C(g,g',2M,M)||f_0||_\infty \int_0^t |\Psi(\mathbf{x},s) - \Phi(\mathbf{x},s)|\, \mathrm{d}s,
\end{aligned}$$

whereas corollary 4.1.6 provides a sufficient estimate for the second term,

$$\begin{aligned}
&\int_0^t |\mathbf{v}_\Psi(\Phi(\mathbf{x},s)) - \mathbf{v}_\Phi(\Phi(\mathbf{x},s))|\, \mathrm{d}s \leq \\
&\qquad\qquad C(g,g',3M,M)||f_0||_\infty \int_0^t \max_{\mathcal{S}^{d-1}} |\Psi(\mathbf{x},s) - \Phi(\mathbf{x},s)|\, \mathrm{d}s.
\end{aligned}$$

□

Straightforward Picard iteration now does the work. Given $\Phi_0(\mathbf{x}) \in \mathcal{O}_{M/2}$, take $T = T(g,g',M,||f_0||_\infty)$ sufficiently small as in propositions 4.2.3 and 4.2.4, and begin by defining $\Phi^0(\mathbf{x},t) \equiv \Phi_0(\mathbf{x})$ for all $t \in [0,T]$. Then, iteratively set

$$\Phi^n(\mathbf{x},t) := A[\Phi^{n-1}](\mathbf{x},t).$$

Inductively, assume that $||\Phi^{n-1} - \Phi_0||_{C^{0,1}}(t) \leq \min\{\frac{M}{2}, \frac{1}{M}\}$ and $\Phi^{n-1}(\mathbf{x}, t) \in \mathcal{O}_M$ for all $t \in [0, T]$. By proposition 4.2.3, $||\Phi^n - \Phi_0||_{C^{0,1}}(t) \leq \min\{\frac{M}{2}, \frac{1}{M}\}$ for all $t \in [0, T]$, so that $\Phi^n(\mathbf{x}, t) \in \mathcal{O}_M$ as well from proposition 4.2.2. Therefore,

$$\sup_{[0,T]} ||\Phi^n - \Phi^{n-1}||_\infty(t) \leq K \sup_{[0,T]} ||\Phi^{n-1} - \Phi^{n-2}||_\infty(t)$$

for some $K < 1$ by proposition 4.2.4, yielding a contraction in $C([0, T]; C^0(\mathcal{S}^{d-1}))$. We therefore have a limit function $\Phi(\mathbf{x}, t) \in C([0, T]; C^0(\mathcal{S}^{d-1}))$ with $||\Phi^n - \Phi||_{C([0,T];C^0(\mathcal{S}^{d-1}))} \to 0$. However, we may note that

$$\sup_{[0,T]} ||\Phi^n - \Phi_0||_{C^{0,1}}(t) \leq \min\left\{\frac{M}{2}, \frac{1}{M}\right\},$$

i.e. that each Φ^n lies in a fixed ball in $C^{0,1}(\mathcal{S}^{d-1})$ with center $\Phi_0(\mathbf{x})$. As they converge uniformly to $\Phi(\mathbf{x}, t)$, we conclude

$$\sup_{[0,T]} ||\Phi - \Phi_0||_{C^{0,1}}(t) \leq \min\left\{\frac{M}{2}, \frac{1}{M}\right\}$$

as well. Proposition 4.2.4 then demonstrates

$$\left|\int_0^t \mathbf{v}_{\Phi^n}(\Phi^n) - \int_0^t \mathbf{v}_\Phi(\Phi)\right| \leq K \sup_{[0,T]} ||\Phi^n - \Phi||_\infty(t) \to 0,$$

so that

$$\Phi(\mathbf{x}, t) = \Phi_0(\mathbf{x}) + \int_0^t \int_{\mathcal{S}^{d-1}} g\left(\frac{1}{2}|\Phi(\mathbf{x}, s) - \Phi(\mathbf{w}, s)|^2\right)(\Phi(\mathbf{x}, s) - \Phi(\mathbf{w}, s)) f_0(\mathbf{w})\, \mathrm{d}\mathcal{S}^{d-1}(\mathbf{w})\mathrm{d}s$$

as desired.

This yields a solution $\Phi(\mathbf{x}, t) \in C([0, T]; C^0(\mathcal{S}^{d-1}))$ that lies in $\mathcal{O}_M$ for each $t \in [0, T]$. However, for $t_1 > t_0$ writing

$$\Phi(\mathbf{x}, t_1) = \Phi(\mathbf{x}, t_0) + \int_{t_0}^{t_1} \mathbf{v}_\Phi(\Phi(\mathbf{x}, s))\, \mathrm{d}s$$

and paralleling the proof of proposition 4.2.3 demonstrates that in fact

$$\Phi(\mathbf{x}, t) \in C([0, T]; C^{0,1}(\mathcal{S}^{d-1}) \cap \mathcal{O}_M).$$

The relation

$$\frac{\partial \Phi(\mathbf{x},t)}{\partial t} = \mathbf{v}_\Phi(\Phi(\mathbf{x},t))$$

and the fact that $\Phi(\mathbf{x},t) \in \mathcal{O}_M$ combine to show that $\frac{\partial \Phi}{\partial t}$ is Lipschitz, by corollary 4.1.5. The contraction furnished by proposition 4.2.4 shows that $\Phi(\mathbf{x},t)$ is the unique solution that lies in $C([0,T];C^{0,1}(\mathcal{S}^{d-1}))$. Finally, each of the preceding arguments work equally well backward in time. All together, this yields theorem 4.2.1.

4.2.1 Differentiability Properties of Solutions

Fix an arbitrary bi-Lipschitz solution $\Phi(\mathbf{x},t)$ to (1.13) on $[0,T]$, and choose $M = M(T)$ so that $\Phi(\mathbf{x},t) \in \mathcal{O}_M$ for all $t \in [0,T]$. For any such solution, we aim in this subsection to prove

Theorem 4.2.5. *Let $\Phi(\mathbf{x},t)$ denote a solution to (1.13) on $[0,T]$ that lies in $\mathcal{O}_M$ for all $t \in [0,T]$. If $D_j\Phi_0(\mathbf{x})$ exists at $\mathbf{x} \in \mathcal{S}^{d-1}$, then $D_j\Phi(\mathbf{x},t) \in C([0,T])$ also exists at $\mathbf{x}$ for all $t \in [0,T]$, and it satisfies the linear ordinary differential equation*

$$\frac{\mathrm{d}D_j\Phi}{\mathrm{d}t}(\mathbf{x},t) = [\nabla \mathbf{v}_\Phi](\Phi(\mathbf{x},t))D_j\Phi(\mathbf{x},t), \quad D_j\Phi(\mathbf{x},0) = D_j\Phi_0(\mathbf{x}). \tag{4.17}$$

In particular, when $\Phi_0(\mathbf{x}) \in C^1(\mathcal{S}^{d-1})$ it follows that if $\Phi(\mathbf{x},t)$ bi-Lipschitz then actually $\Phi(\mathbf{x},t) \in C^1(\mathcal{S}^{d-1})$.

Let $\mathbf{x} \in \mathcal{S}^{d-1}$ denote an arbitrary but fixed point on the sphere, and write $\mathbf{x} = \mathbf{x}(\eta_1,\ldots,\eta_{d-1})$ where $(\eta_1,\ldots,\eta_{d-1}) \in \mathbb{R}^{d-1}$ denote spherical coordinates. For fixed $1 \le j \le d-1$ and any $|h| > 0$ define $\mathbf{x}_j^h = \mathbf{x}(\eta_1,\ldots,\eta_j+h,\ldots,\eta_{d-1}) \in \mathcal{S}^{d-1}$, and for an arbitrary function $\Psi(\mathbf{x}) : \mathcal{S}^{d-1} \to \mathbb{R}^d$ define the difference quotient

$$(D_j^h\Psi)(\mathbf{x}) := \frac{\Psi(\mathbf{x}_j^h) - \Psi(\mathbf{x})}{h}.$$

If the limit of the difference quotient exists as $h \to 0$ then the j^{th} partial derivative D_j of Ψ exists at $\mathbf{x}$, and we write

$$D_j\Psi(\mathbf{x}) := \lim_{h\to 0}(D_j^h\Psi)(\mathbf{x}).$$

As $\Phi(\mathbf{x},t)$ satifies (1.13) for $t \in [0,T]$, we can take difference quotients in the integral form of the equation to find that

$$(D_j^h\Phi)(\mathbf{x},t) = (D_j^h\Phi_0)(\mathbf{x}) + \frac{1}{h}\int_0^t \left(\mathbf{v}_\Phi(\Phi(\mathbf{x}_j^h,s)) - \mathbf{v}_\Phi(\Phi(\mathbf{x},s))\right)\,\mathrm{d}s$$

holds for all $t \in [0,T]$. The fundamental theorem of calculus then shows that

$$(D_j^h\Phi)(\mathbf{x},t) = (D_j^h\Phi_0)(\mathbf{x}) + \int_0^t\int_0^1 [\nabla\mathbf{v}_\Phi](\epsilon\Phi(\mathbf{x}_j^h,s)+(1-\epsilon)\Phi(\mathbf{x},s))(D_j^h\Phi)(\mathbf{x},s)\,\mathrm{d}\epsilon\mathrm{d}s.$$

As $\Phi(\mathbf{x},t) \in \mathcal{O}_M$ for all $t \in [0,T]$, we have that the bound $|\epsilon\Phi(\mathbf{x}_j^h,s)+(1-\epsilon)\Phi(\mathbf{x},s)-\Phi(\mathbf{w})| \leq 2M$ holds independent of the values that s and h assume. By lemma 4.1.3, then,

$$||[\nabla\mathbf{v}_\Phi]||_2(\epsilon\Phi(\mathbf{x}_j^h,s)+(1-\epsilon)\Phi(\mathbf{x},s)) \leq C(g,g',M)||f_0||_\infty \tag{4.18}$$

for C some universal constant.

Now, for an arbitrary $\Psi(t) \in C([0,T];\mathbb{R}^d)$ define a linear operator B_h as

$$B_h[\Psi](t) = \int_0^t\int_0^1 [\nabla\mathbf{v}_\Phi](\epsilon\Phi(\mathbf{x}_j^h,s)+(1-\epsilon)\Phi(\mathbf{x},s))\Psi(s)\,\mathrm{d}\epsilon\mathrm{d}s. \tag{4.19}$$

Due to (4.18), we conclude that for any $t_1,t_2 \in [0,T]$

$$|B_h[\Psi](t_2) - B_h[\Psi](t_1)| \leq ||\Psi||_{C([0,T])}C(g,g',M)||f_0||_\infty|t_2-t_1|.$$

The operator B_h therefore maps $C([0,T];\mathbb{R}^d) \to C([0,T];\mathbb{R}^d)$. Moreover, by taking $t_1 = 0$ we see that if $T' \leq T$ is sufficiently small, depending only on C, then the operator B_h maps $C([0,T];\mathbb{R}^d) \to C([0,T];\mathbb{R}^d)$ with operator norm $||B_h||_{\mathrm{op}} \leq 1/2$. In particular, $\mathrm{Id} - B_h$ is invertible. We therefore have that

$$(D_j^h\Phi)(\mathbf{x},t) = (\mathrm{Id}-B_h)^{-1}[(D_j^h\Phi_0)(\mathbf{x})](t)$$

for all $t \in [0,T']$. Analogously, define the linear operator $B : C([0,T];\mathbb{R}^d) \to C([0,T];\mathbb{R}^d)$ as

$$B[\Psi](t) = \int_0^t [\nabla\mathbf{v}_\Phi](\Phi(\mathbf{x},s))\Psi(s)\,\mathrm{d}s. \tag{4.20}$$

Note that $||B||_{\mathrm{op}} \leq 1/2$ for the same value of T' as well. For these operators, we then have the following lemma:

Lemma 4.2.6. *Let $B_h, B : C([0,T'];\mathbb{R}^d) \to C([0,T'];\mathbb{R}^d)$ denote the linear operators in (4.19) and (4.20), respectively. If $g \in C^1(\mathbb{R}^+ \setminus \{0\})$, satisfies (4.4) and $\Phi(\mathbf{x},t) \in \mathcal{O}_M$ for all $t \in [0,T']$, then $B_h \to B$ as $h \to 0$ in operator norm.*

Proof. Let $\Psi(t) \in C([0,T'];\mathbb{R}^d)$ with $||\Psi||_{C([0,T'])} \leq 1$. Then from the definitions of the operators B_h and B,

$$||(B_h - B)[\Psi]||_{C([0,T'])} \leq$$
$$C\int_0^{T'}\int_0^1 ||[\nabla \mathbf{v}_\Phi](\epsilon\Phi(\mathbf{x}_j^h,s) + (1-\epsilon)\Phi(\mathbf{x},s)) - [\nabla \mathbf{v}_\Phi](\Phi(\mathbf{x},s))||_2 \, \mathrm{d}\epsilon \mathrm{d}s.$$

By definition of the operator norm, then,

$$\lim_{h\to 0}||B_h - B||_{\mathrm{op}} \leq$$
$$C\lim_{h\to 0}\int_0^{T'}\int_0^1 ||[\nabla \mathbf{v}_\Phi](\epsilon\Phi(\mathbf{x}_j^h,s) + (1-\epsilon)\Phi(\mathbf{x},s)) - [\nabla \mathbf{v}_\Phi](\Phi(\mathbf{x},s))||_2 \, \mathrm{d}\epsilon \mathrm{d}s.$$

The matrix $[\nabla \mathbf{v}_\Phi](\mathbf{y})$ is continuous by lemma 4.1.7. This fact combines with the continuity of Φ itself and the fact that $\mathbf{x}_j^h \to \mathbf{x}$ to yield

$$||[\nabla \mathbf{v}_\Phi](\epsilon\Phi(\mathbf{x}_j^h,s) + (1-\epsilon)\Phi(\mathbf{x},s)) - [\nabla \mathbf{v}_\Phi](\Phi(\mathbf{x},s))||_2 \to 0$$

for all $s \in [0,T']$ and $\epsilon \in [0,1]$. The estimate (4.18) and the dominated convergence theorem then show

$$\lim_{h\to 0}||B_h - B|| \leq$$
$$C\int_0^{T'}\int_0^1 \lim_{h\to 0}||[\nabla \mathbf{v}_\Phi](\epsilon\Phi(\mathbf{x}_j^h,s) + (1-\epsilon)\Phi(\mathbf{x},s)) - [\nabla \mathbf{v}_\Phi](\Phi(\mathbf{x},s))||_2 \, \mathrm{d}\epsilon \mathrm{d}s = 0$$

as desired. □

Returning to the task at hand, we have that the uniform estimates $||B_h||_{\mathrm{op}} \leq \frac{1}{2}$ and $||B||_{\mathrm{op}} \leq \frac{1}{2}$ guarantee that both $(\mathrm{Id} - B_h)^{-1}$ and $(\mathrm{Id} - B)^{-1}$ exist. Moreover, by using the power series representations of the inverse operators, the uniform operator norm estimates and the fact that $B_h \to B$ in operator norm we see that $||(\mathrm{Id} - B_h)^{-1} - (\mathrm{Id} - B)^{-1}||_{\mathrm{op}} \to 0$

as well. If $D_j\Phi_0(\mathbf{x})$ exists, we may define the constant functions $\Psi_h, \Psi \in C([0,T'];\mathbb{R}^d)$ by $\Psi_h(t) \equiv (D_j^h\Phi_0)(\mathbf{x})$ and $\Psi(t) \equiv D_j\Phi_0(\mathbf{x})$. Lemma 4.2.6 then shows

$$\begin{aligned}
&|(D_j^h\Phi)(\mathbf{x},t) - (\mathrm{Id}-B)^{-1}[\Psi](t)| = |(\mathrm{Id}-B_h)^{-1}[\Psi_h](t) - (\mathrm{Id}-B)^{-1}[\Psi](t)| \\
&\leq 2||\Psi_h - \Psi||_{C([0,T'])} + ||(\mathrm{Id}-B_h)^{-1} - (\mathrm{Id}-B)^{-1}||_{\mathrm{op}}||\Psi||_{C([0,T'])} \\
&= 2|(D_j^h\Phi_0)(\mathbf{x}) - D_j\Phi_0(\mathbf{x})| + ||(\mathrm{Id}-B_h)^{-1} - (\mathrm{Id}-B)^{-1}||_{\mathrm{op}}|D_j\Phi_0(\mathbf{x})| \to 0
\end{aligned}$$

as $h \to 0$. In other words, $D_j\Phi(\mathbf{x},t)$ exists at $\mathbf{x}$ as well, and we have the representation

$$D_j\Phi(\mathbf{x},t) = (\mathrm{Id}-B)^{-1}[D_j\Phi_0(\mathbf{x})](t) \tag{4.21}$$

Moreover, $D_j\Phi(\mathbf{x},t)$ is a continuous function in t for all $t \in [0,T']$. Pre-multiplying by $(\mathrm{Id}-B)$ in (4.21) and using the definition (4.20) of B then shows that $D_j\Phi(\mathbf{x},t)$ satisfies the integral equation

$$D_j\Phi(\mathbf{x},t) = D_j\Phi_0(\mathbf{x}) + \int_0^t [\nabla \mathbf{v}_\Phi](\Phi(\mathbf{x},s))D_j\Phi(\mathbf{x},s)\,\mathrm{d}s \tag{4.22}$$

on $[0,T']$. Taking $\Phi(\mathbf{x},T')$ as inititial data and applying the same argument then shows that

$$D_j\Phi(\mathbf{x},t) = D_j\Phi(\mathbf{x},T') + \int_{T'}^t [\nabla \mathbf{v}_\Phi](\Phi(\mathbf{x},s))D_j\Phi(\mathbf{x},s)\,\mathrm{d}s$$

for $t \in [T',2T']$, so that (4.22) actually holds on $[0,2T']$. Applying the argument a finite number of times then shows that $D_j\Phi(\mathbf{x},t) \in C([0,T])$ and satisfies (4.22) on $[0,T]$. By the fundamental theorem of calculus, then, (4.17) holds.

For the last statement in theorem 4.2.5, by lemma 4.1.7 the equation (4.17) defines a linear ODE with coefficients that depend continuously on the parameter $\mathbf{x} \in \mathcal{S}^{d-1}$. Its solutions therefore depend continuously on both the parameter $\mathbf{x} \in \mathcal{S}^{d-1}$ and on the initial data. As $\Phi_0(\mathbf{x}) \in C^1(\mathcal{S}^{d-1})$ the initial data also depends continuously on $\mathbf{x} \in \mathcal{S}^{d-1}$, so that the solution $D_j\Phi(\mathbf{x},t) \in C(\mathcal{S}^{d-1})$ as desired.

4.3 Blowup, Collapse, and Global Existence

In the previous section, we demonstrated that if $\Phi_0(\mathbf{x}) \in \mathcal{O}_{\frac{M}{2}}$ then there exists $T = T(M) > 0$ such that integral equation (1.13) has a unique solution $\Phi(\mathbf{x},t)$ on $t \in [0,T]$. The solution

lies in $\mathcal{O}_M$ for all $t \in [0,T]$ as well. Clearly, we can take $\Phi(\mathbf{x},T) \in \mathcal{O}_M$ as initial data and then repeat the argument. This yields a unique solution on some larger time interval $[0,T_1]$ with $T_1 > T$, and this process can continue as long as $\mathrm{Lip}[\Phi](t)$ and $\mathrm{Lip}[\Phi^{-1}](t)$ remain finite. Summarizing, we have the following continuation result:

Theorem 4.3.1. *Let g and Φ_0 satsify the assumptions of theorem 4.2.1 and $\Phi(\mathbf{x},t)$ denote the corresponding solution to the IDE* (1.13)*. If $[0,T_f)$ denotes the largest time interval on which $\Phi(\mathbf{x},t)$ exists as a bi-Lipschitz solution, then at least one of*

$$\text{(i) } \limsup_{t \nearrow T_f} \mathrm{Lip}[\Phi](t) = \infty \quad \text{(ii) } \limsup_{t \nearrow T_f} \mathrm{Lip}[\Phi^{-1}](t) = \infty \quad \text{(iii) } T_f = \infty \tag{4.23}$$

must hold.

By recalling the class of solutions $\Phi(\mathbf{x},t) = R(t)\mathbf{x}$ from example 4.1.2, we find simple examples that demonstrate each of (i), (ii) and (iii) can happen in isolation. Indeed, if $g(s) = s^p$ for $p > 0$ the ODE (4.10) reduces to $R' = C_p R^{1+2p}$; the constant

$$C_p = \mathrm{vol}(\mathcal{S}^{d-2}) \int_{-1}^{1} (1-s)^{1+p} (1-s^2)^{\frac{d-3}{2}} \, \mathrm{d}s$$

is positive. We readily compute the explicit solution and maximal interval of existence $[0,T_f)$ as

$$R(t) = \left(\frac{1}{R(0)^{-2p} - 2pC_p t} \right)^{\frac{1}{2p}}, \quad T_f = \frac{1}{2pC_p R(0)^{2p}}, \tag{4.24}$$

so that (i) occurs as $t \nearrow T_f$ while (ii) remains finite. Conversely, suppose $g(s) = -s^{-p}$ for $0 < p < \frac{d-1}{2}$. Then

$$\begin{aligned} C_p &= \mathrm{vol}(\mathcal{S}^{d-2}) \int_{-1}^{1} (1-s)^{1-p} (1-s^2)^{\frac{d-3}{2}} \, \mathrm{d}s > 0 \\ R(t) &= \left(R(0)^{2p} - 2pC_p t \right)^{\frac{1}{2p}}, \quad T_f = \frac{R(0)^{2p}}{2pC_p} \end{aligned} \tag{4.25}$$

and the solution can collapse to zero in finite time. That is, (ii) occurs at T_f while (i) remains finite.

As these examples indicate, we must prevent both blowup and collapse in order to guarantee the solution exists as a bi-Lipschitz surface for all time. It comes as no surprise that

this amounts to having control over the gradient matrix $[\nabla \mathbf{v}_\Phi](\mathbf{y})$ generated by the Eulerian velocity field $\mathbf{v}_\Phi(\mathbf{y})$, as similar criteria abound for related active scalar problems. Specifically, it proves both necessary and sufficient to have

$$\int_0^T ||\nabla \mathbf{v}_\Phi||_{L^\infty(|\mathbf{y}|\leq||\Phi||_\infty(t))} \mathrm{d}t < \infty \tag{4.26}$$

Precisely analogous conditions guarantee existence for related problems, such as solutions to the Euler equations ([44], Chapter 5) and for the boundary of a vortex patch written in contour dynamics form ([44], Chapter 8).

Theorem 4.3.2. *Suppose $g(s)$ defines an admissible kernel and $f_0 \in L^\infty$. Then the solution $\Phi(\mathbf{x},t) \in C([0,T];C^{0,1}(\mathcal{S}^{d-1}))$ to (1.13) exists as a bi-Lipschitz surface past time T if and only if both $||\Phi||_\infty(T) < \infty$ and (4.26) hold.*

Proof. Clearly, if $\Phi(\mathbf{x},t)$ is bi-Lipschitz on $[0,T']$ for $T' > T$ then $||\Phi||_\infty(T) < \infty$ and $M := \sup_{[0,T]} \mathrm{Lip}[\Phi^{-1}](t) < \infty$ as well. Recalling from (4.14) that

$$\begin{aligned}[\nabla \mathbf{v}_\Phi](\mathbf{y}) = \int_{\mathcal{S}^{d-1}} \Bigg[& g\left(\frac{1}{2}|\mathbf{y}-\Phi(\mathbf{w})|^2\right) \mathrm{Id} + \\ & g'\left(\frac{1}{2}|\mathbf{y}-\Phi(\mathbf{w})|^2\right)(\mathbf{y}-\Phi(\mathbf{w}))(\mathbf{y}-\Phi(\mathbf{w}))^t \Bigg] f_0(\mathbf{w})\, \mathrm{d}\mathcal{S}^{d-1}(\mathbf{w}),\end{aligned}$$

the proof of lemma 4.1.3 shows that $||\nabla \mathbf{v}_\Phi||_\infty(\mathbf{y},t) \leq C(M, D_\mathbf{y})$. The constant C increases with M and $D_\mathbf{y} := \max_{\mathcal{S}^{d-1}} |\mathbf{y}-\Phi(\mathbf{w},t)|$ and remains finite provided M and $D_\mathbf{y}$ stay bounded. Of course $D_\mathbf{y} \leq 2||\Phi||_\infty(t) \leq 2\sup_{[0,T]} ||\Phi||_\infty(t) < \infty$ provided $|\mathbf{y}| \leq ||\Phi||_\infty(t)$, so that

$$||\nabla \mathbf{v}_\Phi||_{L^\infty(|\mathbf{y}|\leq||\Phi||_\infty(t))} \leq C\left(M, 2\sup_{[0,T]} ||\Phi||_\infty(t)\right) < \infty$$

and (4.26) holds.

For the converse, it suffices to show that both $\mathrm{Lip}[\Phi](T)$ and $\mathrm{Lip}[\Phi^{-1}](T)$ remain bounded. To this end, for $\mathbf{x},\mathbf{z} \in \mathcal{S}^{d-1}$ let $\Delta(\mathbf{x},\mathbf{z},t) := \Phi(\mathbf{x},t) - \Phi(\mathbf{z},t)$. The fundamental theorem of calculus then yields

$$\begin{aligned}\frac{1}{2}\frac{\partial}{\partial t}|\Delta(\mathbf{x},\mathbf{z},t)|^2 = & \\ \int_0^1 \langle \Delta(\mathbf{x},\mathbf{z},t), & [\nabla \mathbf{v}_\Phi](\epsilon\Phi(\mathbf{x},t) + (1-\epsilon)\Phi(\mathbf{z},t))\Delta(\mathbf{x},\mathbf{z},t)\rangle \ \mathrm{d}\epsilon.\end{aligned} \tag{4.27}$$

As $|\epsilon\Phi(\mathbf{x},t)+(1-\epsilon)\Phi(\mathbf{z},t)| \leq ||\Phi||_\infty(t)$, the relation (4.27) implies

$$\frac{1}{2}\frac{\partial}{\partial t}|\Delta(\mathbf{x},\mathbf{z},t)|^2 \geq -K||\nabla \mathbf{v}_\Phi||_{L^\infty(|\mathbf{y}|\leq||\Phi||_\infty(t))}|\Delta(\mathbf{x},\mathbf{z},t)|^2$$

for some absolute constant K that depends only on the size of the matrix. By Gronwall's inequality

$$|\Delta(\mathbf{x},\mathbf{z},0)|\mathrm{e}^{-K\int_0^t ||\nabla \mathbf{v}_\Phi||_{L^\infty(|\mathbf{y}|\leq||\Phi||_\infty(s))}\mathrm{d}s} \leq |\Delta(\mathbf{x},\mathbf{z},t)|.$$

Dividing through by $|\mathbf{x}-\mathbf{w}|$ and taking an infimum gives the estimate

$$\mathrm{Lip}[\Phi^{-1}](T) \leq \mathrm{Lip}[\Phi_0^{-1}]\mathrm{e}^{K\int_0^T ||\nabla \mathbf{v}_\Phi||_{L^\infty(|\mathbf{y}|\leq||\Phi||_\infty(s))}\mathrm{d}s} < \infty$$

due to (4.26). Analogously, the fundamental theorem of calculus and the proof of lemma 4.1.3 combine to show

$$\frac{1}{2}\frac{\partial}{\partial t}|\Delta(\mathbf{x},\mathbf{z},t)|^2 \leq C(\mathrm{Lip}[\Phi^{-1}](t), 2||\Phi||_\infty||(t)).$$

Applying Gronwall's inequality, then dividing by $|\mathbf{x}-\mathbf{w}|$ and taking a supremum yields

$$\mathrm{Lip}[\Phi](T) \leq \mathrm{Lip}[\Phi_0]\mathrm{e}^{\int_0^T C(\mathrm{Lip}[\Phi^{-1}](s),2||\Phi||_\infty(s))\,\mathrm{d}s} < \infty.$$

The last inequality holds since $\mathrm{Lip}[\Phi^{-1}](t)$ remains finite on $[0,T]$ due to the previous estimate, and since $||\Phi||_\infty(t)$ remains bounded for all $t \in [0,T]$ by hypothesis. □

Remark 4.3.3. *From the proof of the previous theorem, we can rephrase the result to say that the solution $\Phi(\mathbf{x},t) \in C([0,T];C^{0,1}(\mathcal{S}^{d-1}))$ exists as a bi-Lipschitz surface past time T if and only if both $\mathrm{Lip}[\Phi^{-1}](T)$ and $||\Phi||_\infty(T)$ remain finite. This rephrasing generally proves more useful than the statement in theorem 4.3.2.*

4.3.1 The Osgood Condition for Locally Attractive Kernels

We first focus our attention on the case when $g(s)$ has an attractive (i.e., negative) singularity at the origin, such as $g(s) = -s^{-p}$. From (4.25) we know collapse can occur in finite time, so we wish to characterize precisely when this happens. Earlier studies on the aggregation equation (4.1) have shown that the Osgood condition on the kernel $g(s)$ provides a precise

characterization. Indeed, for initial data $\rho_0 \in L^\infty(\mathbb{R}^d)$ the Osgood condition proves both necessary and sufficient for ρ to remain in L^∞ for all positive times [7]. For initial data in $\rho_0 \in L^p(\mathbb{R}^d)$ with $p > \frac{d}{d-1}$, the Osgood condition proves necessary and sufficient for global existence as well [8]. For our co-dimension one distribution solutions, we show that this characterization holds for the surface equation (1.13) in this section.

Following [7], we say that the kernel $g(s)$ is Osgood if

$$\lim_{\epsilon \downarrow 0} \int_\epsilon^1 \frac{1}{sg(s)} \, \mathrm{d}s = -\infty. \tag{4.28}$$

Adapting the arguments from [7] to our setting easily yields the necessity of (4.28) for global existence, as we demonstrate in the lemma that follows.

Lemma 4.3.4. *Suppose $g(s)$ is non-positive and non-decreasing in some neighborhood $(0, \delta]$ of the origin and that $f_0(\mathbf{w}) \geq 0$. If (4.28) fails, then all solutions with $||\Phi_0||_\infty^2 < \delta/2$ collapse to the origin in finite time.*

Proof. The proof follows exactly as in [7]. As long as $\Phi(\mathbf{x}, t)$ exists, by continuity there exists $\mathbf{x} \in \mathcal{S}^{d-1}$ with $|\Phi(\mathbf{x}, t)| = ||\Phi||_\infty(t)$. From the hypotheses on g, f_0 and the fact that $\langle \Phi(\mathbf{x}, t), \Phi(\mathbf{x}, t) - \Phi(\mathbf{w}, t) \rangle \geq 0$ for all $\mathbf{w} \in \mathcal{S}^{d-1}$ it then follows that

$$\begin{aligned}
&\frac{\partial}{\partial t} |\Phi(\mathbf{x}, t)|^2 = \\
&2 \int_{\mathcal{S}^{d-1}} g\left(\frac{1}{2} |\Phi(\mathbf{x}, t) - \Phi(\mathbf{w}, t)|^2 \right) \langle \Phi(\mathbf{x}, t), \Phi(\mathbf{x}, t) - \Phi(\mathbf{w}, t) \rangle \, f_0(\mathbf{w}) \, \mathrm{d}\mathcal{S}^{d-1}(\mathbf{w}) \\
&\leq 2g\left(2|\Phi(\mathbf{x}, t)|^2\right) \left[\int_{\mathcal{S}^{d-1}} |\Phi(\mathbf{x}, t)|^2 f_0(\mathbf{w}) \, \mathrm{d}\mathcal{S}^{d-1}(\mathbf{w}) - \right. \\
&\qquad\qquad \left. \left\langle \Phi(\mathbf{x}, t), \int_{\mathcal{S}^{d-1}} \Phi(\mathbf{w}, t) f_0(\mathbf{w}) \, \mathrm{d}\mathcal{S}^{d-1}(\mathbf{w}) \right\rangle \right] \\
&= 2M_\rho |\Phi(\mathbf{x}, t)|^2 g\left(2|\Phi(\mathbf{x}, t)|^2\right) \leq 0.
\end{aligned}$$

The last line results from (4.7),(4.8) and our assumption that $\Phi_0(\mathbf{x})$ has zero center of mass. If (4.28) fails, the solution to the ODE

$$\frac{\mathrm{d}r}{\mathrm{d}t} = 2M_\rho r g(2r) \quad r(0) = ||\Phi_0||_\infty^2 \tag{4.29}$$

reaches zero in finite time, whence $||\Phi||_\infty(t)$ must reach zero in finite time as well. □

As a consequence, in general (4.28) must hold in order to guarantee that solutions to (1.13) do not collapse in finite time. We therefore assume (4.28), and turn our attention toward demonstrating the sufficiency of the Osgood condition for global existence. For this it will prove useful to rewrite $g(s)$ in the form

$$g(s) = \frac{h\left((2s)^p\right)}{(2s)^p},\ 0 < p \leq 1/2, \tag{4.30}$$

so that the Osgood condition then reads

$$\lim_{\epsilon \downarrow 0} \int_{\epsilon}^{1} \frac{1}{h(u)}\, \mathrm{d}u = -\infty. \tag{4.31}$$

Following [8], we shall say $h(r)$ defines a natural kernel provided it satisfies the following regularity, boundedness and monotonicity conditions:

Definition 4.3.5. *Let $g(s)$ satisfy (4.30) for some $0 < p \leq 1/2$ if $d > 2$ and $0 < p < 1/2$ if $d = 2$. We then say $h(r)$ defines a* ***natural kernel*** *if*

(H1) $h(r) \in C^1\left(\mathbb{R}^+ \setminus \{0\}\right)$

(H2) $h(r) \in L^\infty(\mathbb{R}^+)$

(H3) $h'(r)$ *is monotonic (either increasing or decreasing) near zero*

Remark 4.3.6. *The additional restriction $0 < p < 1/2$ if $d = 2$ arises due to the integrability constraint (4.4).*

Using the arguments from [8], we establish

Lemma 4.3.7. *Let $h(r)$ define a natural kernel with $h(0) = 0$. Then either*

(a) $\min\left\{\frac{h(r)}{r}, h'(r)\right\} \geq C_0$ *for some $C_0 > -\infty$ and all $r \in [0,1]$, or both*

(b1) $\frac{h(r)}{r} \to -\infty$ *and* $h'(r) \to -\infty$ *as* $r \to 0^+$, *and*

(b2) $\exists \delta > 0$ *such that* $\forall r \in (0, \delta]$ $h'(r) \geq \frac{h(r)}{r}$, $\frac{h(r)}{r}$ *increases*, $h(r)$ *decreases*, *and if* $\delta_1 \leq \delta$ *then* $\inf_{r \geq \delta_1} \frac{h(r)}{r} = \frac{h(\delta_1)}{\delta_1}$ *and* $\inf_{r \geq \delta_1} h'(r) = h'(\delta_1)$.

Proof. Suppose first that there exists $C_1 > -\infty$ such that

$$\liminf_{r\to 0^+} \frac{h(r)}{r} > C_1.$$

As $h(0) = 0$, given any r sufficiently small there exists $s < r$ with

$$h'(s) = \frac{h(r)}{r} > C_1.$$

It then follows from (H3) that $\lim_{r\to 0^+} h'(r) \geq C_0$. Thus $h'(r)$ is bounded from below in a neighborhood of the origin as well, so (a) holds. Otherwise, there exists sequences $r_n \to 0^+$ and $s_n < r_n$ with

$$\lim_{n\to\infty} \frac{h(r_n)}{r_n} = h'(s_n) = -\infty. \tag{4.32}$$

When combined with (H3), this gives both that $h'(r) \to -\infty$ and that $h'(r)$ is increasing on some neighborhood $(0, \sigma]$ of zero. Clearly h decreases in this neighborhood as $h' < 0$. Moreover, for any $r \in (0, \sigma]$ there exists $s < r \leq \sigma$ with

$$\frac{h(r)}{r} = h'(s) \leq h'(r)$$

as desired. This also gives that $\frac{\mathrm{d}}{\mathrm{d}r}\left(\frac{h(r)}{r}\right) = \frac{1}{r}\left(h'(r) - \frac{h(r)}{r}\right) \geq 0$, so that $\frac{h(r)}{r}$ increases. Coupled with (4.32) this shows $\frac{h(r)}{r} \to -\infty$, completing the proof of (b1). Finally, from these statements it follows that $\frac{h(r)}{r}$ and $h'(r)$ are monotonic in $(0, \sigma]$ and tend to $-\infty$ as $r \to 0^+$, so the remainder of (b2) follows provided $\delta \leq \sigma$ is sufficiently small. □

Note that if $g(s)$ is Osgood, it follows from (4.31) that necessarily $h(0) = 0$. We can therefore apply lemma 4.3.7 to such kernels, and this allows us to provide a lower bound for the time of collapse of $1/\mathrm{Lip}[\Phi^{-1}](t)$ to zero in terms of the solution to an ODE. When part (a) of the lemma holds, a crude estimate suffices to demonstrate global existence from this ODE. When (b1) and (b2) hold the ODE proves more complicated. However, as $g(s)$ is Osgood, the solution to this ODE still remains positive for all time, and this yields global existence in the second case.

Lemma 4.3.8. *Let $h(r)$ define a natural kernel $g(s)$ that is Osgood. Suppose further that $f_0(\mathbf{z}) \geq 0$. If (a) in lemma 4.3.7 holds then the solution $\Phi(\mathbf{x}, t)$ exists globally in time.*

Proof. By the remark following theorem 4.3.2, this follows from a straightforward upper bound for $\mathrm{Lip}[\Phi^{-1}](t)$ and $||\Phi||_\infty(T)$. For $\mathbf{x}, \mathbf{w}, \mathbf{z} \in \mathcal{S}^{d-1}$ and $\epsilon \in \mathbb{R}$ let $\Delta(\mathbf{x}, \mathbf{w}, t) := \Phi(\mathbf{x}, t) - \Phi(\mathbf{w}, t)$ and

$$L_\epsilon(\mathbf{x}, \mathbf{w}, \mathbf{z}) = \epsilon\Phi(\mathbf{x}, t) + (1-\epsilon)\Phi(\mathbf{w}, t) - \Phi(\mathbf{z}, t). \tag{4.33}$$

Using the fundamental theorem of calculus as before shows

$$\begin{aligned}\frac{1}{2}\frac{\partial}{\partial t}|\Delta(\mathbf{x}, \mathbf{w}, t)|^2 =& |\Delta|^2 \int_0^1 \int_{\mathcal{S}^{d-1}} \left[\frac{h(|L_\epsilon|^{2p})}{|L_\epsilon|^{2p}} \left(1 - 2p\cos^2(\theta_\epsilon)\right) + \right. \\ & \left. h'(|L_\epsilon|^{2p}) 2p\cos^2(\theta_\epsilon) \right] f_0(\mathbf{z})\, \mathrm{d}\mathcal{S}^{d-1}(\mathbf{z}) \mathrm{d}\epsilon, \end{aligned} \tag{4.34}$$

where θ_ϵ denotes the angle between L_ϵ and Δ. Let

$$C_0(t) = C_0(||\Phi||_\infty(t)) = \inf_{r \in \left[0, 2^{2p}||\Phi||_\infty^{2p}(t)\right]} \min\left\{ \frac{h(r)}{r}, h'(r) \right\}$$

When (a) holds, it follows from (H1) that $C_0(t) > -\infty$ provided $||\Phi||_\infty(t)$ remains finite. Therefore,

$$\frac{1}{2}\frac{\partial}{\partial t}|\Delta(\mathbf{x}, \mathbf{w}, t)|^2 \geq C_0(t) M_\rho |\Delta(\mathbf{x}, \mathbf{w}, t)|^2.$$

Gronwall's inequality then yields

$$|\Delta(\mathbf{x}, \mathbf{w}, t)| \geq |\Delta(\mathbf{x}, \mathbf{w}, 0)| \mathrm{e}^{M_\rho \int_0^t C_0(s)\mathrm{d}s}.$$

Dividing through by $|\mathbf{x} - \mathbf{w}|$ and taking an infimum yields

$$\mathrm{Lip}[\Phi^{-1}](t) \leq \mathrm{Lip}[\Phi_0^{-1}] \mathrm{e}^{-M_\rho \int_0^t C_0(s)\mathrm{d}s},$$

so that $\mathrm{Lip}[\Phi^{-1}](t)$ remains bounded for all finite times provided $||\Phi||_\infty(t)$ does. As $h(r)$ defines a natural kernel, the hypotheses (H2) shows that

$$\frac{\partial}{\partial t}||\Phi||_\infty(t) \leq K||\Phi||_\infty^{1-2p}(t),$$

for some absolute constant K, so that $||\Phi||_\infty(t)$ does indeed remain bounded for all finite time as desired. □

Now let us turn to the second case, i.e. that (b1) and (b2) from lemma 4.3.7 hold. For use in the following lemma, let us define the quantity we wish to estimate, $r(t) := 1/\text{Lip}[\Phi^{-1}](t)$, and the integral

$$\mathcal{I}(r^{2p}(t)) = \int_{-1}^{1} \frac{h\left(r^{2p}(t)2^{-p}(1-s)^p\right)}{2^{-p}(1-s)^p}(1-s^2)^{\frac{d-3}{2}}\,\mathrm{d}s. \tag{4.35}$$

With these definitions, and taking δ as in lemma 4.3.7 part (b2) we can demonstrate

Lemma 4.3.9. *Let $h(r)$ define a natural kernel $g(s)$ that is Osgood. Suppose further that $f_0(\mathbf{z}) \geq 0$ and $0 < r(t_0) < \delta$ for some $t_0 \geq 0$. If* (b1) *and* (b2) *in lemma 4.3.7 holds, then $r^{2p}(t)$ remains bounded below by the solution $q(t)$ to the ODE*

$$\frac{\mathrm{d}q}{\mathrm{d}t} = 2p\left[\text{vol}(\mathcal{S}^{d-2})||f_0||_\infty \mathcal{I}(q(t)) + M_\rho h(q(t))\right], \quad q(t_0) = r^{2p}(t_0) \tag{4.36}$$

for all $t \geq t_0$.

Proof. Use the fundamental theorem of calculus as in the first case, define L_ϵ as in (4.33) and let $f(\epsilon, \mathbf{z})$ denote the integrand. Then split the resulting integral (4.34) into two terms to find

$$\begin{aligned}\int_0^1 \int_{\mathcal{S}^{d-1}} f(\epsilon,\mathbf{z})\,\mathrm{d}\mathcal{S}^{d-1}(\mathbf{z})\mathrm{d}\epsilon =& \int_0^1 \int_{\mathcal{S}^{d-1}\cap\{|L_\epsilon|^{2p}\leq\delta_1\}} + \int_0^1 \int_{\mathcal{S}^{d-1}\cap\{|L_\epsilon|^{2p}\geq\delta_1\}} \\ :=& \mathrm{I} + \mathrm{II}.\end{aligned}$$

For any $\delta_1 \leq \delta$ with δ as in lemma 4.3.7, as $h'(|L_\epsilon|^{2p}) \geq \frac{h(|L_\epsilon|^{2p})}{|L_\epsilon|^{2p}}$ and $h \leq 0$ it follows that

$$\mathrm{I} \geq ||f_0||_\infty \int_0^1 \int_{\mathcal{S}^{d-1}\cap\{|L_\epsilon|^{2p}\leq\delta_1\}} \frac{h(|L_\epsilon|^{2p})}{|L_\epsilon|^{2p}}\,\mathrm{d}\mathcal{S}^{d-1}(\mathbf{z}).$$

Let $\mathbf{x}_0 = \mathbf{x}_0(\epsilon)$ denote a minimizer of $|\epsilon\Phi(\mathbf{x},t) + (1-\epsilon)\Phi(\mathbf{w},t) - \Phi(\mathbf{z},t)|$ over $\mathbf{z} \in \mathcal{S}^{d-1}$, so that

$$|L_\epsilon| \geq \frac{1}{2}|\Phi(\mathbf{x}_0,t) - \Phi(\mathbf{z},t)| \geq \frac{r(t)}{2}|\mathbf{x}_0 - \mathbf{z}|.$$

Combining this with the facts that $\frac{h(r)}{r}$ is non-decreasing and that $h \leq 0$ then shows

$$\begin{aligned}\mathrm{I} \geq& 2^{2p}||f_0||_\infty \int_0^1 \int_{\{|L_\epsilon|^{2p}\leq\delta_1\}} \frac{h\left(r^{2p}(t)2^{-2p}|\mathbf{x}_0-\mathbf{z}|^{2p}\right)}{r^{2p}(t)|\mathbf{x}_0-\mathbf{z}|^{2p}}\,\mathrm{d}\mathcal{S}^{d-1}(\mathbf{z})\mathrm{d}\epsilon \geq \\ & 2^{2p}||f_0||_\infty \int_0^1 \int_{\{r^{2p}(t)2^{-2p}|\mathbf{x}_0-\mathbf{z}|^{2p}\leq\delta_1\}} \frac{h\left(r^{2p}(t)2^{-2p}|\mathbf{x}_0-\mathbf{z}|^{2p}\right)}{r^{2p}(t)|\mathbf{x}_0-\mathbf{z}|^{2p}}\,\mathrm{d}\mathcal{S}^{d-1}(\mathbf{z})\mathrm{d}\epsilon.\end{aligned}$$

The case $l = 0$ of theorem 4.1.1 then implies

$$\mathrm{I} \geq \mathrm{vol}(\mathcal{S}^{d-2})||f_0||_\infty \int_{\{(r^2(1-s)/2)^p \leq \delta_1\}} \frac{h\left(r^{2p}(t)2^{-p}(1-s)^p\right)}{r^{2p}(t)2^{-p}(1-s)^p}(1-s^2)^{\frac{d-3}{2}}\ \mathrm{d}s.$$

For II, using the last part of (b2) it follows that $\frac{h(r)}{r} \geq \frac{h(\delta_1)}{\delta_1}$ for all $r \geq \delta_1$ and similarly that $h'(r) \geq h'(\delta_1) \geq \frac{h(\delta_1)}{\delta_1}$ provided $\delta_1 \leq \delta$. Therefore

$$\mathrm{II} \geq \frac{h(\delta_1)}{\delta_1}\int_0^1 \int_{\mathcal{S}^{d-1}} f_0(\mathbf{z})\ \mathrm{d}\mathcal{S}^{d-1}(\mathbf{z})\mathrm{d}\epsilon = M_\rho \frac{h(\delta_1)}{\delta_1}.$$

For any time when $r^{2p}(t) < \delta$, the choice $\delta_1 = r^{2p}(t)$ yields

$$\frac{1}{2}\frac{\partial}{\partial t}|\Delta|^2 \geq |\Delta|^2\left[\mathrm{vol}(\mathcal{S}^{d-2})||f_0||_\infty \mathcal{I}(r^{2p}(t)) + M_\rho h(r^{2p}(t))\right] r^{-2p}(t). \tag{4.37}$$

An application of Gronwall's inequality then shows

$$|\Delta(\mathbf{x},\mathbf{w},t)|^{2p} \geq |\Delta(\mathbf{x},\mathbf{w},0)|^{2p} \exp\left(2p\int_{t_0}^t \left[\mathrm{vol}(\mathcal{S}^{d-2})||f_0||_\infty \mathcal{I}(r^{2p}(s)) + M_\rho h(r^{2p}(s))\right] r^{-2p}(s)\ \mathrm{d}s\right).$$

Dividing through by $|\mathbf{x}-\mathbf{w}|$ and taking infimums yields the estimate

$$r^{2p}(t)/r^{2p}(t_0) \geq \exp\left(2p\int_{t_0}^t \left[\mathrm{vol}(\mathcal{S}^{d-2})||f_0||_\infty \mathcal{I}(r^{2p}(s)) + M_\rho h(r^{2p}(s))\right] r^{-2p}(s)\ \mathrm{d}s\right) \tag{4.38}$$

which holds for all $t \geq t_0$ such that $r^{2p}(t) < \delta$ on $[t_0, t]$. Using (4.38) and a standard bootstrap argument shows that $r^{2p}(t) \geq q(t)$ for all such $t \geq t_0$. Of course, $q(t) < \delta$ for all $t \geq t_0$ as $h \leq 0$ on $(0, \delta]$, so that in fact $r^{2p}(t) \geq q(t)$ for all $t \geq t_0$. □

The last ingredient we need demonstrates that in the second case, the solution to (4.36) remains positive for all time when $h(r)$ defines a natural, Osgood kernel.

Lemma 4.3.10. *Let $h(r)$ define a natural, Osgood kernel satisfying* (b1) *and* (b2)*, and take $\delta > 0$ as in lemma 4.3.7. Then the solution $\Phi(\mathbf{x}, t)$ with initial data $\Phi_0(\mathbf{x})$ exists globally in time.*

Proof. It suffices to show that $\mathcal{I}(q(t)) \geq Ch(q(t))$ where C denotes some finite, positive constant. Indeed, as $h(r)$ defines an Osgood kernel the solution to (4.36) then remains positive for all time, whence $\text{Lip}[\Phi^{-1}](t)$ remains finite for all time by lemma 4.3.9. From (H2) it follows that $||\Phi||_\infty(t)$ also remains bounded for all time, and the claim then follows.

To see that $\mathcal{I}(q(t)) \geq Ch(q(t))$ holds, recall from lemma 4.3.7 part (b2) that $h(r)$ decreases on $(0, \delta]$. As $q(t)2^{-p}(1-s)^p \leq q \leq \delta$ for $s \in [-1, 1]$, it then follows that

$$\begin{aligned}\mathcal{I}(q(t)) &:= \int_{-1}^{1} \frac{h\left(q(t)2^{-p}(1-s)^p\right)}{2^{-p}(1-s)^p}(1-s^2)^{\frac{d-3}{2}}\,\mathrm{d}s \\ &\geq 2^p h(q(t)) \int_{-1}^{1} (1-s)^{\frac{d-3}{2}-p}(1+s)^{\frac{d-3}{2}}\,\mathrm{d}s.\end{aligned}$$

As $p < \frac{d-1}{2}$ by hypothesis, the last integral is finite, which gives $\mathcal{I}(q(t)) \geq Ch(q(t))$ as desired. □

We may now encapsulate the previous lemmas into the main result of this section, i.e. the following theorem demonstrating the equivalence between the Osgood condition (4.31) and the global existence of all solutions to the IDE (1.13) for the class of natural kernels.

Theorem 4.3.11. *(Necessary and Sufficient Condition for Global Existence) Let $g(s)$ satisfy* (4.30)*, where $h(r)$ defines a natural kernel and $h(r) \leq 0$ in a neighborhood of the origin. Then all solutions to* (1.13) *exist globally in time if and only if* (4.31) *holds.*

Proof. Suppose first that (4.31) fails. Then either $h(0) < 0$ or $h(0) = 0$. In the first case, there exists $\epsilon > 0$ so that

$$g(s) < \frac{h(0)}{2(2s)^p},$$

for some $p > 0$ and all $s \in [0, \epsilon]$. The proof of lemma 4.3.4 then shows that all solutions with $||\Phi_0||_\infty^2 \leq \epsilon/2$ collapse to the origin in finite time. In the second case, either (a) or (b1,b2) in lemma 4.3.7 holds. If (a) holds then $\exists C_0 > 0$ so that

$$h(r) \geq -C_0 r$$

for all r in a neighborhood of the origin. This contradicts the assumption that (4.31) fails, so both (b1) and (b2) must hold. As a consequence, $g(s)$ is non-negative and non-decreasing

in a neighborhood of the origin. Lemma 4.3.4 then applies, so that all solutions with $||\Phi_0||_\infty$ sufficiently small must collapse in finite time.

Conversely, if (4.31) holds then necessarily $h(0) = 0$. Thus either lemma 4.3.8 or lemma 4.3.10 applies, yielding global existence of all solutions in either case. □

4.3.2 Locally Repulsive Kernels

Lastly, we provide a global existence result for locally repulsive kernels, i.e. when $g(s)$ has a positive singularity near the origin. As before, we assume

$$g(s) = \frac{h\left((2s)^p\right)}{(2s)^p},$$

for some $0 < p \leq 1/2$ and $p < 1/2$ if $d = 2$. We modify the assumtions on $h(r)$ slightly, in that we replace the monotonicity condition (H3) with a boundedness condition (H4). We therefore assume

$$\begin{aligned} &\text{(H1) } h(r) \in C^1\left(\mathbb{R}^+ \setminus \{0\}\right) \\ &\text{(H2) } h(r) \in L^\infty(\mathbb{R}^+) \\ &\text{(H4) } \inf_{(0,1)} h'(r) > -\infty. \end{aligned} \tag{4.39}$$

These hypotheses include many kernels that appear in applications, including the power laws $g(s) = s^{-p}$ for $p \leq \frac{1}{2}$ as well as the ubiquitous Morse potential [38, 24]

$$g(s) = \frac{\mathrm{e}^{-\sqrt{2s}} - F\mathrm{e}^{-L\sqrt{2s}}}{\sqrt{2s}}.$$

Under these assumptions, we have the following global existence result:

Theorem 4.3.12. *Let $g(s) = h((2s)^p)(2s)^{-p}$ for some $0 < p \leq 1/2$ if $d \geq 3$ and $p < 1/2$ if $d = 2$. Let $h(r)$ satisfy (4.39) and $f_0(\mathbf{w}) \geq 0$. If there exists a neighborhood $(0, \delta]$ of the origin on which $h(r) \geq 0$, then the solution $\Phi(\mathbf{x}, t)$ given by theorem 4.2.1 exists globally in time.*

Proof. Again using the remark following theorem 4.3.2, this follows from a straightforward upper bound for $\mathrm{Lip}[\Phi^{-1}](t)$ and $||\Phi||_\infty(T)$. For $\mathbf{x}, \mathbf{w}, \mathbf{z} \in \mathcal{S}^{d-1}$ and $\epsilon \in \mathbb{R}$ let $\Delta(\mathbf{x}, \mathbf{w}, t) :=$

$\Phi(\mathbf{x},t)-\Phi(\mathbf{w},t)$ and

$$L_\epsilon(\mathbf{x},\mathbf{w},\mathbf{z})=\epsilon\Phi(\mathbf{x},t)+(1-\epsilon)\Phi(\mathbf{w},t)-\Phi(\mathbf{z},t).$$

Then as before it follows that

$$\begin{aligned}\frac{1}{2}\frac{\partial}{\partial t}|\Delta(\mathbf{x},\mathbf{w},t)|^2 =&|\Delta|^2\int_0^1\int_{\mathcal{S}^{d-1}}\left[\frac{h(|L_\epsilon|^{2p})}{|L_\epsilon|^{2p}}\left(1-2p\cos^2(\theta_\epsilon)\right)+\right.\\ &\left.h'(|L_\epsilon|^{2p})2p\cos^2(\theta_\epsilon)\right]f_0(\mathbf{z})\,\mathrm{d}\mathcal{S}^{d-1}(\mathbf{z})\mathrm{d}\epsilon,\end{aligned}$$

where θ_ϵ denotes the angle between L_ϵ and Δ. As $h\geq 0$ when $|L_\epsilon|^{2p}<\delta$ and h' is bounded below it follows that

$$\begin{aligned}&\frac{1}{2}\frac{\partial}{\partial t}|\Delta(\mathbf{x},\mathbf{w},t)|^2\geq|\Delta|^2\int_0^1\int_{\mathcal{S}^{d-1}}\left[\frac{h(|L_\epsilon|^{2p})}{|L_\epsilon|^{2p}}\left(1-2p\cos^2(\theta_\epsilon)\right)\mathbf{1}_{\{|L_\epsilon|^{2p}\geq\delta\}}+\right.\\ &\left.h'(|L_\epsilon|^{2p})2p\cos^2(\theta_\epsilon)\right]f_0(\mathbf{z})\,\mathrm{d}\mathcal{S}^{d-1}(\mathbf{z})\mathrm{d}\epsilon\geq\\ &|\Delta|^2\mathrm{vol}(\mathcal{S}^{d-1})||f_0||_\infty\left(\min\left\{\inf_{r\in(0,2^{2p}||\Phi||_\infty^{2p}(t)]}h'(r),0\right\}-\frac{||h||_\infty}{\delta}\right).\end{aligned}$$

Using Gronwall's inequality as before shows that $\mathrm{Lip}[\Phi^{-1}](t)$ remains finite for all time provided $||\Phi||_\infty(t)$ does. However, as in lemma 4.3.8 the hypothesis (H2) shows that

$$\frac{\partial}{\partial t}||\Phi||_\infty(t)\leq K||\Phi||_\infty^{1-2p}(t),$$

for some absolute constant K, so that $||\Phi||_\infty(t)$ does remains bounded for all finite time as desired. □

4.4 Concluding Remarks

This chapter provided the basic local in time well-posedness theory for an aggregation sheet, i.e. a solution to the aggregation equation (4.1) that concentrates on a co-dimension one manifold. We dedicated our efforts on the case when the evolution equation (1.13) is linearly well-posed, and demonstrated that this aspect of the linear theory used the linear well-posedness condition to demonstrate that nonlinear well-posedness also holds. This condition enforces regularity in the kernel, and we therefore assumed only a modest amount regularity

for the sheet itself. This contrasts to similar problems in the linearly ill-posed regime, most notably the Birkhoff-Rott equation, where local existence results have been known for some time for analytic sheets in two and three dimensions [60], and for chord-arc initial data [73] in two dimensions. Demonstrating local existence of sheet solutions to the aggregation equation (4.1) in the ill-posed regime proves an interesting open problem.

Regarding global existence, we showed that for attractive kernels the Osgood condition (4.28) determines whether or not solutions collapse in finite time. This makes a nice connection to the existing literature on the co-dimension zero aggregation equation, where similar results exist [7, 8]. For a class of kernels with a repulsive singularity near the origin we provided a simple global existence result. While this class includes many kernels that appear in applications, such as the Morse potential, it fails to capture reasonable examples such as the power laws $g(s) = s^{-p}$ for $p > 1/2$. Our current methods for demonstrating global existence do not apply to such kernels, so we leave the problem of proving global existence for a broader class of repulsive kernels for future research.

References

[1] Eric L. Altschuler, Timothy J. Williams, Edward R. Ratner, Robert Tipton, Richard Stong, Farid Dowla, and Frederick Wooten. Possible global minimum lattice configurations for thomson's problem of charges on a sphere. Phys. Rev. Lett., 78(14):2681–2685, Apr 1997.

[2] Anna M. Barry, Glen R. Hall, and C. Eugene Wayne. Relative Equilibria of the $(1+N)$-Vortex Problem. arXiv, 1012.1002v1, 2010.

[3] N. Bellomo, H. Berestycki, F. Brezzi, and J.-P. Nadal. Mathematics and complexity in life and human sciences. Math. Mod. Meth. Appl. Sci., 20(1 suppl.):1391–1395, 2010.

[4] D. Benedetto, E. Caglioti, and M. Pulvirenti. A kinetic equation for granular media. Math. Mod. Num. Anal., 31(5):615–641, 1997.

[5] A.J. Bernoff and C.M. Topaz. A primer of swarm equilibria. SIAM J. Appl. Dyn. Syst., 10:212–250, 2011.

[6] A.L. Bertozzi and T. Laurent. Finite-time blow-up of solutions of an aggregation equation in $\mathbb{R}^n$. Comm. Math. Phys., 274:717–735, 2007.

[7] Andrea Bertozzi, Jose Carrillo, and Thomas Laurent. Blowup in multidimensional aggregation equations with mildly singular interaction kernels. Nonlinearity, 22(3):683–710, 2009.

[8] Andrea Bertozzi, Thomas Laurent, and Jesus Rosado. L^p theory for the multidimensional aggregation equation. Commun. Pure Appl. Math., 64(1):45–83, 2011.

[9] Andrea L. Bertozzi, John B. Garnett, and Thomas Laurent. Characterization of radially symmetric finite time blowup in multidimensional aggregation equations. SIAM J. of Math. Anal., accepted, 2011.

[10] M. Bodnar and J.J.L. Velázquez. An integro-differential equation arising as a limit of individual cell-based models. J. Diff. Eq., 222:341–380, 2006.

[11] Michael P. Brenner, Peter Constantin, Leo P. Kadanoff, Alain Schenkel, and Shankar C. Venkataramani. Diffusion, attraction and collapse. Nonlinearity, 12(4):1071, 1999.

[12] J.L. Burchnall and A. Lakin. The theorems of Saalschütz and Dougall. Quart. J. Math., 2(1), 1950.

[13] Scott Camazine, Jean-Louis Deneubourg, Nigel R. Franks, James Sneyd, Guy Theraulaz, and Eric Bonabeau. Self-Organization in Biological Systems. Princeton Univ. Press, Princeton, 2003.

[14] J.A. Carillo, M. DiFrancesco, A. Figalli, T. Laurent, and D. Slepcev. Global-in-time weak measure solutions and finite-time aggregation for nonlocal interaction equations. Duke Math. Journ., 156(2):229–271, 2011.

[15] J. A. Carrillo, R. J. McCann, and C. Villani. Contractions in the 2-wasserstein length space and thermalization of granular media. Arch. Rat. Mech. Anal., 179(2):217–263, 2006.

[16] S. J. Chapman, J. Rubinstein, and M. Schatzman. A mean-field model of superconducting vortices. Euro. Journ. Appl. Math., 7:97–111, 1996.

[17] Yao-Li Chuang, Y.R. Huang, M.R. D'Orsogna, and A.L. Bertozzi. Multi-vehicle flocking: Scalability of cooperative control algorithms using pairwise potentials. In Robotics and Automation, 2007 IEEE International Conference on, pages 2292 –2299, 2007.

[18] Henry Cohn and Abhinav Kumar. Universally optimal distribution of points on spheres. J. Amer. Math. Soc., 20(1):99–148, 2007.

[19] Henry Cohn and Abhinav Kumar. Algorithmic design of self-assembling structures. PNAS, 106(24):9570–9575, 2009.

[20] I. D. Couzin, J. Krauss, N. R. Franks, and S. A. Levin. Effective leadership and decision-making in animal groups on the move. Nature, 433:513–516, 2005.

[21] Anna M. Delprato, Azadeh Samadani, A. Kudrolli, and L. S. Tsimring. Swarming ring patterns in bacterial colonies exposed to ultraviolet radiation. Phys. Rev. Lett., 87(15):158102, Sep 2001.

[22] H. Dong. The aggregation equation with power-law kernels: ill-posedness, mass concentration and similarity solutions. Comm. Math. Phys., 304(3):649–664, 2011.

[23] H. Dong. On similarity solutions to the multidimensional aggregation equation. SIAM J. Math. Anal., 43:1995–2008, 2011.

[24] M. R. D'Orsogna, Y. L. Chuang, A. L. Bertozzi, and L. S. Chayes. Self-propelled particles with soft-core interactions: Patterns, stability, and collapse. Phys. Rev. Lett., 96(10):104302, Mar 2006.

[25] Leah Edelstein-Keshet, James Watmough, and Daniel Grunbaum. Do travelling band solutions describe cohesive swarms? An investigation for migratory locusts. Journal of Mathematical Biology, 36:515–549, 1998. 10.1007/s002850050112.

[26] K. Fellner and G. Raoul. Stability of stationary states of non-local equations with singular interaction potentials. Mathematical and Computer Modelling, 53(7-8), 2011.

[27] K. Fellner and G. Raoul. Stable stationary states of non-local interaction equations. Mathematical Models and Methods in Applied Sciences, 20(12), 2011.

[28] R. C. Fetecau, Y. Huang, and T. Kolokolnikov. Swarm dynamics and equilibria for a nonlocal aggregation model. Nonlinearity, 24(10):2681–2716, 2011.

[29] George Gasper and Walter Trebels. A Riemann-Lebesgue lemma for Jacobi expansions. In A.I. Zayed M.E.H. Ismail, M.Z. Nashed and A.F. Gholeb, editors, Conf. on Mathematical Analysis, Wavelets, and Signal Processing, volume 90 of Contemporary Mathematics. Amer. Math. Soc., Providence, R.I., 1995.

[30] J. H. Irving and J. G. Kirkwood. The statistical mechanical theory of transport processes. iv. the equations of hydrodynamics. J. Chem. Phys., pages 817–829, 1950.

[31] Mohamed I. Jamaloodeen and Paul K. Newton. The N-vortex problem on a rotating sphere. II. heterogeneous platonic solid equilibria. Proc. R. Soc. A, 462(2075):3277–3299, 2008.

[32] S. A. Kaufmann. The Origins of Order: Self-Organization and Selection in Evolution. Oxford University Press, New York, 1933.

[33] E. F. Keller and L. A. Segel. Initiation of slime mold aggregation viewed as an instability. J. Theor. Biol., 26:399–415, 1970.

[34] Evelyn F. Keller and Lee A. Segel. Model for chemotaxis. Journal of Theoretical Biology, 30(2):225 – 234, 1971.

[35] T. Kolokolnikov, H. Sun, D. Uminsky, and A. L. Bertozzi. Stability of ring patterns arising from two-dimensional particle interactions. Phys. Rev. E, 84(1):015203, Jul 2011.

[36] Robert Krasny. A study of singularity formation in a vortex sheet by the point-vortex approximation. J. Fluid Mech., 167:65–93, 1986.

[37] A. B. Kuijlaars and E. B. Saff. Asymptotics for minimal discrete energy on the sphere. Trans. Amer. Math. Soc., 350(2):523–538, 1998.

[38] Andrew J. Leverentz, Chad M. Topaz, and Andrew J. Bernoff. Asymptotic dynamics of attractive-repulsive swarms. SIAM J. Appl. Dyn. Syst., 8:880–908, 2009.

[39] Herbert Levine, Wouter-Jan Rappel, and Inon Cohen. Self-organization in systems of self-propelled particles. Phys. Rev. E, 63(1):017101, Dec 2000.

[40] F. Lin and P. Zhang. On the hydrodynamic limit of ginzburg-landau vortices. Disc. Cont. Dyn. Sys., 6:121–142, 2000.

[41] Ryan Lukemana, Yue-Xian Lib, and Leah Edelstein-Keshet. Inferring individual rules from collective behavior. PNAS, 10(107), 2010.

[42] R. Mach and F. Schweitzer. Modeling vortex swarming in daphnia. Bull. Math. Bio, 69:539–562, 2007.

[43] A. Majda. Vorticity and the mathematical theory of incompressible flow. Commun. Pure Appl. Math., 39(1):5187–5220, 1986.

[44] Andrew Majda and Andrea Bertozzi. Vorticity and Incompressible Flow. Cambridge University Press, 2002.

[45] A. Mogilner and L. Edelstein-Keshet. A non-local model for a swarm. Journal of Mathematical Biology, 38:534–570, 1999.

[46] A. Mogilner, L. Edelstein-Keshet, L. Bent, and A. Spiros. Mutual interactions, potentials, and individual distance in a social aggregation. Journal of Mathematical Biology, 47:353–389, 2003. 10.1007/s00285-003-0209-7.

[47] Paul K. Newton and Takashi Sakajo. The N-vortex problem on a rotating sphere. III. ring configurations coupled to a background field. Proc. R. Soc. A, 463(2080):961–977, 2007.

[48] Paul K. Newton and Takashi Sakajo. Point vortex equilibria and optimal packings of circles on a sphere. Proc. R. Soc. A, 2010.

[49] J. K. Parrish and L. Edelstein-Keshet. Complexity, Pattern, and Evolutionary Trade-Offs in Animal Aggregation. Science, 284(99), 1999.

[50] A. Pérez-Garrido, M. J. W. Dodgson, and M. A. Moore. Influence of dislocations in thomson's problem. Phys. Rev. B, 56(7):3640–3643, Aug 1997.

[51] F. Poupad. Diagonal defect measures, adhesion dynamics and the Euler equation. Meth. Appl. Anal., 9:533–561, 2002.

[52] I. Prigogine. Order Out of Chaos. Bantam, New York, 1984.

[53] G. Raoul. Non-local interaction equations: Stationary states and stability analysis, 2011.

[54] Mikael C. Rechtsman, Frank H. Stillinger, and Salvatore Torquato. Optimized interactions for targeted self-assembly: Application to a honeycomb lattice. Phys. Rev. Lett., 95(22):228301, Nov 2005.

[55] Mikael C. Rechtsman, Frank H. Stillinger, and Salvatore Torquato. Designed interaction potentials via inverse methods for self-assembly. Phys. Rev. E, 73(1):011406, Jan 2006.

[56] Mikael C. Rechtsman, Frank H. Stillinger, and Salvatore Torquato. Self-assembly of the simple cubic lattice with an isotropic potential. Phys. Rev. E, 74(2):021404, Aug 2006.

[57] R.T. Seeley. Spherical harmonics. The American Mathematical Monthly, 73(4), 1966.

[58] L.J. Slater. Generalized hypergeometric functions. Cambridge University Press, 1966.

[59] S. Smale. Mathematical problems for the next century. Mathematics: frontiers and perspectives, pages 271–294, 2000.

[60] C. Sulem, P.L. Sulem, C. Bardos, and U. Frisch. Finite Time Analyticity for the Two and Three Dimensional Kelvin-Helmholtz Instability. Commun. Math. Phys., 80:485–516, 1981.

[61] H. Sun, D. Uminsky, and A. L. Bertozzi. A generalized Birkhoff-Rott Equation for 2D Active Scalar Problems. accepted to SIAM J. Appl. Math, 2011.

[62] G. Szegö. Orthogonal Polynomials. Amer. Math. Soc., Providence, RI, 4th edition, 1975.

[63] J. J. Thomson. On the structure of the atom. Philosophical Magazine, 7(39):237–265, 1904.

[64] C. M. Topaz, A. J. Bernoff, S. Logan, and W. Toolson. A model for rolling swarms of locusts. The European Physical Journal - Special Topics, 157:93–109, 2008. 10.1140/epjst/e2008-00633-y.

[65] Chad M. Topaz and Andrea L. Bertozzi. Swarming patterns in a two-dimensional kinematic model for biological groups. SIAM J. on Appl. Math., 65(1):152–174, 2004.

[66] Salvatore Torquato. Inverse optimization techniques for targeted self-assembly. Soft Matter, 5:1157–1173, 2009.

[67] G. Toscani. One-dimensional kinetic models of granular flows. Math. Mod. Num. Anal., 34(6).

[68] Lev Tsimring, Herbert Levine, Igor Aranson, Eshel Ben-Jacob, Inon Cohen, Ofer Shochet, and William N. Reynolds. Aggregation patterns in stressed bacteria. Phys. Rev. Lett., 75(9):1859–1862, Aug 1995.

[69] James H. von Brecht and Andrea L. Bertozzi. Well-posedness theory for aggregation sheets. Commun. Math. Phys., submitted, 2012.

[70] James H. von Brecht and David Uminsky. Linearized inverse statistical mechanics. J. Nonlinear Sci., to appear, 2012.

[71] James H. von Brecht, David Uminsky, Theodore Kolokolnikov, and Andrea L. Bertozzi. Predicting pattern formation in particle interactions. Math. Mod. Meth. Appl. Sci., Suppl. 4, 2012.

[72] McKay Hayley Wales, David J. and Eric L. Altschuler. Defect motifs for spherical topologies. Phys. Rev. B, 79(22):224115, Jun 2009.

[73] Sijue Wu. Mathematical Analysis of Vortex Sheets. Commun. Pure Appl. Math., 59(1):1065–1206, 2005.

[74] Wen Yang, A.L. Bertozzi, and Xiaofan Wang. Stability of a second order consensus algorithm with time delay. In Decision and Control, 2008. CDC 2008. 47th IEEE Conference on, pages 2926 –2931, 2008.

[75] R. Zandi, D. Reguera, R.F. Bruinsma, W.M. Gelbart, and J. Rudnick. Origin of icosahedral symmetry in viruses. PNAS, 101(44):15556–60, 2004.